Title

Targeted delivery of LIF to dystrophic muscles by macrophages reduces muscle fibrosis and inflammation

Author

Flores, Ivan

Publication Date

2021

Peer reviewed|Thesis/dissertation

UNIVERSITY OF CALIFORNIA

Los Angeles

Targeted delivery of transgenic LIF to dystrophic muscles by macrophages reduces muscle fibrosis and inflammation

A dissertation submitted in partial satisfaction of the requirements for the degree of Doctor of Philosophy in Molecular, Cellular, and Integrative Physiology

by

Ivan Flores

2021

ABSTRACT OF THE DISSERTATION

Targeted delivery of transgenic LIF to dystrophic muscles by macrophages reduces muscle fibrosis and inflammation

by

Ivan Flores

Doctor of Philosophy in Molecular, Cellular, and Integrative Physiology

University of California, Los Angeles, 2021

Professor James G. Tidball, Chair

Progressive fibrosis of muscles in Duchenne muscular dystrophy impairs muscle function and contributes to premature death of patients. The use of many potentially-therapeutic molecules is limited by an inability to target their delivery specifically to sites of active muscle pathology. In this dissertation research, we tested the hypothesis that inflammatory cells can function as vectors to deliver therapeutic molecules to sites of active pathology in dystrophic muscle. We designed a transgene in which expression of leukemia inhibitory factor (LIF) is driven by the promoter for CD11b, a surface marker highly expressed by mature macrophages. Expression of the transgene (CD11b/LIF) in the mdx mouse model of Duchenne muscular dystrophy increased LIF protein content at inflammatory muscle lesions without off-target expression. Transplantation of transgenic bone marrow cells to non-transgenic, mdx mice showed that a

single intervention can provide long-term benefits to dystrophic muscles. The primary benefit of the transgene was reduced fibrosis. Transgenic LIF inhibited fibrogenesis by reducing transforming growth factor-β expression and reducing the numbers of fibro/adipogenic progenitor cells in mdx muscles. CD11b/LIF expression also biased macrophages away from a CD163+/CD206+, pro-fibrotic phenotype and reduced their intramuscular numbers. Reduced chemotactic response of CD11b/LIF+ macrophages to C-C motif chemokine ligand-2 contributed to the reduced macrophage numbers. The dispersion of cytolytic, CD68+ macrophages was impaired in transgenic muscles early in the pathology. Localized accumulation of CD68+ macrophages increased the numbers of injured fibers. At later stages of the pathology, the transgene did not affect macrophage distribution but did reduce muscle damage. Collectively, our observations show that targeted expression of the CD11b/LIF transgene improves dystrophic muscle health. More importantly, we have shown that genetically-modified macrophages can be used as vectors for the delivery of therapeutic molecules to diseased tissues with a significant inflammatory component.

The dissertation of Ivan Flores is approved.

Kenneth Dorshkind

Tomas Ganz

Sergio Armando Villalta

James G. Tidball, Committee Chair

University of California, Los Angeles

2021

Dedication

I dedicate this dissertation to Karin.

Table of Contents

List of Figures and Tables

Chapter 2

Chapter 3

ACKNOWLEDGEMENTS

I am extremely grateful to have received mentorship from Dr. Tidball during my training at UCLA. I began my research experience in his laboratory as a transfer, undergraduate student. Despite my lack of experience, his direct guidance, encouragement, and trust made me feel like a competent scientist. That great experience continued through my doctoral training, during which I have felt fortunate to have Dr. Tidball serve as a role model for being a scientist and caring leader. Although I am leaving his laboratory, the strong work ethic he helped me develop will continue to aid me in accomplishing my new goals. I also leave the Tidball laboratory with great memories provided by current and past members. The friendship they provided made it a joy to be in the laboratory every day and celebrate our successes with each other.

I would also like to thank Dr. Diana Azurdia, Dr. Dwayne Simmons, Dr. Sonia Zarate, and Dr. Tama Hasson for administering the training programs that enriched my academic studies at UCLA. The MARC undergraduate program and the Bridge to the Doctorate graduate program used challenging curriculums to improve my skills in scientific writing and presenting. More importantly, the programs helped me succeed in graduate school by providing guidance that a first-generation college student, like myself, would not have had access to.

Lastly, it is a privilege to have Dr. Armando Villalta, Dr. Kenneth Dorshkind, and Dr. Tomas Ganz be a part of my committee. Their valuable input will ensure that the time and effort I have invested in my doctoral work is well presented in this dissertation.

The work presented in Chapter 2 was completed under the guidance of James G. Tidball and is a reprint of “Welc, S. S., Flores, I., Wehling-Henricks, M., Ramos, J., Wang, Y., Bertoni, C. and Tidball, J. G. (2019) Targeting a therapeutic LIF transgene to muscle via the immune system

ameliorates muscular dystrophy. *Nat. Commun.*, 10, 1–17." Primary authorship is shared by Steven S. Welc and Ivan Flores. The experimental design for the investigation was done by Steven S. Welc, Ivan Flores, Michelle Wehling-Henricks, and James G. Tidball. Experiments were completed by all listed authors. Steven S. Welc, Ivan Flores, and James G. Tidball analyzed the experimental data and prepared the manuscript.

The work presented in Chapter 3 was completed under the guidance of James G. Tidball and is a version of, "Flores, I., Welc, S.S., Wehling-Henricks, M., and Tidball, J. G. (2021) Myeloid cell-mediated targeting of LIF to dystrophic muscle causes transient increases in muscle fiber lesions by disrupting the recruitment and dispersion of macrophages in muscle. *Hum. Mol. Genet.*, (in press)." All authors contributed to experimental design and completion of experiments. Ivan Flores and James G. Tidball analyzed the experimental data and prepared the manuscript.

Research reported in this dissertation was supported by an F31 fellowship from the National Institute of Arthritis and Musculoskeletal and Skin Diseases of the National Institutes of Health (F31AR071783) and a Bridge to the Doctorate fellowship from the National Science Foundation. This work was also supported by the following fellowships awarded by the University of California, Los Angeles: Eugene V. Cota-Robles Fellowship, Charles E. and Sue K. Young Fellowship, and a Dissertation Year Fellowship.

Vita

Education

University of California, Los Angeles 2012 — 2014

- Physiological Sciences, B.S.

Fellowships

Dissertation Year Fellowship, UCLA 2020 — 2021

Charles E. and Sue K. Young Fellowship, UCLA 2020 — 2021

F31 Pre-doctoral Fellowship, NIH 2017 — 2019

Eugene V. Cota-Robles Fellowship, UCLA 2016 — 2017

Bridge to the Doctorate, NSF 2015 — 2016

Awards

Society for Muscle Biology, Frontiers in Myogenesis Conference 2019

- Best Trainee Award, Poster Presentation (3rd place)

Emerging Researchers National Conference 2015

- Graduate Student Oral Presentation (1st place)

Publications

1. Welc, S. S.*, Flores, I.*, Wehling-Henricks, M., Ramos, J., Wang, Y., Bertoni, C. and Tidball, J. G. (2019) Targeting a therapeutic LIF transgene to muscle via the immune system ameliorates muscular dystrophy. *Nat. Commun.*, **10**, 1–17.

- * denotes primary co-authorship.

2. Tidball, J. G., Flores, I., Welc, S. S., Wehling-Henricks, M., and Ochi, E. (2021) Aging of the immune system and impaired muscle regeneration: A failure of immunomodulation of adult myogenesis. *Exp. Gerontol.,* **145,** 111200.

3. Flores, I., Welc, S.S., Wehling-Henricks, M., and Tidball, J. G. (2021) Myeloid cell-mediated targeting of LIF to dystrophic muscle causes transient increases in muscle fiber

lesions by disrupting the recruitment and dispersion of macrophages in muscle. *Hum. Mol. Genet.*, **(in press).**

Chapter 1:

Introduction

Duchenne muscular dystrophy (DMD) is a muscle-debilitating disease.

Duchenne muscular dystrophy (DMD) is a muscle-wasting disease that has no cure and affects one in every 3,600 – 6,000 male births [1–5]. The progressive muscle deterioration results in the loss of patient ambulation in the second decade of life and patient mortality in the third to fourth decades due to limb, respiratory, and cardiac muscle failure [6,7]. Muscle weakness in DMD patients is caused by a null mutation in the dystrophin gene, resulting in the reduction of the dystrophin-associated protein complex (DAPC) from the muscle fiber membrane (sarcolemma) [8–11]. A major role of the DAPC is to provide structural integrity by tethering the muscle cytoskeleton to the extracellular membrane (ECM) [12]. Absence of the DAPC dramatically increases the susceptibility of muscle to damage during mechanical stress. Repeated bouts of mechanical injury lead to cycles of degeneration and regeneration that chronically-activate the immune response [8,12–14]. Prolonged immune activity exacerbates the dystrophic pathology by increasing muscle damage and promoting fibrosis, the process through which contractile muscle tissue is replaced by non-contractile collagen [15–17]. This effect contrasts with the temporary inflammatory response that is indispensable for muscle regeneration in acute, sterile injuries.

The differing roles that the immune response plays in acute versus chronic muscle injuries can be partially explained by a dysregulation in the activity of macrophages in pathologically-inflamed muscle. For example, depletion of infiltrating macrophages to acutely injured muscles will impair repair, while macrophage depletion at the onset of the dystrophic pathology can reduce damage to the sarcolemma [13,18,19]. Therefore, treatment strategies that can modify the inflammatory response in dystrophic muscles can be especially effective. In this introduction, I review the roles of macrophages in muscle damage and regeneration following acute injury and how those processes are disrupted in dystrophic muscles.

Macrophages promote myogenesis in acutely injured muscle.

Acute muscle repair relies on myogenesis.

The regenerative capacity of skeletal muscle depends on the presence of myogenic progenitor cells, called satellite cells, and their ability to proceed through sequential stages of myogenesis to form syncytial muscle fibers [20,21]. Myogenesis following injury can be divided into early myogenesis, early differentiation, and terminal differentiation. The progression of muscle cells through each stage can be identified by their sequential expression of the muscle-specific transcription factors Pax7, MyoD, myogenin, and myogenic regulatory factor 4 (MRF4) [21–23].

Early myogenesis begins when quiescent satellite cells (Pax7+MyoD-) are activated to myoblasts in response to the physical disruption of their niche and an increase in pro-inflammatory cytokine availability associated with early muscle damage [20,21,23]. Myoblasts (Pax7-MyoD+) will proliferate asymmetrically so that one daughter cell can re-enter quiescence to replenish the satellite cell pool, while the other daughter cell becomes a post-mitotic myocyte (myogenin+) during early differentiation. Myogenin drives the expression of genes necessary for muscle cell fusion, marking the start of terminal differentiation. Myocytes can contribute to muscle regeneration by fusing with other myogenin+ cells to form *de novo* fibers that will replace necrotic fibers, or by fusing with injured fibers to promote fiber repair [24,25]. Myogenesis concludes with fiber growth to mature, functional muscle fibers (MRF4+) [23]. Although factors intrinsic to muscle cells play a dominant role in regulating myogenesis, extrinsic factors provided by other cells, such as macrophages, can have important influences on myogenesis.

Macrophages are recruited to sites of injury.

Macrophages recruited to injured muscles are derived from monocytes that reside in the bone marrow and circulatory system [26]. Monocytes infiltrate muscles in response to chemoattractants

produced by resident macrophages and neutrophils [14,27,28]. Resident macrophages are intramuscular cells that normally reside in a quiescent state but are rapidly activated in response to damage. Damage-associated permeability of the sarcolemma allows for passive release of molecules that are normally compartmentalized within muscle fibers [14,29]. Once released, the molecules function as damage-associated molecular patterns (DAMPs) and become ligands to toll-like receptors (TLRs) on the surface of resident macrophages [29]. Ligand binding to TLRs induces resident macrophage activation and their production of pro-inflammatory cytokines, including chemoattractants [30–32]. The initial myeloid cell population to respond to the increase in chemoattractants are neutrophils, which will reach peak intramuscular numbers and begin to decline within 24 hours of injury [33,34]. Although their presence is brief, neutrophils contribute to the production of chemoattractants for macrophage recruitment [35,36].

An important macrophage chemoattractant is C-C motif chemokine ligand 2 (CCL2) [37]. CCL2 binds to its receptor, C-C motif chemokine receptor 2 (CCR2), on the surface of monocytes to mediate their recruitment to injured tissue [30,38–41]. While CCR2 is also expressed by other leukocytes, acute injuries to muscles of CCL2-/- and CCR2-/- mice show that intramuscular numbers of macrophages are reduced without decreases in the numbers of neutrophils, T cells, or B cells [26,38]. Those observations suggest that monocytes are the primary leukocytes recruited by CCL2-CCR2 signaling. Additionally, proper macrophage recruitment requires CCL2 expression by bone marrow cells and circulating cells in addition to the CCL2 produced at the site of injury [26]. Bone marrow transplantation (BMT) of CCL2-/- cells to wild-type (WT) mice reduced the numbers of intramuscular macrophages following an acute injury when compared to acutely-injured, WT mice that received BMT of WT cells. Similarly, intramuscular macrophage numbers were reduced in WT mice that received intravenous injection of CCL2-/- bone marrow

cells (BMCs) at the same time of acute injury administration, relative to mice receiving intravenous injection of WT BMCs [39].

In addition to CCL2, high mobility group box 1 (HMGB1) can recruit macrophages to injured muscles [42–45]. HMGB1 is a DAMP that is normally restricted to the cell nucleus but can be passively released by damaged cells in muscle tissue or actively released by activated macrophages [46–49]. Exogenous HMGB1 can form a heterocomplex with C-X-C motif chemokine ligand 12 (CXCL12) to mediate chemotaxis of myeloid cells by binding to (C-X-C motif chemokine receptor 4) CXCR4 [42,44,50]. Additionally, HMGB1 can function as a ligand to TLR4 on the surface of myeloid cells to induce their expression of nuclear factor kappa-B (NF-κB) [43,45,45,47]. NF-κB is a transcription factor that promotes the production of Th1 cytokines that will condition the injured muscle toward a pro-inflammatory environment that will influence the activity of infiltrating macrophages [30,31,51,52].

Recruited macrophages have a high degree of phenotypic plasticity that is influenced by changes in the cytokine profile at their site of infiltration [14,20,21]. Although the phenotypic state of macrophages lies on a continuum, they can generally be categorized as M1-biased, pro-inflammatory or M2-biased, anti-inflammatory macrophages. M1-biased macrophages are activated by Th1, pro-inflammatory cytokines and can be identified in injured muscles by their relatively high expression of inducible nitric oxide synthase (iNOS), tumor necrosis factor alpha (TNF-α), CD68, and Ly6C [16,20,21,53–55]. In contrast, M2-biased macrophages are activated by Th2, anti-inflammatory cytokines and can be identified in injured muscles by their expression of arginase-1 (Arg-1), transforming growth factor β (TGF-β), CD163, and CD206 [15,20,21,54–60]. The progression of macrophages from an M1- to an M2-biased phenotype is associated with the progression of muscle cells through myogenesis.

M1-biased macrophages promote early myogenesis.

Significant infiltration of macrophages begins 24 hours post-injury, concurrent with the decline of intramuscular neutrophil numbers [21]. The abundance of Th1 cytokines activates the recruited macrophages toward an M1-biased phenotype. M1-biased macrophages further produce Th1 cytokines that can promote satellite cell proliferation. For example, interferon gamma (IFNγ) and interleukin-6 (IL-6) maintain macrophages in an M1-biased state, and act directly on myoblasts to promote their proliferation *in vitro* [20,61,62]. Additionally, TNF-α maintains a Th1 response and while inhibiting muscle cell differentiation by reducing myogenin expression in cell cultures [63–65]. The combined effect of these cytokines is an expansion of myoblast numbers prior to myogenic differentiation.

M1-biased macrophages can also promote regeneration by clearing muscle debris that provides a physical obstacle for nascent fiber growth. In part, the clearance of debris by macrophages depends on their production of reactive oxygen species (ROS) that are generated by iNOS and myeloperoxidase shifts [14,16,66]. ROS can oxidize necrotic tissue and cause its further breakdown. M1-biased macrophages can then phagocytose necrotic muscle fibers, while leaving the basement membrane that surrounds the sarcolemma intact [14,17,67,68]. The basement membrane is later used by myocytes as scaffolding to generate new fibers that retain a normal size and shape [17]. M1 macrophages also phagocytose apoptotic neutrophils, a process that contributes to an active switch to an anti-inflammatory, M2-biased phenotype that promotes muscle repair.

M2-biased macrophages promote myogenic differentiation and fiber growth.

The macrophage transition to an M2-biased phenotype is characterized by their increased expression of Th2 cytokines [14,20,21]. An increase in available anti-inflammatory cytokines can

contribute to muscle regeneration by activating newly-recruited macrophages to an M2-biased phenotype and by promoting myogenic differentiation. For example, IL-10 can directly deactivate the M1-biased phenotype by reducing NF-κB expression in macrophages [56,57,60,69–71]. IL-10 can also activate AMP-activated protein kinase (AMPK) to induce a switch from the glycolytic metabolism favored by M1-biased macrophages to the oxidative metabolism favored by M2-biased macrophages [20,72]. *In vitro* studies have also demonstrated that IL-10 can promote early differentiation in myoblasts by blocking the inhibitory effect of TNF-α and IL-1β on the expression of myogenin [73,74]. IL-4, another Th2 cytokine, can also act as myoblast chemoattractant and induce expression of myogenin, facilitating muscle cell fusion *in vitro* [75–77]. The importance of Th2 cytokines to muscle repair is highlighted by impaired muscle regeneration observed in dystrophic muscle with an IL-10 deficiency and in acutely-injured muscle with an IL-4 deficiency [57,76]. Similarly, regeneration is impaired in muscles following modified muscle loading when macrophages are depleted at the stage associated with the M1- to M2-biased phenotype switch [18]. The regenerative capacity of muscle can also be impaired by inhibiting the M1- to M2-biased phenotype transition by ablating insulin-like growth factor-1 (IGF-1) in myeloid cells [78]. IGF-1 is a molecule expressed by M1- and M2-biased macrophages that can act as an anti-inflammatory cytokine to promote the M2-biased phenotype [79]. IGF-1 can also act directly on muscle cells as a growth factor to increase myoblast proliferation and increase muscle fiber growth by promoting protein synthesis [78–80]. In addition to influencing myogenesis, macrophages contribute to successful muscle repair by modulating a transient increase in ECM synthesis following an injury.

Macrophages limit connective tissue deposition.

ECM produced in response to injury provides structural integrity to the compromised muscle and aids the basement membrane in providing a scaffold to satellite cells during nascent fiber

growth [17]. Major components of the ECM are fibrils composed of collagens type 1, 3, and 5 [81,82]. Collagen type 5 functions as a central axis around which collagen type 1 or type 3 form heterofibrils [83]. Following an injury, fibrils primarily composed of collagen type 3 are synthesized at the injury site [17,82]. As the scarring matures during the regenerative process, collagen type 3 fibrils are replaced by fibrils primarily composed of collagen type 1. Collagen type 1 fibrils provide greater stability to injured muscle due to their greater diameter compared to collagen type 3 fibrils [84]. M2-biased macrophages contribute to the formation of collagen fibrils by producing proline through arginine metabolism by Arg-1 [15,20,83,85]. Proline is a structural component necessary for the formation of collagen fibrils [83]. As nascent fibers are formed and fiber growth progresses, the temporary ECM scaffold is degraded by matrix metalloproteinases produced by M1-biased macrophages [14,17,86,87]. Macrophages further modulate this process by regulating the activity of fibro-adipogenic progenitor cells (FAPs).

FAPs are a mesenchymal cell population that can be identified by their expression of platelet-derived growth factor receptor alpha (PDGFRα) [88–90]. Under homeostatic conditions, FAPs reside in a quiescent state, but are rapidly activated in response to inflammatory cytokines [14,88]. *In vitro* stimulation of FAPs with IL-4, IL-13, and TGF-β activate quiescent FAPs and promote their differentiation to fibroblasts while inhibiting their differentiation into adipose-producing cells [91–93]. FAP-derived fibroblasts are the primary source of collagens in injured muscles, and collagen expression by fibroblasts is further promoted by *in vitro* stimulation with TGF-β [88,89,93,94]. The pro-fibrotic effects of FAPs can have a detrimental role in the repair process following an injury. Administration of a TGF-β inhibitor to acutely-injured mice resulted in reduced numbers of FAPs and accumulation of connective tissue [95]. The expression of atrogin-1, associated with muscle atrophy, was also reduced in mice with reduced TGF-β activity. As regeneration progresses to fiber growth, macrophage-derived TNF-α induces FAP apoptosis to prevent

abnormal accumulation of collagens that results in fibrosis [88]. Co-cocultures of FAPs and M1-biased macrophages isolated from acutely injured muscles showed increased apoptosis of FAPs when compared to FAP-only cultures. The apoptotic effect mediated by the M1-biased macrophages was reduced in co-cultures treated with an TNF-α-neutralizing antibody. Additionally, co-cultures of fibroblasts with human macrophages activated to an M1-biased phenotype reduced the production of collagen in the co-cultures, which was quantified by measuring hydroxyproline content [87]. The importance of macrophages in regulating FAP activity is shown in a CCR2-/- mouse model of acute injury in which myeloid cell infiltration was reduced [88]. In that model, reduced muscle repair was associated by increased collagen accumulation. The increased collagen content was caused by prolonged elevations in intramuscular FAP numbers and their increased expression of genes associated with ECM synthesis. The perturbation in FAP activity was associated with reduced FAP apoptosis that was caused by decreased TNF-α derived from myeloid cells in the injured muscle.

Dysregulation of the immune response in dystrophic muscle.

The *mdx* mouse model.

Much of our understanding of dystrophic pathologies comes from studying the *mdx* mouse model of DMD. Similar to DMD patients, *mdx* mice are affected by a null mutation of the dystrophin gene that results in muscle susceptibility to chronic injury [11,96,97]. Although the muscle deterioration that occurs in *mdx* mice is not as severe as the pathology observed in DMD muscles, *mdx* mice share many of the pathological characteristics that are observed in humans. The acute onset of the *mdx* pathology that occurs at 1-month of age is accompanied by a large infiltration of macrophages that are phenotypically-similar to inflammatory cells observed in DMD muscles [14,16,20,20,53,57]. Following the acute pathological stage, *mdx* muscles undergo a regenerative stage at 3-months of age that is followed by progressive deterioration and

inflammation that begins at 12-months of age [13–15,20,69]. By the 12-month time-point, significant muscle fibrosis that is especially obvious in the diaphragm muscle has occurred and continues until death [8,11,15,98–100]. These characteristics allow the *mdx* mouse to be used as an efficient model to test therapeutic strategies that can modulate inflammation and fibrosis along the course of the dystrophic pathology.

Chronic macrophage recruitment to dystrophic muscles.

Chronic muscle damage is associated with elevated levels of chemoattractants in DMD patients and *mdx* mice. Muscles from DMD patients have elevated CCL2 protein content that localizes to blood vessels and intramuscular macrophages, while *in situ* hybridization shows that regenerating muscle fibers express CCL2 [101]. Similarly, CCL2 expression is elevated in *mdx* muscle lysates and CCL2 protein co-localizes with mononuclear cells and injured fibers [102]. CCL2 protein content is also elevated in the serum of DMD patients and *mdx* mice [103]. Additionally, serum from DMD patients and *mdx* mice contains increased amounts of HMGB1 [46]. HMGB1 protein content is also elevated in lysates of DMD and *mdx* muscles [46]. The pathologically-elevated levels of chemoattractants in dystrophic muscles cause increased recruitment of leukocytes to sites of active pathology. Approximately 90% of the infiltrating inflammatory cells are identified as macrophages, which can reach average densities of approximately 75,000 cells / mm^3 [13,101]. Experimentation in *mdx* mice shows that reducing CCL2-CCR2 signaling by genetic ablation of CCR2 or by delivering an inactive form of CCL2 can decrease the numbers of macrophages recruited to diseased muscles [41,104]. Intramuscular macrophage numbers can also be reduced by inhibiting the release of HMGB1 from cells in the muscles of *mdx* mice [47]. The reduced macrophage numbers in *mdx* muscles associated with inhibition of chemotaxis are associated with reductions in collagen accumulation and numbers of injured muscle fibers.

M1-biased macrophages promote muscle damage.

Mdx muscles at the acute onset of pathology experience overlapping cycles of injury in which muscle fibers can be found at different stages of the regenerative process, causing prolonged elevations of both pro- and anti-inflammatory cytokines [14,20]. Chronic exposure of recruited macrophages to pro-inflammatory cytokines will activate the macrophages toward a cytolytic, M1-biased phenotype [14,16,20]. However, the concurrent exposure of the macrophages to anti-inflammatory cytokines increases their expression of TGF-β. The result is a cytotoxic, M1-biased phenotype that is identified by the elevated expression of the M1-related genes TNF-α an iNOS, as well as the M2-related gene, TGF-β [14–16,88]. Pathologically-activated, M1-biased macrophages cause an increase in dystrophic muscle damage by their elevated production of ROS [16,66,105]. While a transient increase in ROS is needed for effective debris clearance, pathologically-high levels of ROS can cause sarcolemma lysis of non-necrotic fibers. Previous work in our lab has demonstrated that reducing ROS levels in *mdx* muscles by knocking out iNOS expression reduces the proportion of injured fibers *in vivo* and reduces macrophage-mediated permeabilization of muscle cells *in vitro* [16]. M1-biased macrophages can also exacerbate the dystrophic pathology by phagocytosing the basement membrane of necrotic fibers before it can serve as a scaffold for nascent fibers [17]. Without a scaffold template, nascent fibers will have variable arrangement and growth that deviates from the uniform arrangement of healthy muscle fibers.

Additionally, M1-biased macrophages found in dystrophic muscles are incapable of inducing FAP apoptosis to limit fibrotic cell numbers [88]. *Mdx* muscles show increased accumulation of FAPs when compared to age-matched, wild-type mice. The increased numbers of FAPs correlate with an increase in the accumulation of collagen type 1 in *mdx* muscles relative to wild-

type mice [90]. Researchers have shown that the elevated expression of TGF-β by M1-biased macrophages in *mdx* muscles is responsible for the anti-apoptotic effect [88]. Co-cultures of FAPs with M1-biased macrophages isolated from *mdx* muscles failed to induce FAP apoptosis, in contrast to high levels of FAP apoptosis induced by M1-biased macrophages isolated from acutely-injured muscles. However, M1-biased macrophages from *mdx* muscles were able to induce FAP apoptosis when the co-cultures were treated with a pharmacological inhibitor for TGF-β [88]. In addition to inhibiting FAP apoptosis, pathologically-elevated TGF-β has the aforementioned effects of promoting FAP differentiation to fibroblasts and increasing the expression of collagens in fibroblasts. The pro-fibrotic effects of TGF-β are maintained past the acute inflammatory stage of the *mdx* pathology.

M2-biased macrophages promote fibrosis.

Progression of the *mdx* pathology to later stages is associated with an increase in the protein content of IL-4 and IL-10 in *mdx* muscle lysates [16]. The increased availability of Th2 cytokines shifts the activation state of recruited macrophages from an M1-biased to an M2-biased phenotype. Muscle macrophages isolated from 3-month-old, *mdx* mice have reduced iNOS protein content compared to muscle macrophages from 1-month-old, *mdx* mice [16,53]. In contrast, expression of CD163 and CD206 is elevated in muscles of 3-month-old, *mdx* mice relative to the 1-month time-point [16,53]. The switch to an M2-biased phenotype can contribute to the age-dependent increases in TGF-β protein content observed in *mdx* muscles [106]. Macrophages stimulated to an M2-biased phenotype with IL-4 or IL-10 show increased expression of TGF-β when compared to macrophages stimulated to an M1-biased phenotype with IFN-γ [107].

Elevations in TGF-β can induce fibrogenesis of muscle cells in addition to increasing the fibrotic activity of FAPs. In a lineage tracing study, researchers labeled Pax7+ cells and their progeny

with yellow fluorescent protein (YFP) in *mdx* and WT mice [108]. Muscle cross-sections from 12-month-old mice were labeled with a cocktail of antibodies for Pax7, MyoD, and myogenin. Samples from the WT mice showed that 97% of YFP+ cells expressed at least one of the transcription factors, while as little as 80% of the YFP+ cells from *mdx* mice showed transcription factor expression. QPCR analysis of muscle cells isolated from the YFP+/*mdx* mice showed an increase in the expression of collagen type 1 and fibronectin, an additional ECM component, in comparison to YFP+/WT mice. Additionally, the researchers showed that culturing satellite cells isolated from *mdx* mice in the presence of a TGF-β-neutralizing antibody reduced their expression of collagen type 1 and fibronectin, while increasing their expression of Pax7 and MyoD. *In vitro* experimentation using the C2C12 muscle cell line also provided evidence of the fibrogenic effect of TGF-β on muscle cells. C2C12 cells stimulated with TGF-β showed increased expression of collagen type 1 and connective tissue growth factor, but reduced expression of myogenin [109,110]. The reduction in myogenin may contribute to reductions in C2C12 cell differentiation and fusion in the presence of TGF-β stimulation [109,110]. The reduced fusion was rescued by including a TGF-β receptor inhibitor in C2C12 cell cultures treated with TGF-β [110].

The shift of macrophage activation toward an M2-biased phenotype can further promote fibrosis by modifying arginine metabolism. Metabolism of arginine by iNOS expressed in M1-biased macrophages increases the availability of cytolytic ROS [16]. In contrast, Arg-1 expressed by M2-biased macrophages metabolizes arginine to increase the amounts of proline available for collagen fibril synthesis [15,16]. The age-dependent reductions in iNOS protein of *mdx* muscles is accompanied with an age-dependent increase in the expression of Arg-1 and Arg-2 in *mdx* muscles [16,53]. Additionally, changes in the availability of inflammatory cytokines can regulate the expression of iNOS and Arg-1 in macrophages. Stimulation of muscle macrophages from *mdx*

mice with IFN-γ and TNF-α increased their protein expression of iNOS while reducing Arg-1 protein content [16]. In contrast, stimulation with IL-4 and IL-10 reduced iNOS protein expression while increasing Arg-1 protein levels in *mdx* muscle macrophages [16]. The progressive characteristic of muscle fibrosis may be partly caused by intrinsic changes in macrophages from dystrophic muscles due to aging. Muscle macrophages isolated from 12-month-old, *mdx* muscles show increased induction of Arg-1 protein expression in response to IL-10 stimulation relative to the effect of IL-10 on macrophages isolated from 1-month-old, *mdx* muscles [15]. Age-related increases in TGF-β availability may also increase Arg-1 expression by macrophages. Stimulation of macrophages with TGF-β can increase the rate of iNOS protein degradation while increasing arginase activity [111–113].

Current treatment strategies for dystrophic pathologies.

Delivery of therapeutic molecules.

Many molecules with therapeutic potential for improving dystrophic muscle health have been identified. However, current methods for the delivery of the molecules limit their clinical use. For example, molecules that can improve muscle health can also have negative effects on non-muscle tissue. This issue is highlighted by the use of glucocorticoids as the most common treatment method for DMD patients [114,115]. Glucocorticoids are anti-inflammatory molecules that can activate macrophages toward an M2-biased phenotype and reduce sarcolemma permeabilization [115,116]. Long-term glucocorticoid use can improve muscle force production and reduce the rate at which force production is reduced as the pathology progresses [1,117]. The improvements in muscle health prolong ambulation of DMD patients and reduce the need for spinal surgery to correct scoliosis due to the deterioration of postural muscles [117,118]. However, systemic administration of glucocorticoids is required for the efficient delivery of the molecules to all muscles, which account for approximately 40% of total body mass [1,7,119]. Systemic

elevations of glucocorticoids can cause adverse effects which include obesity, osteoporosis, the development of cataracts, adrenal insufficiencies, delayed puberty, and behavioral changes [115,120,121]. Despite the benefits of glucocorticoids in improving the quality of life for DMD patients, continued observation of patient health is required to determine whether treatment should be discontinued.

Alternatively, molecules that can cause adverse, systemic effects can be used to improve dystrophic muscle health without off-target effects when the molecules are targeted to muscles. For example, leukemia inhibitory factor (LIF) is a pleiotropic molecule that can cause muscle wasting and cause death when its levels are elevated systemically [122–125]. However, targeted delivery of LIF to muscles can improve muscle repair following an acute injury and can improve the health of *mdx* muscles. The potential for LIF as pro-regenerative molecule was recognized by investigators who showed that LIF expression is increased in regenerating muscles following an acute injury, while its expression is reduced in *mdx* muscles [126–128]. Exogenous administration of LIF by the implantation of an osmotic pump at the site of acute muscle injury can increase the fiber size of regenerating fibers [129,130]. Additionally, implantation of LIF-infused alginate rods at one side of *mdx* diaphragms for six months can reduce progressive fibrosis [131]. However, in that investigation, the side opposite to the site of rod implantation did not receive the benefits of LIF treatment. Those results show that the targeted delivery of molecules provides benefits only to portions of the muscle adjacent to the site of delivery, without providing benefits to portions of the same muscle distant from the delivery site. More importantly, currently available delivery methods are not sensitive to the dynamic aspect of dystrophic pathologies, in which muscle damage occurs at different magnitudes and times in different muscles [132]. The efficacy of therapeutic molecules could be increased by the development of treatment strategies

that retain their effectiveness following fewer administrations and respond to the stage of the dystrophic pathology.

Cell transplantation strategies.

Researchers have taken advantage of the syncytial characteristics of muscle fibers to use cell transplantation strategies to improve dystrophic muscle health. Elegant studies have shown that transplantation of wild-type or genetically modified populations of stem cells, including BMCs, can engraft onto dystrophic host muscles and contribute myonuclei to regenerating fibers [133–138]. Impressively, donor myonuclei were able to restore dystrophin expression in host muscles [139–141]. However, the low survival and engraftment rates of transplanted cells have prevented these strategies from becoming viable treatment options in humans [134,142,143].

Innovation of our approach.

Using stem cells as a vector source.

In contrast to previous treatment strategies that use BMCs as a source of myonuclei, we have designed a strategy in which genetically-modified BMCs are used as a source of vectors for the delivery of therapeutic molecules. We designed a transgene in which expression of a therapeutic molecule is controlled by the CD11b promoter in *mdx* mice. CD11b is a cell surface integrin that is expressed at varying levels in leukocyte populations [144,145]. However, endogenous expression of CD11b is much higher in myeloid cells compared to lymphocytes [146]. Amongst myeloid cell populations, including myeloid precursor cells, CD11b expression is highest in mature macrophages [144,145]. Additionally, macrophages are the most numerous inflammatory cell population found in dystrophic muscles [20,147]. Because intramuscular macrophage numbers are proportional to the magnitude and location of the pathology, and HMGB1 signaling through TLR4 can increase CD11b expression, significant delivery of the

transgene will only occur at inflammatory lesions containing macrophages [35,43,148–150]. As inflammation and macrophages numbers decrease, so will transgene expression. Our approach allows for the delivery of therapeutic molecules to muscles in a manner that is responsive to the location, time, and magnitude of the dystrophic pathology. The use of BMT provides a method through which genetically-modified BMCs can be delivered to humans. Investigators have shown that BMCs of donor origin can be found in hosts more than 10 years after a single BMT procedure [139,151,152]. These findings suggest that our treatment strategy would provide benefits for more than a decade after a single therapeutic intervention.

The CD11b/LIF transgene.

We have chosen LIF as the cargo molecule to be driven by the CD11b promoter (CD11b/LIF transgene). In addition to the pro-regenerative effects of exogenous LIF on muscles *in vivo*, *in vitro* studies have demonstrated that LIF can modulate myogenesis. Stimulation of muscle cells with LIF can promote early myogenesis by increasing the proliferation of muscles cells and reducing their apoptosis [124,153,154]. LIF stimulation can also inhibit early differentiation of muscle cells, as shown by the inhibition of myotube formation by LIF [155]. However, administration of LIF to myotubes during the stage of late differentiation can increase the rate of protein synthesis, which may contribute to the increases in fiber size mediated by exogenous LIF administration to injured muscles *in vivo* [156]. LIF can also shift macrophages toward an anti-inflammatory, M2-biased phenotype. *In vitro* stimulation of macrophages with LIF reduces their expression of TNF-α while increasing their expression of CD163 relative to unstimulated macrophages [157]. Additionally, administration of a LIF receptor antagonist to acutely injured muscles resulted in an increased pro-inflammatory response and reduced area of regenerating fibers [127]. The pro-regenerative effects of LIF will allow us to test whether the CD11b/LIF transgene can improve the health of limb and respiratory muscles without off-target LIF expression.

Specific Aims.

In this investigation, we developed an *mdx* mouse line expressing the CD11b/LIF transgene (LIF/*mdx* mouse) and assessed transgene effects on muscle health along the course of the *mdx* pathology. Additionally, we performed BMT of CD11b/LIF+ BMCs to non-transgenic, *mdx* mice (LIF BMT/*mdx* mice) to address the following questions:

Aim 1: Can genetically-modified macrophages be used as vectors for the delivery of therapeutic molecules in a manner that is intrinsically regulated by the *mdx* pathology without off-target transgene expression?

Aim 2: Is BMT of genetically-modified cells a viable strategy for the long-term delivery of therapeutic molecules to dystrophic muscles after a single transplantation?

Aim 3: Can the continuous and targeted delivery of LIF to *mdx* muscles improve the dystrophic pathology?

References

1. Bushby, K., Finkel, R., Birnkrant, D. J., Case, L. E., Clemens, P. R., Cripe, L., Kaul A., Kinnett, K., McDonald, C., Pandya, S., Poysky, J., Shapiro, F., Tomezsko, J. and Tomezsko, J. (2010) Diagnosis and management of Duchenne muscular dystrophy, part 1: diagnosis, and pharmacological and psychosocial management. *Lancet Neurol.*, **9**, 77–93.

2. Mah, J. K., Korngut, L., Dykeman, J., Day, L., Pringsheim, T. and Jette, N. (2014) A systematic review and meta-analysis on the epidemiology of Duchenne and Becker muscular dystrophy. *Neuromuscul. Disord.*, **24**, 482–491.

3. Romitti, P., Puzhankara, S., Mathews, K., Zamba, G., Cunniff, C., Andrews, J., Matthews, D., James, K., Miller, L., Druschel, C., Fox, D., Pandya, S., Ciafaloni, E., Adams, M., Mandel, D., Ouyang, L., Constantin, C. and Costa, P. (2009) Prevalence of Duchenne/Becker muscular dystrophy among males aged 5-24 years - four states, 2007. *Morb. Mortal. Wkly. Rep.*, **58**, 1119–1122.

4. Romitti, P. A., Zhu, Y., Puzhankara, S., James, K. A., Nabukera S. K., Zamba, G. K. D., Ciafaloni, E., Cunniff, C., Druschel, C. M., Mathews, K. D., Matthews, D. J., Meaney, F. J., Andrews, J. G., Conway, K. M. C., Fox, D. J., Street, N., Adams, M. M. and Bolen, J. (2015) Prevalence of Duchenne and Becker muscular dystrophies in the United States. *Pediatrics*, **135**, 513–521.

5. Emery, A. E. H. (1991) Population frequencies of inherited neuromuscular diseases—A world survey. *Neuromuscul. Disord.*, **1**, 19–29.

6. Passamano, L., Taglia, A., Palladino, A., Viggiano, E., D'Ambrosio, P., Scutifero, M., Rosario, C. M., Torre, V., De Luca, F., Picillo, E., Paciello, O., Piluso, G., Nigro, G. and Politano, L. (2012) Improvement of survival in Duchenne Muscular Dystrophy: retrospective analysis of 835 patients. *Acta Myol.*, **31**, 121–125.

7. Eagle, M., Baudouin, S. V., Chandler, C., Giddings, D. R., Bullock, R. and Bushby, K. (2002) Survival in Duchenne muscular dystrophy: improvements in life expectancy since 1967 and the impact of home nocturnal ventilation. *Neuromuscul. Disord.*, **12**, 926–929.

8. Petrof, B. J., Shrager, J. B., Stedman, H. H., Kelly, A. M. and Sweeney, H. L. (1993) Dystrophin protects the sarcolemma from stresses developed during muscle contraction. *Proc. Natl. Acad. Sci.*, **90**, 3710–3714.

9. Pasternak, C., Wong, S. and Elson, E. L. (1995) Mechanical function of dystrophin in muscle cells. *J. Cell Biol.*, **128**, 355–361.

10. Menke, A. and Jockusch, H. (1995) Extent of shock-induced membrane leakage in human and mouse myotubes depends on dystrophin. *J. Cell Sci.*, **108**, 727–733.

11. McArdle, A., Edwards, R. H. T. and Jackson, M. J. (1995) How does dystrophin deficiency lead to muscle degeneration? — Evidence from the MDX mouse. *Neuromuscul. Disord.*, **5**, 445–456.

12. O'Brien, K. F. and Kunkel, L. M. (2001) Dystrophin and Muscular Dystrophy: Past, Present, and Future. *Mol. Genet. Metab.*, **74**, 75–88.

13. Wehling, M., Spencer, M. J. and Tidball, J. G. (2001) A nitric oxide synthase transgene ameliorates muscular dystrophy in mdx mice. *J. Cell Biol.*, **155**, 123–132.

14. Dort, J., Fabre, P., Molina, T. and Dumont, N. A. (2019) Macrophages are key regulators of stem cells during skeletal muscle regeneration and diseases. *Stem Cells Int.*, **2019**.

15. Wehling-Henricks, M., Jordan, M. C., Gotoh, T., Grody, W. W., Roos, K. P. and Tidball, J. G. (2010) Arginine metabolism by macrophages promotes cardiac and muscle fibrosis in mdx muscular dystrophy. *PLoS ONE*, **5**, e10763.

16. Villalta, S. A., Nguyen, H. X., Deng, B., Gotoh, T. and Tidball, J. G. (2009) Shifts in macrophage phenotypes and macrophage competition for arginine metabolism affect the severity of muscle pathology in muscular dystrophy. *Hum. Mol. Genet.*, **18**, 482–496.

17. Serrano, A. L. and Muñoz-Cánoves, P. (2010) Regulation and dysregulation of fibrosis in skeletal muscle. *Exp. Cell Res.*, **316**, 3050–3058.

18. Tidball, J. G. and Wehling-Henricks, M. (2007) Macrophages promote muscle membrane repair and muscle fibre growth and regeneration during modified muscle loading in mice in vivo. *J. Physiol.*, **578**, 327–336.

19. Kawanishi, N., Mizokami, T., Niihara, H., Yada, K. and Suzuki, K. (2015) Macrophage depletion by clodronate liposome attenuates muscle injury and inflammation following exhaustive exercise. *Biochem. Biophys. Rep.*, **5**, 146–151.

20. Tidball, J. G. (2017) Regulation of muscle growth and regeneration by the immune system. *Nat. Rev Immunol.*, **17**, 165–178.

21. Tidball, J. G. and Villalta, S. A. (2010) Regulatory interactions between muscle and the immune system during muscle regeneration. *Am. J. Physiol., Regul, Integr. Comp. Physiol.*, **298**, R1173–R1187.

22. Sincennes, M. C., Brun, C. E. and Rudnicki, M. A. (2016) Concise review: epigenetic regulation of myogenesis in health and disease. *Stem Cells Transl. Med.*, **5**, 282–290.

23. Zammit, P. S. (2017) Function of the myogenic regulatory factors Myf5, MyoD, Myogenin and MRF4 in skeletal muscle, satellite cells and regenerative myogenesis. *Semin. Cell Dev. Biol.*, **72**, 19–32.

24. Petrany, M. J. and Millay, D. P. (2019) Cell fusion: merging membranes and making muscle. *Trends Cell Biol.*, **29**, 964–973.

25. Petrany, M. J., Song, T., Sadayappan, S. and Millay, D. P. (2020) Myocyte-derived myomaker expression is required for regenerative fusion but exacerbates membrane instability in dystrophic myofibers. *JCI Insight*, **5**, e136095.

26. Lu, H., Huang, D., Ransohoff, R. M. and Zhou, L. (2011) Acute skeletal muscle injury: CCL2 expression by both monocytes and injured muscle is required for repair. *FASEB J.*, **25**, 3344–3355.

27. Brigitte, M., Schilte, C., Plonquet, A., Baba-Amer, Y., Henri, A., Charlier, C., Tajbakhsh, S., Albert, M., Gherardi, R. K. and Chretien, F. (2010) Muscle resident macrophages control the immune cell reaction in a mouse model of notexin-induced myoinjury. *Arthritis Rheum.*, **62**, 268–279.

28. Wang, Y.-T., Zaitsev, K., Lu, Q., Li, S., Schaiff, W. T., Kim. K., Droit, L., Wilen, C. B., Desai, C., Balce, D. R., Orchard, R. C., Orvedahl, A., Park, S., Kreamalmeyer, D., Handley, S. A., Pfeifer, J. D., Baldridge, M. T., Artyomov, M. N., Stallings, C. L. and Virgin, H. W. (2020) Select autophagy genes maintain quiescence of tissue-resident macrophages and increase susceptibility to Listeria monocytogenes. *Nature Microbiol.*, **5**, 272–281.

29. Zhang, X. and Mosser, D. M. (2008) Macrophage activation by endogenous danger signals. *J. Pathol.*, **214**, 161–178.

30. Akhter, N., Hasan, A., Shenouda, S., Wilson, A., Kochumon, S., Ali, S., Tuomilehto, J., Sindhu, S. and Ahmad, R. (2018) TLR4/MyD88 -mediated CCL2 production by lipopolysaccharide (endotoxin): Implications for metabolic inflammation. *J. Diabetes Metab. Disord.*, **17**, 77–84.

31. Thompson, W. L. and Van Eldik, L. J. (2009) Inflammatory cytokines stimulate the chemokines CCL2/MCP-1 and CCL7/MCP-3 through NFkB and MAPK dependent pathways in rat astrocytes [corrected]. *Brain Res.*, **1287**, 47–57.

32. Gschwandtner, M., Derler, R. and Midwood, K. S. (2019) More than just attractive: How CCL2 influences myeloid cell behavior beyond chemotaxis. *Front. Immunol.*, **10**, 2759.

33. Toumi, H., F'guyer, S. and Best, T. M. (2006) The role of neutrophils in injury and repair following muscle stretch. *J. Anat.*, **208**, 459–470.

34. Wang, J. (2018) Neutrophils in tissue injury and repair. *Cell Tissue Res.*, **371**, 531–539.

35. Zhou, X., Gao, X.-P., Fan, J., Liu, Q., Anwar, K. N., Frey, R. S. and Malik, A. B. (2005) LPS activation of Toll-like receptor 4 signals CD11b/CD18 expression in neutrophils. *Am. J. Physiol. Lung Cell Mol. Physiol.*, **288**, L655-662.

36. Tecchio, C. and Cassatella, M. A. (2016) Neutrophil-derived chemokines on the road to immunity. *Semin Immunol*, **28**, 119–128.

37. Shireman, P. K., Contreras-Shannon, V., Ochoa, O., Karia, B. P., Michalek, J. E. and McManus, L. M. (2007) MCP-1 deficiency causes altered inflammation with impaired skeletal muscle regeneration. *J. Leukoc. Biol.*, **81**, 775–785.

38. Martinez, C. O., McHale, M. J., Wells, J. T., Ochoa, O., Michalek, J. E., McManus, L. M. and Shireman, P. K. (2010) Regulation of skeletal muscle regeneration by CCR2-activating chemokines is directly related to macrophage recruitment. *Am. J. Physiol. Regul. Integr. Comp. Physiol*, **299**, R832–R842.

39. Warren, G. L., O'Farrell, L., Summan, M., Hulderman, T., Mishra, D., Luster, M. I., Kuziel, W. A. and Simeonova, P. P. (2004) Role of CC chemokines in skeletal muscle functional restoration after injury. *Am. J. Physiol. Cell Physiol.*, **286**, C1031–C1036.

40. Warren, G. L., Hulderman, T., Mishra, D., Gao, X., Millecchia, L., O'Farrell, L., Kuziel, W. A. and Simeonova, P. P. (2004) Chemokine receptor CCR2 involvement in skeletal muscle regeneration. *FASEB J.*, **19**, 413–415.

41. Mojumdar, K., Liang, F., Giordano, C., Lemaire, C., Danialou, G., Okazaki, T., Bourdon, J., Rafei, M., Galipeau, J., Devangahi, M. and Petrof, B. J. (2014) Inflammatory monocytes promote progression of Duchenne muscular dystrophy and can be therapeutically targeted via CCR2. *EMBO Mol. Med.*, **6**, 1476–1492.

42. Schiraldi, M., Raucci, A., Muñoz, L. M., Livoti, E., Celona, B., Venereau, E., Apuzzo, T., De Marchis, F., Pedotti, M., Bachi, A., Thelen, M., Varani, L., Mellado, M., Proudfoot, A.,

Bianchi, M. E. and Uguccioni, M. (2012) HMGB1 promotes recruitment of inflammatory cells to damaged tissues by forming a complex with CXCL12 and signaling via CXCR4. *J. Exp. Med.*, **209**, 551–563.

43. Yang, H., Hreggvidsdottir, H. S., Palmblad, K., Wang, H., Ochani, M., Li, J., Lu, B., Chavan, S., Rosas-Ballina, M., Al-Abed, Y., Akira, S., Bierhaus, A., Erlandsson-Haris, H., Andersson, U. and Tracey, K. J. (2010) A critical cysteine is required for HMGB1 binding to Toll-like receptor 4 and activation of macrophage cytokine release. *Proc. Natl. Acad. Sci. U. S. A.*, **107**, 11942–11947.

44. Kew, R. R., Penzo, M., Habiel, D. M. and Marcu, K. B. (2012) The IKKα-Dependent NF-κB p52/RelB noncanonical pathway is essential to sustain a CXCL12 autocrine loop in cells migrating in response to HMGB1. *J. Immunol.*, **188**, 2380–2386.

45. Andersson, U. and Tracey, K. J. (2011) HMGB1 is a therapeutic target for sterile inflammation and infection. *Annu. Rev. Immunol.*, **29**, 139–162.

46. Careccia, G., Saclier, M., Tirone, M., Ruggieri, E., Principi, E., Raffaghello, L., Torchio, S., Recchia, D., Canepari, M., Gorzanelli, A., Ferrara, M., Rovere-Querini, P., Casalgrandi, M., Preti, A., Lorenzetti, I., Bruno, C., Bottinelli, R., Brunelli, S., Previtali, S. C., Bianchi, M. E., Messina, G. and Venereau, E. (2021) Rebalancing expression of HMGB1 redox isoforms to counteract muscular dystrophy. *Sci. Transl. Med.*, **13**.

47. Giordano, C., Mojumdar, K., Liang, F., Lemaire, C., Li, T., Richardson, J., Divangahi, M., Qureshi, S. and Petrof, B. J. (2015) Toll-like receptor 4 ablation in mdx mice reveals innate immunity as a therapeutic target in Duchenne muscular dystrophy. *Hum. Mol. Genet.*, **24**, 2147–2162.

48. Tang, D., Shi, Y., Kang, R., Li, T., Xiao, W., Wang, H. and Xiao, X. (2007) Hydrogen peroxide stimulates macrophages and monocytes to actively release HMGB1. *J. Leukoc. Biol.*, **81**, 741–747.

49. Yuan, S., Liu, Z., Xu, Z., Liu, J. and Zhang, J. (2020) High mobility group box 1 (HMGB1): a pivotal regulator of hematopoietic malignancies. *J. Hematol. Oncol.*, **13**, 91.

50. Campana, L., Bosurgi, L., Bianchi, M. E., Manfredi, A. A. and Rovere–Querini, P. (2009) Requirement of HMGB1 for stromal cell–derived factor–1/CXCL12–dependent migration of macrophages and dendritic cells. *J. Leukoc. Biol.*, **86**, 609–615.

51. Li, H., Malhotra, S. and Kumar, A. (2008) Nuclear factor-kappa B signaling in skeletal muscle atrophy. *J. Mol. Med.*, **86**, 1113–1126.

52. Leclercq, I. A., Farrell, G. C., Sempoux, C., dela Peña, A. and Horsmans, Y. (2004) Curcumin inhibits NF-kappaB activation and reduces the severity of experimental steatohepatitis in mice. *J. Hepatol.*, **41**, 926–934.

53. Villalta, S. A., Deng, B., Rinaldi, C., Wehling-Henricks, M. and Tidball, J. G. (2011) IFN-γ promotes muscle damage in the mdx mouse model of Duchenne muscular dystrophy by suppressing M2 macrophage activation and inhibiting muscle cell Proliferation. *J. Immunol.*, **187**, 5419–5428.

54. Arnold, L., Henry, A., Poron, F., Baba-Amer, Y., van Rooijen, N., Plonquet, A., Gherardi, R. K. and Chazaud, B. (2007) Inflammatory monocytes recruited after skeletal muscle injury switch into antiinflammatory macrophages to support myogenesis. *J. Exp. Med.*, **204**, 1057–1069.

55. Murray, P. J., Allen, J. E., Biswas, S. K., et al. (2014) Macrophage Activation and Polarization: Nomenclature and Experimental Guidelines. *Immunity*, **41**, 14–20.

56. Mosser, D. M. and Zhang, X. (2008) Interleukin-10: new perspectives on an old cytokine. *Immunol. Rev.*, **226**, 205–218.

57. Villalta, S. A., Rinaldi, C., Deng, B., Liu, G., Fedor, B. and Tidball, J. G. (2011) Interleukin-10 reduces the pathology of mdx muscular dystrophy by deactivating M1 macrophages and modulating macrophage phenotype. *Hum. Mol. Genet.*, **20**, 790–805.

58. Crane, M. J., Daley, J. M., van Houtte, O., Brancato, S. K., Henry, W. L. and Albina, J. E. (2014) The monocyte to macrophage transition in the murine sterile wound. *PLoS One*, **9**, e86660.

59. Murray, P. J. (2006) Understanding and exploiting the endogenous interleukin-10/STAT3-mediated anti-inflammatory response. *Curr. Opin. Pharmacol.*, **6**, 379–386.

60. Lang, R., Patel, D., Morris, J. J., Rutschman, R. L. and Murray, P. J. (2002) Shaping Gene Expression in Activated and Resting Primary Macrophages by IL-10. *J. Immunol.*, **169**, 2253–2263.

61. Cheng, M., Nguyen, M.-H., Fantuzzi, G. and Koh, T. J. (2008) Endogenous interferon-γ is required for efficient skeletal muscle regeneration. *Am. J. Physiol. Cell Physiol.*, **294**, C1183–C1191.

62. Serrano, A. L., Baeza-Raja, B., Perdiguero, E., Jardí, M. and Muñoz-Cánoves, P. (2008) Interleukin-6 is an essential regulator of satellite cell-mediated skeletal muscle hypertrophy. *Cell Metab.*, **7**, 33–44.

63. Langen, R. C. J., Schols, A. M. W. J., Kelders, M. C. J. M., van der Velden, J. L. J., Wouters, E. F. M. and Janssen-Heininger, Y. M. W. (2002) Tumor necrosis factor-α inhibits myogenesis through redox-dependent and -independent pathways. *Am. J. Physiol. Regul. Integr. Comp. Physiol.*, **283**, C714–C721.

64. Langen, R. C. J., Velden, J. L. J. van der, Schols, A. M. W. J., Kelders, M. C. J. M., Wouters, E. F. M. and Janssen-Heininger, Y. M. W. (2004) Tumor necrosis factor-alpha inhibits myogenic differentiation through MyoD protein destabilization. *FASEB J.*, **18**, 227–237.

65. Langen, R. C. J., Schols, A. M. W. J., Kelders, M. C. J. M., Wouters, E. F. M. and Janssen-Heininger, Y. M. W. (2001) Inflammatory cytokines inhibit myogenic differentiation through activation of nuclear factor-κB. *FASEB J.*, **15**, 1169–1180.

66. Nguyen, H. X., Lusis, A. J. and Tidball, J. G. (2005) Null mutation of myeloperoxidase in mice prevents mechanical activation of neutrophil lysis of muscle cell membranes in vitro and in vivo. *J. Physiol.*, **565**, 403–413.

67. Kozakowska, M., Pietraszek-Gremplewicz, K., Jozkowicz, A. and Dulak, J. (2015) The role of oxidative stress in skeletal muscle injury and regeneration: focus on antioxidant enzymes. *J. Muscle. Res. Cell. Motil.*, **36**, 377–393.

68. Disatnik, M.-H., Dhawan, J., Yu, Y., Beal, M. F., Whirl, M. M., Franco, A. A. and Rando, T. A. (1998) Evidence of oxidative stress in mdx mouse muscle: Studies of the pre-necrotic state. *J. Neurol. Sci.*, **161**, 77–84.

69. Mosser, D. M. (2003) The many faces of macrophage activation. *J. Leukoc. Biol.*, **73**, 209–212.

70. Mourkioti, F. and Rosenthal, N. (2008) NF-κB signaling in skeletal muscle: prospects for intervention in muscle diseases. *J. Mol. Med. (Berl.)*, **86**, 747–759.

71. Fiorentino, D. F., Zlotnik, A., Mosmann, T. R., Howard, M. and O'Garra, A. (1991) IL-10 inhibits cytokine production by activated macrophages. *J. Immunol.*, **147**, 3815–3822.

72. Mounier, R., Théret, M., Arnold, L., et al. (2013) AMPKα1 regulates macrophage skewing at the time of resolution of inflammation during skeletal muscle regeneration. *Cell Metab.*, **18**, 251–264.

73. Strle, K., MCusker, R. H., Tran, L., King, A., Johnson, R. W., Freund, G. G., Dantzer, R. and Kelley, K. W. (2007) Novel activity of an anti-inflammatory cytokine: IL-10 prevents TNFα-induced resistance to IGF-I in myoblasts. *J. Neuroimmunol.*, **188**, 48–55.

74. Strle, K., McCusker, R. H., Johnson, R. W., Zunich, S. M., Dantzer, R. and Kelley, K. W. (2008) Prototypical anti-inflammatory cytokine IL-10 prevents loss of IGF-I-induced myogenin protein expression caused by IL-1β. *Am. J. Physiol. Endocrinol. Metab.*, **294**, E709–E718.

75. Hindi, S. M., Tajrishi, M. M. and Kumar, A. (2013) Signaling mechanisms in mammalian myoblast fusion. *Sci. Signal.*, **6**, re2.

76. Horsley, V., Jansen, K. M., Mills, S. T. and Pavlath, G. K. (2003) IL-4 acts as a myoblast recruitment factor during mammalian muscle growth. *Cell*, **113**, 483–494.

77. Possidonio, A. C. B., Senna, M. L., Portilho, D. M., Pontes Soares, C., da Silva Sampaio, L., Einicker-Lamas, M., Castelo Branco, M. T. L., Costa, M. L. and Mermelstein, C. (2011) α-Cyclodextrin enhances myoblast fusion and muscle differentiation by the release of IL-4. *Cytokine*, **55**, 280–287.

78. Tonkin, J., Temmerman, L., Sampson, R. D., Gallego-Colon, E., Barberi, L., Bilbao, D., Schneider, M. D., Musarò, A. and Rosenthal, N. (2015) Monocyte/macrophage-derived IGF-1 orchestrates murine skeletal muscle regeneration and modulates autocrine polarization. *Mol. Ther.*, **23**, 1189–1200.

79. Lu, H., Huang, D., Saederup, N., Charo, I. F., Ransohoff, R. M. and Zhou, L. (2010) Macrophages recruited via CCR2 produce insulin-like growth factor-1 to repair acute skeletal muscle injury. *FASEB J.*, **25**, 358–369.

80. Barton-Davis, E. R., Shoturma, D. I., Musaro, A., Rosenthal, N. and Sweeney, H. L. (1998) Viral mediated expression of insulin-like growth factor I blocks the aging-related loss of skeletal muscle function. *Proc. Natl. Acad. Sci. U. S. A.*, **95**, 15603–15607.

81. Birk, D. E. and Bruckner, P. (2005) Collagen suprastructures. In Brinckmann, J., Notbohm, H., Müller, P. K. (eds.), *Collagen: primer in structure, processing and assembly*, Topics in Current Chemistry, Springer, Berlin, Heidelberg, pp. 185–205.

82. Lehto, M., Sims, T. J. and Bailey, A. J. (1985) Skeletal muscle injury—molecular changes in the collagen during healing. *Res. Exp. Med.*, **185**, 95–106.

83. Gelse, K., Pöschl, E. and Aigner, T. (2003) Collagens—structure, function, and biosynthesis. *Adv. Drug Deliv. Rev.*, **55**, 1531–1546.

84. Wiedemann, H., Fujii, T., Kühn, K., Chung, E. and Miller, E. J. (1975) Comparative electron-microscope studies on type-III and type-I collagens. *Eur. J. Biochem.*, **51**, 363–368.

85. Shosha, E., Fouda, A. Y., Narayanan, S. P., Caldwell, R. W. and Caldwell, R. B. (2020) Is the arginase pathway a novel therapeutic avenue for diabetic retinopathy? *J. Clin. Med.*, **9**, 425.

86. Ploeger, D. T., Hosper, N. A., Schipper, M., Koerts, J. A., de Rond, S. and Bank, R. A. (2013) Cell plasticity in wound healing: paracrine factors of M1/ M2 polarized macrophages influence the phenotypical state of dermal fibroblasts. *Cell Commun. Signal.*, **11**, 29.

87. Song, E., Ouyang, N., Hörbelt, M., Antus, B., Wang, M. and Exton, M. S. (2000) Influence of alternatively and classically activated macrophages on fibrogenic activities of human fibroblasts. *Cell. Immunol.*, **204**, 19–28.

88. Lemos, D. R., Babaeijandaghi, F., Low, M., Chang, C.-K., Lee, S. T., Fiore, D., Zhang, R.-H., Natarajan, A., Nedospasov, S. A. and Rossi, F. M. V. (2015) Nilotinib reduces muscle fibrosis in chronic muscle injury by promoting TNF-mediated apoptosis of fibro/adipogenic progenitors. *Nat. Med.*, **21**, 786–794.

89. Uezumi, A., Ito, T., Morikawa, D., Shimizu, N., Yoneda, T., Segawa, M., Yamaguchi, M., Ogawa, R., Matev, M. M., Miyagoe-Suzuki, Y., Takeda, S., Tsujikawa, K., Tsuchida, K., Yamamoto, H. and Fukada, S. (2011) Fibrosis and adipogenesis originate from a common mesenchymal progenitor in skeletal muscle. *J. Cell Sci.*, **124**, 3654–3664.

90. Contreras, O., Rebolledo, D. L., Oyarzún, J. E., Olguín, H. C. and Brandan, E. (2016) Connective tissue cells expressing fibro/adipogenic progenitor markers increase under chronic damage: relevance in fibroblast-myofibroblast differentiation and skeletal muscle fibrosis. *Cell Tissue Res*, **364**, 647–660.

91. Heredia, J. E., Mukundan, L., Chen, F. M., Mueller, A. A., Deo, R. C., Locksley, R. M., Rando, T. A. and Chawla, A. (2013) Type 2 Innate Signals Stimulate Fibro/Adipogenic Progenitors to Facilitate Muscle Regeneration. *Cell*, **153**, 376–388.

92. Contreras, O., Cruz-Soca, M., Theret, M., Soliman, H., Tung, L. W., Groppa, E., Rossi, F. M. and Brandan, E. (2019) Cross-talk between TGF-β and PDGFRα signaling pathways regulates the fate of stromal fibro–adipogenic progenitors. *J. Cell Sci.*, **132**, jcs232157.

93. Contreras, O., Soliman, H., Theret, M., Rossi, F. M. V. and Brandan, E. (2020) TGF-β-driven downregulation of the TCF7L2/TCF4 transcription factor affects Wnt/β-Catenin signaling in PDGFRα+ fibroblasts. *J. Cell Sci.*, **133**, jcs242297.

94. Parker, E. and Hamrick, M. W. (2021) Role of fibro-adipogenic progenitor cells in muscle atrophy and musculoskeletal diseases. *Curr. Opin. Pharmacol.*, **58**, 1–7.

95. Davies, M. R., Liu, X., Lee, L., Laron, D., Ning, A. Y., Kim, H. T. and Feeley, B. T. (2016) TGF-β small molecule inhibitor SB431542 reduces rotator cuff muscle fibrosis and fatty infiltration by promoting fibro/adipogenic progenitor apoptosis. *PLoS ONE*, **11**, e0155486.

96. Willmann, R., Possekel, S., Dubach-Powell, J., Meier, T. and Ruegg, M. A. (2009) Mammalian animal models for Duchenne muscular dystrophy. *Neuromuscul. Disord.*, **19**, 241–249.

97. Bulfield, G., Siller, W. G., Wight, P. A. and Moore, K. J. (1984) X chromosome-linked muscular dystrophy (mdx) in the mouse. *Proc. Natl. Acad. Sci. U. S. A.*, **81**, 1189–1192.

98. Ishizaki, M., Suga, T., Kimura, E., Shiota, T., Kawano, R., Uchida, Y., Uchino, K., Yamashita, S., Maeda, Y. and Uchino, M. (2008) Mdx respiratory impairment following fibrosis of the diaphragm. *Neuromuscul. Disord.*, **18**, 342–348.

99. Taniguti, A. P. T., Pertille, A., Matsumura, C. Y., Neto, H. S. and Marques, M. J. (2011) Prevention of muscle fibrosis and myonecrosis in mdx mice by suramin, a TGF-β1 blocker. *Muscle Nerve*, **43**, 82–87.

100. Inkley, S. R., Oldenburg, F. C. and Vignos, P. J. (1974) Pulmonary function in Duchenne muscular dystrophy related to stage of disease. *Am. J. Med.*, **56**, 297–306.

101. Paepe, B. D., Creus, K. K., Martin, J.-J. and Bleecker, J. L. D. (2012) Upregulation of chemokines and their receptors in duchenne muscular dystrophy: potential for attenuation of myofiber necrosis. *Muscle Nerve*, **46**, 914–916.

102. Porter, J. D., Guo, W., Merriam, A. P., Khanna, S., Cheng, G., Zhou, X., Andrade, F. H., Richmonds, C. and Kaminski, H. J. (2003) Persistent over-expression of specific CC class chemokines correlates with macrophage and T-cell recruitment in mdx skeletal muscle. *Neuromuscul. Disord.*, **13**, 223–235.

103. Ogundele, M., Zhang, J. S., Goswami, M. V., Barbieri, M. L., Dang, U. J., Novak, J. S., Hoffman, E. P., Nagaraju, K. and Yetrib, H. (2021) Validation of Chemokine Biomarkers in Duchenne Muscular Dystrophy. *Life*, **11**, 827.

104. Zhao, W., Wang, X., Ransohoff, R. M. and Zhou, L. (2016) CCR2 deficiency does not provide sustained improvement of muscular dystrophy in mdx5cv mice. *FASEB J.*, **31**, 35–46.

105. Nguyen, H. X. and Tidball, J. G. (2003) Interactions between neutrophils and macrophages promote macrophage killing of rat muscle cells in vitro. *J. Physiol.*, **547**, 125–132.

106. Andreetta, F., Bernasconi, P., Baggi, F., Ferro, P., Oliva, L., Arnoldi, E., Cornelio, F., Mantegazza, R. and Confalonieri, P. (2006) Immunomodulation of TGF-beta1 in mdx mouse inhibits connective tissue proliferation in diaphragm but increases inflammatory response: Implications for antifibrotic therapy. *J. Neuroimmunol.*, **175**, 77–86.

107. Mantovani, A., Sica, A., Sozzani, S., Allavena, P., Vecchi, A. and Locati, M. (2004) The chemokine system in diverse forms of macrophage activation and polarization. *Trends Immunol.*, **25**, 677–686.

108. Biressi, S., Miyabara, E. H., Gopinath, S. D., Carlig, P. M. M. and Rando, T. A. (2014) A Wnt-TGFβ2 axis induces a fibrogenic program in muscle stem cells from dystrophic mice. *Sci. Transl. Med.*, **6**, 267ra176.

109. Hillege, M. M. G., Galli Caro, R. A., Offringa, C., de Wit, G. M. J., Jaspers, R. T. and Hoogaars, W. M. H. (2020) TGF-β regulates collagen type I expression in myoblasts and myotubes via transient ctgf and fgf-2 expression. *Cells*, **9**, 375.

110. Shi, A., Hillege, M. M. G., Wüst, R. C. I., Wu, G. and Jaspers, R. T. (2021) Synergistic short-term and long-term effects of TGF-β1 and 3 on collagen production in differentiating myoblasts. *Biochem. Biophys. Res. Commun.*, **547**, 176–182.

111. Ding, A., Nathan, C. F., Graycar, J., Derynck, R., Stuehr, D. J. and Srimal, S. (1990) Macrophage deactivating factor and transforming growth factors-beta 1 -beta 2 and -beta 3 inhibit induction of macrophage nitrogen oxide synthesis by IFN-gamma. *J. Immunol.*, **145**, 940–944.

112. Takaki, H., Minoda, Y., Koga, K., Takaesu, G., Yoshimura, A. and Kobayashi, T. (2006) TGF-beta1 suppresses IFN-gamma-induced NO production in macrophages by suppressing STAT1 activation and accelerating iNOS protein degradation. *Genes Cells*, **11**, 871–882.

113. Boutard, V., Havouis, R., Fouqueray, B., Philippe, C., Moulinoux, J. P. and Baud, L. (1995) Transforming growth factor-beta stimulates arginase activity in macrophages. Implications for the regulation of macrophage cytotoxicity. *J Immunol*, **155**, 2077–2084.

114. Manzur, A. Y., Kuntzer, T., Pike, M. and Swan, A. V. (2016) Glucocorticoid corticosteroids for Duchenne muscular dystrophy. *Cochrane Database Sys. Rev.*, **5**, CD003725.

115. Zhang, T. and Kong, X. (2021) Recent advances of glucocorticoids in the treatment of Duchenne muscular dystrophy (Review). *Exp. Ther. Med.*, **21**, 1–7.

116. Schaer, D. J., Boretti, F. S., Schoedon, G. and Schaffner, A. (2002) Induction of the CD163-dependent haemoglobin uptake by macrophages as a novel anti-inflammatory action of glucocorticoids. *Br. J. Haematol.*, **119**, 239–243.

117. Matthews, E., Brassington, R., Kuntzer, T., Jichi, F. and Manzur, A. Y. (2016) Corticosteroids for the treatment of Duchenne muscular dystrophy. *Cochrane Database Sys. Rev.*, **5**, CD003725.

118. Lebel, D. E., Corston, J. A., McAdam, L. C., Biggar, W. D. and Alman, B. A. (2013) Glucocorticoid treatment for the prevention of scoliosis in children with Duchenne muscular dystrophy: long-term follow-up. *J. Bone Jt. Surg.*, **95**, 1057–1061.

119. Janssen, I., Heymsfield, S. B., Wang, Z. and Ross, R. (2000) Skeletal muscle mass and distribution in 468 men and women aged 18–88 yr. *J. Appl. Physiol.*, **89**, 81–88.

120. Rice, M. L., Wong, B., Horn, P. S. and Yang, M. B. (2018) Cataract development associated with long-term glucocorticoid therapy in Duchenne muscular dystrophy patients. *J. APPOS*, **22**, 192–196.

121. Bowden, S. A., Connolly, A. M., Kinnett, K. and Zeitler, P. S. (2019) Management of adrenal insufficiency risk after long-term systemic glucocorticoid therapy in Duchenne muscular dystrophy: clinical practice recommendations. *J. Neuromuscul. Dis.*, **6**, 31–41.

122. Metcalf, D. and Gearing, D. P. (1989) Fatal syndrome in mice engrafted with cells producing high levels of the leukemia inhibitory factor. *Proc. Natl. Acad. Sci. U. S. A.*, **86**, 5948–5952.

123. Seto, D. N., Kandarian, S. C. and Jackman, R. W. (2015) A Key Role for Leukemia Inhibitory Factor in C26 Cancer Cachexia. *J. Biol. Chem.*, **290**, 19976–19986.

124. Metcalf, D., Nicola, N. A. and Gearing, D. P. (1990) Effects of injected leukemia inhibitory factor on hematopoietic and other tissues in mice. *Blood*, **76**, 50–56.

125. Metcalf, D. (2003) The unsolved enigmas of leukemia inhibitory factor. *Stem Cells*, **21**, 5–14.

126. Kurek, J. B., Nouri, S., Kannourakis, G., Murphy, M. and Austin, L. (1996) Leukemia inhibitory factor and interleukin-6 are produced by diseased and regenerating skeletal muscle. *Muscle Nerve*, **19**, 1291–1301.

127. Hunt, L. C., Upadhyay, A., Jazayeri, J. A., Tudor, E. M. and White, J. D. (2013) An anti-inflammatory role for leukemia inhibitory factor receptor signaling in regenerating skeletal muscle. *Histochem. Cell. Biol.*, **139**, 13–34.

128. Hunt, L. C., Anthea Coles, C., Gorman, C. M., Tudor, E. M., Smythe, G. M. and White, J. D. (2011) Alterations in the expression of leukemia inhibitory factor following exercise: comparisons between wild-type and mdx muscles. *PLoS Curr.*, **3**, RRN1277.

129. Barnard, W., Bower, J., Brown, M. A., Murphy, M. and Austin, L. (1994) Leukemia inhibitory factor (LIF) infusion stimulates skeletal muscle regeneration after injury: Injured muscle expresses lif mRNA. *J. Neurol. Sci.*, **123**, 108–113.

130. Kurek, J. B., Bower, J. J., Romanella, M., Koentgen, F., Murphy, M. and Austin, L. (1997) The role of leukemia inhibitory factor in skeletal muscle regeneration. *Muscle Nerve*, **20**, 815–822.

131. Austin, L., Bower, J. J., Bennett, T. M., Lynch, G. S., Kapsa, R., White, J. D., Barnard, W., Gregorevic, P. and Byrne, E. (2000) Leukemia inhibitory factor ameliorates muscle fiber degeneration in the mdx mouse. *Muscle Nerve*, **23**, 1700–1705.

132. Dadgar, S., Wang, Z., Johnston, H., Kesari, A, Nagaraju, K., Chen, Y.-W., Hill, D. A., Partridge, T. A., Giri, M., Freishtat, R. J., Nazarian, J., Xuan, J., Wang, Y. and Hoffman, E. P. (2014) Asynchronous remodeling is a driver of failed regeneration in Duchenne muscular dystrophy. *J. Cell Biol.*, **207**, 139–158.

133. Mueller, A. L. and Bloch, R. J. (2020) Skeletal muscle cell transplantation: models and methods. *J. Muscle Res. Cell Motil.*, **41**, 297–311.

134. Ito, N., Shimizu, N., Tanaka, H. and Takeda, S. Enhancement of satellite cell transplantation efficiency by leukemia inhibitory factor. *J. Neuromuscul. Dis.*, **3**, 201–207.

135. Judson, R. N. and Rossi, F. M. V. (2020) Towards stem cell therapies for skeletal muscle repair. *npj Regen. Med.*, **5**, 1–6.

136. Lapidos, K. A., Chen, Y. E., Earley, J. U., Heydemann, A., Huber, J. M., Chien, M., Ma, A. and McNally, E. M. (2004) Transplanted hematopoietic stem cells demonstrate impaired sarcoglycan expression after engraftment into cardiac and skeletal muscle. *J. Clin. Invest.*, **114**, 1577–1585.

137. Gang, E. J., Darabi, R., Bosnakovski, D., Xu, Z., Kamm, K. E., Kyba, M. and Perlingeiro, R. C. R. (2009) Engraftment of mesenchymal stem cells into dystrophin-deficient mice is not accompanied by functional recovery. *Exp. Cell Res.*, **315**, 2624–2636.

138. Nitahara-Kasahara, Y., Hayashita-Kinoh, H., Ohshima-Hosoyama, S., Okada, H., Wada-Maeda, M., Nakamura, A., Okada, T. and Takeda, S. (2012) Long-term engraftment of multipotent mesenchymal stromal cells that differentiate to form myogenic cells in dogs with Duchenne muscular dystrophy. *Mol. Ther.*, **20**, 168–177.

139. Gussoni, E., Bennett, R. R., Muskiewicz, K. R., Meyerrose., T., Nolta, J. A., Gilgoff, I., Stein, J., Chan, Y.-M., Lidov, H. G., Bonnermann, C. G., von Moers, A., Morris, G. E., den Dunnen, J. T., Chamberlain, J. S., Kunkel, L. M. and Weinberg, K. (2002) Long-term persistence of donor nuclei in a Duchenne muscular dystrophy patient receiving bone marrow transplantation. *J. Clin. Invest.*, **110**, 807–814.

140. Gussoni, E., Soneoka, Y., Strickland, C. D., Buzney, E. A., Khan, M. K., Flint, A. F., Kunkel, L. M. and Mulligan, R. C. (1999) Dystrophin expression in the mdx mouse restored by stem cell transplantation. *Nature*, **401**, 390–394.

141. Meng, J., Counsell, J. R., Reza, M., Laval, S. H., Danos, O., Thrasher, A., Lochmüller, H., Muntoni, F. and Morgan, J. E. (2016) Autologous skeletal muscle derived cells expressing a novel functional dystrophin provide a potential therapy for Duchenne Muscular Dystrophy. *Sci. Rep.*, **6**, 19750.

142. Bencze, M., Negroni, E., Vallese, D., Yacoub-Yousseff, H., Chaouch, S., Wolff, A., Aamiri, A., Di Santo, J. P., Chazaud, B., Butler-Browne, G., Savino, W., Mouly, V. and Rieder, I. (2012) Proinflammatory macrophages enhance the regenerative capacity of human myoblasts by modifying their kinetics of proliferation and differentiation. *Mol. Ther.*, **20**, 2168–2179.

143. Negroni, E., Vallese, D., Vilquin, J.-T., Butler-Browne, G., Mouly, V. and Trollet, C. (2011) Current advances in cell therapy strategies for muscular dystrophies. *Expert Opin. Biol. Ther.*, **11**, 157–176.

144. Rosmarin, A. G., Weil, S. C., Rosner, G. L., Griffin, J. D., Arnaout, M. A. and Tenen, D. G. (1989) Differential expression of CD11b/CD18 (Mo1) and myeloperoxidase genes during myeloid differentiation. *Blood*, **73**, 131–136.

145. Sanchez-Madrid, F., Nagy, J. A., Robbins, E., Simon, P. and Springer, T. A. (1983) A human leukocyte differentiation antigen family with distinct alpha-subunits and a common beta-subunit: the lymphocyte function-associated antigen (LFA-1), the C3bi complement receptor (OKM1/Mac-1), and the p150,95 molecule. *J. Exp. Med.*, **158**, 1785–1803.

146. Miller, L. J., Schwarting, R. and Springer, T. A. (1986) Regulated expression of the Mac-1, LFA-1, p150,95 glycoprotein family during leukocyte differentiation. *J. Immunol.*, **137**, 2891–2900.

147. Spencer, M. J., Montecino-Rodriguez, E., Dorshkind, K. and Tidball, J. G. (2001) Helper (CD4+) and cytotoxic (CD8+) T cells promote the pathology of Dystrophin-deficient muscle. *Clin. Immunol.*, **98**, 235–243.

148. Yu, M., Wang, H., Ding, A., Golenbock, D. T., Latz, E., Czura, C. J., Fenton, M. J., Tracey, K. J. and Yang, H. (2006) HMGB1 signals through toll-like receptor (TLR) 4 and TLR2. *Shock*, **26**, 174–179.

149. Kim, S., Kim, S. Y., Pribis, J. P., Lotze, M., Mollen, K. P., Shapiro, R., Loughran, P., Scott, M. J. and Billiar, T. R. (2013) Signaling of high mobility group box 1 (HMGB1) through toll-like receptor 4 in macrophages requires CD14. *Mol. Med.*, **19**, 88–98.

150. Hietaranta, A., Mustonen, H., Puolakkainen, P., Haapiainen, R. and Kemppainen, E. (2004) Proinflammatory effects of pancreatic elastase are mediated through TLR4 and NF-κB. *Biochem. Biophys. Res. Commun.*, **323**, 192–196.

151. Reuter, U., Roesler, J., Thiede, C., Schulz, A., Classen, C. F., Oelschlägel, U., Debatin, K.-M. and Friedrich, W. (2002) Correction of complete interferon-γ receptor 1 deficiency by bone marrow transplantation. *Blood*, **100**, 4234–4235.

152. Ball, L. M., Lankester, A. C., Giordano, P. C., van Weel, M. H., Harteveld, C. L., Bredius, R. G. M., Smiers, F. J., Egeler, R. M. and Vossen, J. M. J. J. (2003) Paediatric allogeneic bone marrow transplantation for homozygous β -thalassaemia, the Dutch experience. *Bone Marrow Transplant.*, **31**, 1081–1087.

153. Austin, L. and Burgess, A. W. (1991) Stimulation of myoblast proliferation in culture by leukaemia inhibitory factor and other cytokines. *J. Neurol. Sci.*, **101**, 193–197.

154. Broholm, C., Laye, M. J., Brandt, C., Vadalasetty, R., Pilegaard, H., Pedersen, B. K. and Scheele, C. (2011) LIF is a contraction-induced myokine stimulating human myocyte proliferation. *J. Appl. Physiol.*, **111**, 251–259.

155. Hunt, L. C., Upadhyay, A., Jazayeri, J. A., Tudor, E. M. and White, J. D. (2011) Caspase-3, myogenic transcription factors and cell cycle inhibitors are regulated by leukemia inhibitory factor to mediate inhibition of myogenic differentiation. *Skelet. Muscle*, **1**, 17.

156. Gao, S., Durstine, J. L., Koh, H.-J., Carver, W. E., Frizzell, N. and Carson, J. A. (2017) Acute myotube protein synthesis regulation by IL-6-related cytokines. *Am. J. Physiol. Cell Physiol.*, **313**, C487–C500.

157. Duluc, D., Delneste, Y., Tan, F., Moles, M.-P., Grimaud, L., Lenoir, J., Preisser, L., Anegon, I., Catala, L., Ifrah, N., Descamps, P., Gamelin, E., Gascan, H., Hebbar, M. and Jeannin, P. (2007) Tumor-associated leukemia inhibitory factor and IL-6 skew monocyte differentiation into tumor-associated macrophage-like cells. *Blood*, **110**, 4319–4330.

Chapter 2:

Targeting a therapeutic LIF transgene to muscle via the immune system ameliorates muscular dystrophy

nature COMMUNICATIONS

ARTICLE

https://doi.org/10.1038/s41467-019-10614-1 OPEN

Targeting a therapeutic LIF transgene to muscle via the immune system ameliorates muscular dystrophy

Steven S. Welc[1,5], Ivan Flores[2,5], Michelle Wehling-Henricks[1], Julian Ramos[1], Ying Wang[2], Carmen Bertoni[3] & James G. Tidball[1,2,4]

Many potentially therapeutic molecules have been identified for treating Duchenne muscular dystrophy. However, targeting those molecules only to sites of active pathology is an obstacle to their clinical use. Because dystrophic muscles become extensively inflamed, we tested whether expressing a therapeutic transgene in leukocyte progenitors that invade muscle would provide selective, timely delivery to diseased muscle. We designed a transgene in which leukemia inhibitory factor (LIF) is under control of a leukocyte-specific promoter and transplanted transgenic cells into dystrophic mice. Transplantation diminishes pathology, reduces Th2 cytokines in muscle and biases macrophages away from a CD163+/CD206+ phenotype that promotes fibrosis. Transgenic cells also abrogate TGFβ signaling, reduce fibro/adipogenic progenitor cells and reduce fibrogenesis of muscle cells. These findings indicate that leukocytes expressing a LIF transgene reduce fibrosis by suppressing type 2 immunity and highlight a novel application by which immune cells can be genetically modified as potential therapeutics to treat muscle disease.

[1] Department of Integrative Biology and Physiology, University of California, Los Angeles, CA 90095-1606, USA. [2] Molecular, Cellular & Integrative Physiology Program, University of California, Los Angeles, CA 90095-1606, USA. [3] Department of Neurology, David Geffen School of Medicine at UCLA, University of California, Los Angeles, CA 90095, USA. [4] Department of Pathology and Laboratory Medicine, David Geffen School of Medicine at UCLA, University of California, Los Angeles, CA 90095, USA. [5] These authors contributed equally: Steven S. Welc, Ivan Flores. Correspondence and requests for materials should be addressed to J.G.T. (email: jtidball@physci.ucla.edu)

Over recent years, investigators have identified numerous, potentially-therapeutic molecules for the treatment of Duchenne muscular dystrophy (DMD), a lethal and incurable muscle-wasting disease. For example, systemic delivery of therapeutic agents that can inhibit fibrosis (e.g., block TGFβ function[1–3]), inhibit muscle wasting (e.g., myostatin blocking molecules[4]), and increase numbers of muscle stem cells called satellite cells (e.g., Klotho[5]) all reduce pathology in the *mdx* mouse model of DMD. However, systemic delivery of any of these molecules presents risks of unintended off-target effects which provide an obstacle to their clinical application for the treatment of DMD. In addition, the occurrence of muscle pathology is not synchronized in DMD patients. The unpredictable timing and severity of disease vary between muscles in a single individual at any given time, and also vary between locations in a single muscle[6]. Even if a therapeutic agent were specifically targeted to dystrophic muscle, achieving delivery only when pathology is active presents an additional challenge.

Nature has provided a naturally-occurring system for targeted delivery of potentially-therapeutic molecules to dystrophic muscle at stages of the disease when pathology is active. Coinciding with the unpredictable ebb and flow of pathology in muscular dystrophy, inflammatory cells invade in numbers that coincide with the magnitude of muscle pathology. Although the immune cell infiltrate in dystrophin-deficient muscle is complex[7–12], macrophages comprise the vast majority and they can reach concentrations that exceed 10^7 cells per pound of muscle at the peak of *mdx* pathology[7]. They are also rich sources of regulatory molecules that can amplify muscle damage but also promote muscle repair and regeneration in muscular dystrophy[7,13,14]. Thus, the introduction of therapeutic transgenes that are expressed at elevated levels in activated macrophages or other immune cells could provide a strategy for intrinsically-regulated targeting of therapeutic molecules specifically to dystrophic muscles at the time of active pathology and at levels that were commensurate with the extent of pathology.

In this investigation, we test whether transplantation of bone marrow cells (BMCs) into which we have introduced a leukemia inhibitory factor (LIF) transgene controlled by the human CD11b promoter reduces the pathology of *mdx* dystrophy. Although *mdx* pathology is less severe than DMD pathology, they share the pathological features of muscle inflammation and progressive fibrosis that persist over the entire lifespan and impair muscle function, reduce health and increase mortality. The CD11b promoter was chosen to drive the therapeutic transgene because CD11b is expressed at low or undetectable levels in myeloid precursors, but at increasingly elevated levels during myeloid cell differentiation and activation[15–17]. LIF was selected as a therapeutic molecule to test this system because it is expressed by macrophages and can influence muscle growth, fibrosis, and inflammation during disease or following injury[18–21]. Our findings show that this intervention significantly modifies intramuscular macrophage phenotype and reduces inflammation and fibrosis of dystrophic muscle, thereby reducing pathology. Perhaps more valuable, the findings indicate that inflammatory cells can be exploited as natural vectors to deliver therapeutic transgenes for the treatment of chronic diseases in which there is a significant inflammatory component.

Results

A CD11b regulated LIF transgene suppresses M2-biased markers. We generated mice with a LIF transgene under control of the CD11b promoter (CD11b/LIF transgenic mice). Quantitative PCR (QPCR) analysis of *Cd11b* mRNA levels confirmed that *Cd11b* expression increased as BMCs differentiate into bone marrow-derived macrophages (BMDMs) (Fig. 1a). Freshly-isolated bone marrow mononuclear cells (BMMCs) from transgenic *mice* had a ~2.8-fold higher *Lif* expression compared to wild-type (WT). After 9 days of culture, *Lif* expression was ~10-fold higher in transgenic BMDMs than WT (Fig. 1b). Thus, LIF transgene expression increased with increased CD11b promoter activation as monocytes differentiate into mature macrophages. Upon becoming fully-differentiated macrophages, the CD11b/LIF transgene had an autocrine effect on macrophage phenotype, increasing expression of *Cd68* by ~31% and reducing *Cd163* and arginase-1 (*Arg1*) by 47% and 42%, respectively (Fig. 1c). CD68 is present at high levels in macrophages that are biased to a pro-inflammatory phenotype (M1-biased). Arginase and CD163 are present in macrophages that are biased toward a pro-fibrotic and reparative phenotype (M2-biased)[22].

CD11b/LIF transgene reduces mdx muscle inflammation and fibrosis. We assayed whether the expression of the CD11b/LIF transgene affected *mdx* pathology, focusing on influences on muscle inflammation and fibrosis. We confirmed elevated expression of *Lif* in the tibialis anterior (TA) and diaphragm muscles of transgenic mice (CD11b/LIF *mdx* mice) (Fig. 2a) and observed that cells in inflammatory lesions in CD11b/LIF *mdx* mice showed higher levels of LIF protein than non-transgenic mice (Fig. 2b–d). However, sera from transgenic mice showed no elevation in LIF protein assayed by ELISA (mean ± sem: WT/*mdx* 19.25 ± 1.85 and LIF/*mdx* 26.19 ± 4.86 pg/ml , $n = 3$ per data set, $P = 0.25$; two-tailed *t*-test). We also found no significant differences in the concentrations of cytokines previously implicated in influencing the pathology of muscular dystrophy (IFNγ, TNF, IL-4, and IL-10) in the serum of transgenic mice, compared to non-transgenic mice (Supplementary Fig. 1).

We assessed effects of the transgene on *mdx* pathology over the course of the disease, sampling at the acute onset of pathology (1-month-old), the period of successful regeneration (3-months-old), and the late, progressive stage of pathology (12-months-old) in TA muscles. Diaphragm muscles show a progressive pathology following disease onset. The CD11b/LIF transgene reduced numbers of macrophages expressing the pan-macrophage marker F4/80 at the stages of pathology characterized by extensive, muscle inflammation (1-month-old in TA; 12-months-old in diaphragm) (Fig. 2e–g). The transgene also reduced numbers of CD163+ macrophages at the acute onset of pathology in both TA and diaphragm (Fig. 2h–j) but did not affect numbers of CD68+ macrophages in either muscle at any stage of the disease that we tested (Supplementary Fig. 2).

We tested whether the CD11b/LIF transgene reduced collagen accumulation in *mdx* muscles, which would be consistent with a reduction in numbers or activity of CD163 macrophages that promote fibrosis of dystrophic muscle[23]. Both the TA and diaphragm showed significant reductions in collagen type 1 at the acute onset of pathology, and the transgene completely abrogated collagen type 1 accumulation in the TA muscle, at least until 12-months-old (Fig. 2k–m). The CD11b/LIF transgene also reduced accumulation of collagen type 1 in diaphragms (Fig. 2n–p) and reduced accumulation of collagen types 3 and 5 in diaphragms at late stages of pathology and reduced collagen type 5 in 3-month-old TA muscles (Supplementary Fig. 3).

Because the CD11b/LIF transgene prevented collagen type 1 accumulation in TA muscles and collagen type 1 is primarily responsible for increased muscle stiffness caused by fibrosis, we assayed for changes in the passive mechanical properties of TA muscles in CD11b/LIF transgenic *mdx* mice. We subjected TA muscles to cyclic, dynamic loading using 20% strains at a 0.6/s strain rate, which is within the physiological range. Lissajous

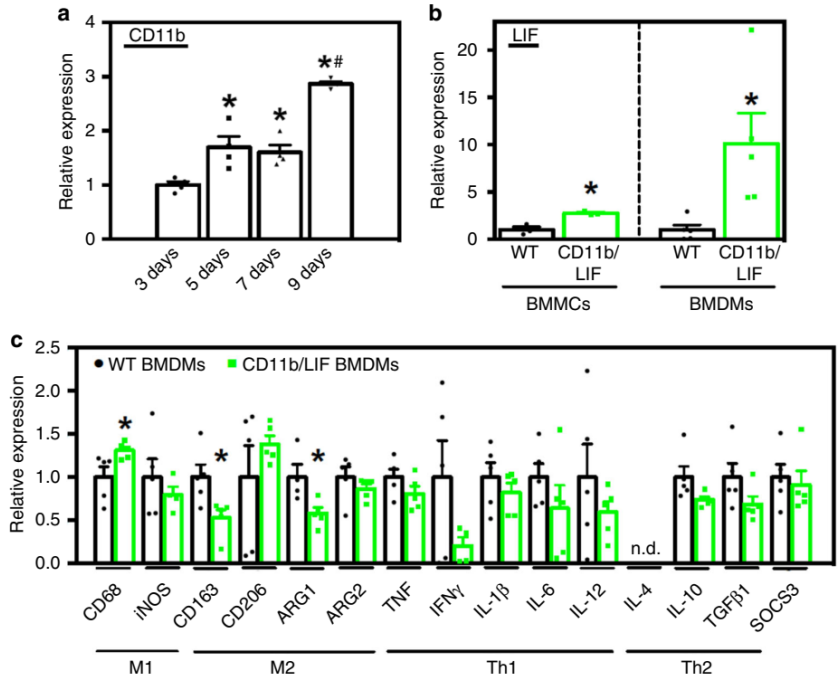

Fig. 1 Differentiation of BMCs into macrophages increases CD11b/LIF transgene expression, causing suppression of M2-biased macrophage markers. **a** QPCR data showing differences in the level of *Cd11b* expression in C57BL6 BMCs stimulated with MCSF and differentiated to macrophages for 3–9 days. Values are normalized to 3-day cultures, $n = 4$ for each data set; * indicates significantly different from 3-day data set and # indicates significantly different from 5- and 7-day data sets at $P < 0.05$. *P*-values based on ANOVA with Tukey's multiple comparison test. For all histograms in the figure, the bars indicate mean ± sem. **b** QPCR data showing increased *Lif* expression in freshly-isolated BMMCs and BMDMs cultured for 9 days from CD11b/LIF transgenic mice compared to transgene negative littermate controls (WT). Data are presented as mean ± sem. BMCs were isolated from three independent donors, $n = 3$ per data set. * Indicates significantly different from WT at $P < 0.05$. *P*-values based on two-tailed *t*-test. *F*-test BMDMs day 9 ($P = 0.0038$). **c** QPCR analysis shows that CD11b/LIF BMDMs have increased the expression of *Cd68* and reduced the expression of *Cd163* and *Arg1*. Data are presented as mean ± sem, $n = 5$ for each data set, $n = 4$ for WT BMDMs *Inos*, and CD11b/LIF BMDMs *Arg1* data sets ($P < 0.05$). n.d. indicates that no expression was detected. Data presented for BMDMs (**b**, **c**) were isolated from a single donor animal of each genotype and cultured as $n = 5$ technical replicates. Significant findings were verified with biological replicates of experiments from independent donors. * Indicates significantly different from WT BMDMs at $P < 0.05$. *P*-values based on two-tailed *t*-test. *F*-test *Cd206* ($P = 0.0258$) and *Il10* ($P = 0.0311$). Source data are provided as a Source Data file

figures obtained by measuring force–strain relationships showed that muscle stiffness (indicated by the slope of the tangent to the loading phase of each cycle) was significantly less in CD11b/LIF transgenic *mdx* mice (Fig. 2q, r). In addition, the transgenic *mdx* muscles showed less energy dissipation during each cycle of loading (proportional to the area inside each hysteresis loop during a cycle of loading/unloading) (Fig. 2q, s), indicating higher mechanical efficiency in the CD11b/LIF transgenic muscles.

CD11b/LIF transgene does not impair muscle growth. Although previous investigations showed that M2-biased macrophages promote muscle fibrosis, they also promote regeneration[23,24]. We tested this possibility by assaying for effects of the transgene on TA muscle fiber cross-sectional area as an index of regeneration and found no difference in TA fiber size between transgenic and non-transgenic *mdx* mice at any age sampled (Supplementary Fig. 4A). We also assayed for the proportion of muscle fibers that expressed developmental myosin heavy chain (dMHC), which is upregulated in regenerating fibers. We observed a higher proportion of dMHC+ fibers in TAs of CD11b/LIF transgenic *mdx* mice at 3-months-old and a trend for more dMHC+ fibers at 1-month and 12-months-old, compared to non-transgenic *mdx* mice (Supplementary Fig. 4B). Similarly, the proportions of dMHC+ fibers in 3-months-old and 12-months-old diaphragms were increased by the transgene (Supplementary Fig. 4C). Collectively, these observations indicate that the CD11b/LIF transgene does not impair muscle growth or regeneration, despite the reduction of CD163+ cells.

Transplanted CD11b/LIF cells reduce inflammation. Our analyses of CD11b/LIF transgenic *mdx* mice showed that the transgene reduces muscle inflammation and fibrosis, thereby validating the transgene as a therapeutic molecule for muscular dystrophy. However, our primary goal in the investigation was to determine whether transplanted bone marrow derived cells (BMDCs) could serve as vehicles to deliver therapeutic molecules to dystrophic muscle through a clinically-relevant approach; in particular, we questioned whether transplantation of genetically-modified BMCs into dystrophic animals provides a strategy for targeted delivery of therapeutic cargo to diseased muscle. We assayed treatment effects in 6-months-old *mdx* mice at 4 months post-bone marrow transplantation (BMT) for scientific and technical reasons. First, we anticipated that a likely, beneficial outcome of leukocyte delivery of a LIF transgene to muscle would be reductions in fibrosis. Our previous work[5] showed that 6-months-old *mdx* muscles show significantly elevated

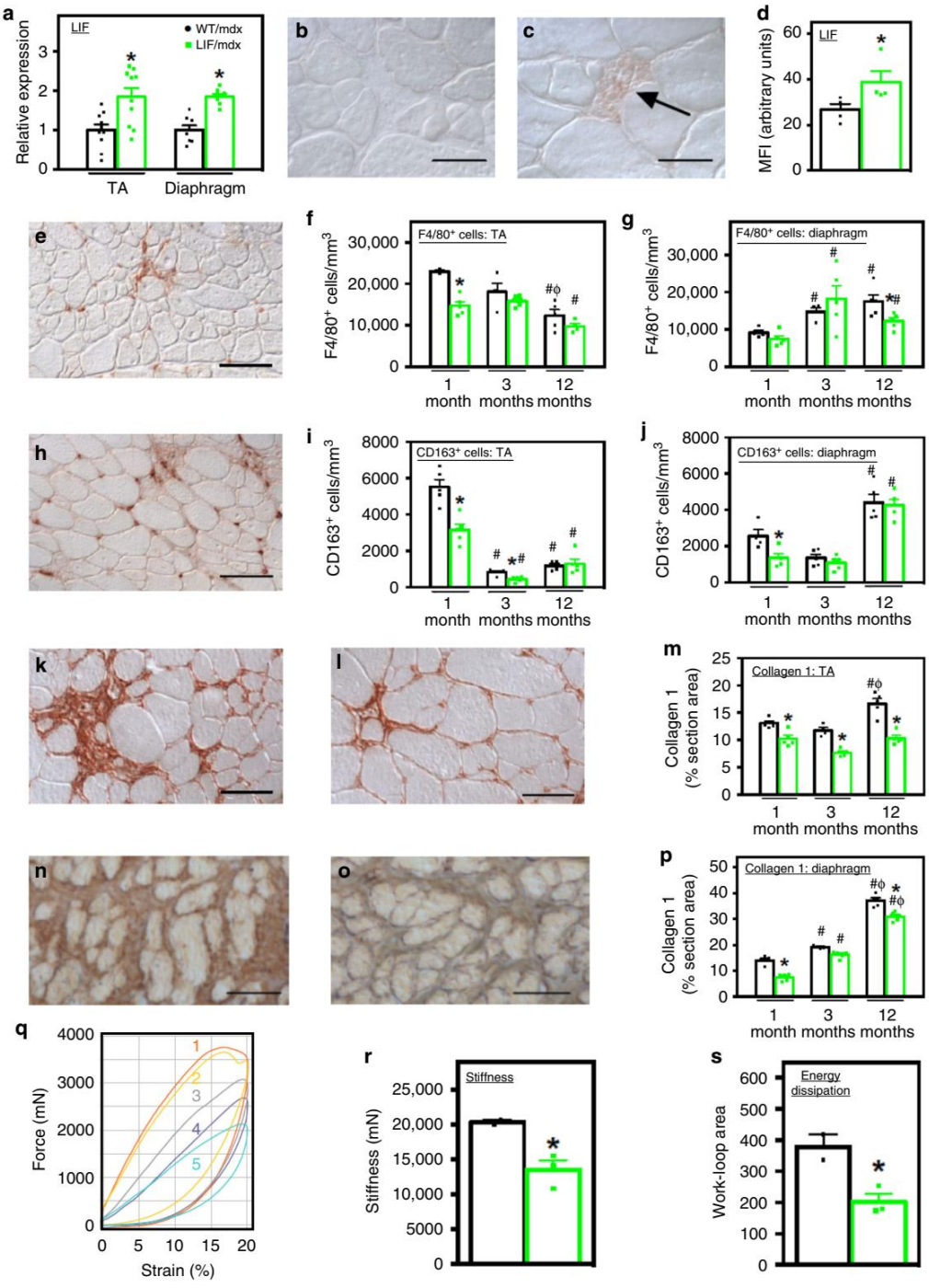

accumulation of type I and type III collagen. We also showed that at 6-months-old, *mdx* limb muscles contain elevated numbers of M2-biased macrophages that contribute to muscle fibrosis[5]. The technical rationale for sampling at 6 months is that engraftment of transplanted cells takes time and our preliminary experiments showed that high levels of engraftment could be achieved by 4 months post-BMT.

At the time of tissue collection from transplant recipients, circulating leukocytes were 86.6% donor-derived (sem = 1.14; $n = 25$). QPCR of muscles showed that CD11b/LIF recipients

Fig. 2 CD11b/LIF transgene expression modulates inflammation and reduces fibrosis. **a** QPCR data showing *Lif* expression in muscles of CD11b/LIF transgenic *mdx* mice (LIF/*mdx*) and non-transgenic littermates (WT/*mdx*), normalized to WT/*mdx*. TA muscles: $n = 10$. Diaphragm muscles: $n = 8$ or 7 for WT/*mdx* and LIF/*mdx* data sets, respectively. * Indicates significant difference versus WT/*mdx* ($P < 0.05$). For all histograms, bars indicate mean ± sem. **b**, **c** Cross-sections of WT/*mdx* (**b**) and LIF/*mdx* (**c**) TA muscles labeled with anti-LIF. Bars = 50 μm. **d** Mean fluorescence intensity (MFI) of inflammatory lesions in sections immunolabeled for LIF. * Indicates significant difference from WT/*mdx* ($n = 4$; $P < 0.05$). **e**–**j** Cross-sections of muscles from WT/*mdx* and LIF/*mdx* mice were immunolabeled with antibodies to F4/80 (**e**) and CD163 (**h**). Numbers of F4/80+ (**f**, **g**) and CD163+ (**i**, **j**) cells were normalized to muscle volume. Labeling of F4/80+ (**e**) and CD163+ (**h**) cells in TA muscle from 1-month-old WT/*mdx* muscle. Bars = 100 μm. $N = 5$ for each group, except $n = 4$ for F4/80 WT/*mdx* 1- and 12-month TA, LIF/*mdx* 12-month TA, WT/*mdx* 1- and 3-month diaphragm, and CD163 WT/*mdx* 12-month TA data sets. **k**–**p** Cross-sections of TA (**k**, **i**) and diaphragm (**n**, **o**) muscles from 12-month-old WT/*mdx* (**k**, **n**) and LIF/*mdx* (**l**, **o**) mice were immunolabeled with anti-collagen type 1. Bars = 50 μm. The volume fraction of muscle occupied by collagen type 1 (**m**, **p**). $N = 5$ for each group, except $n = 4$ for 3-month TA. * Indicates significant difference versus age-matched WT/*mdx* mice ($P < 0.05$). # and Φ indicate significant difference versus 1- and 3-months-old, genotype-matched mice, respectively ($P < 0.05$). *P*-values based on two-tailed *t*-test. **q**–**s** The passive mechanical properties of TA muscles of WT/*mdx* (curves 1 and 2) and LIF/*mdx* (curves 3–5) mice were measured in-situ. Lissajous curves (**q**) show passive stiffness (**r**) and energy dissipation (**s**) of TAs. $N = 2$ and 3 for WT/*mdx* and LIF/*mdx* groups, respectively. * Indicates significant difference versus WT/*mdx* mice. *P*-values based on two-tailed *t*-test. Source data are provided as a Source Data file

(LIF BMT/*mdx* mice) had reduced expression of the M2-biased markers *Cd163*, CD206 (*Mrc1*), and arginase-2 (*Arg2*) expression by 51%, 49%, and 43%, respectively (Fig. 3a). This effect resembles the autocrine effect of CD11b/LIF on macrophages in vitro (Fig. 1c). Additionally, the transgene affected the expression of Th2 cytokines associated with M2-biased macrophage activation, IL-4 (*Il4*) and IL-10 (*Il10*), which were reduced by ~79% and ~84%, respectively (Fig. 3a). Reduced cytokine expression was accompanied by a ~2.8-fold increase in the expression of suppressor of cytokine signaling 3 (*Socs3*) in CD11b/LIF BMT recipients (Fig. 3a). *Socs3* expression is activated by LIF[25] and its elevation in muscles of CD11b/LIF BMT recipients verifies an increase in LIF signaling in muscle.

We tested the effect of CD11b/LIF BMT on macrophage numbers and phenotype because changes in macrophages have profound effects on dystrophic muscle pathology[7,13,14,26]. We performed immunohistochemistry using anti-F4/80, to identify total macrophage populations, or anti-CD68 (M1-biased macrophages), anti-CD163 (M2-biased), or anti-CD206 (M2-biased). *Mdx* mice that received CD11b/LIF BMCs had 37% fewer F4/80+ cells compared to mice receiving WT BMCs (Fig. 3b). Quantitation of CD68+, CD163+ and CD206+ macrophages showed no difference in CD68+ cells (mean ± sem: WT BMT/*mdx* 17,525 ± 1502 and LIF BMT/*mdx* 16,377 ± 1440 cells/mm^3, $n = 5$ per data set, $P = 0.60$; two-tailed *t*-test), a 32% reduction of CD163+ cells (Fig. 3e) and 46% fewer CD206+ cells (Fig. 3h) in the dystrophic muscle. However, numbers of CD4+ T-cells and neutrophils in *mdx* muscles were unaffected by transplantation of CD11b/LIF BMCs (Fig. 3k, l), indicating a selective reduction of M2-biased macrophages caused by transgenic BMDCs.

LIF reduces *Ccl2* expression in muscle and macrophages. The large reductions of M2-biased macrophages in dystrophic muscle of mice transplanted with CD11b/LIF BMCs (Fig. 3) suggest that LIF inhibits their recruitment. Because abrogation of CCR2 signaling reduces macrophage accumulation in dystrophic muscle[27], we tested whether CCR2 signaling was affected by LIF. QPCR assays showed reduced expression of Ccr2 and its ligands *Ccl2*, *Ccl8* and *Ccl12* in muscles of CD11b/LIF BMT recipients, and a strong trend for lower levels of *Ccl7* expression ($P = 0.06$) (Fig. 4a).

We next tested the possibility that LIF acts directly on macrophages to inhibit CCR2 signaling in vitro. Unexpectedly, brief periods of macrophage stimulation with LIF had no effect on *Ccr2* expression and extended periods significantly increased *Ccr2* expression (Fig. 4b). We assayed whether the CD11b/LIF transgene affected the numbers of intramuscular macrophages that expressed detectible CCR2 but found that the proportion of CD68+ or CD206+ macrophages that expressed CCR2 was not influenced by the transgene (Fig. 4c, d). This indicates that reductions in macrophage-derived CCR2 in muscles reflect reductions in macrophage numbers, rather than ablating the expression of CCR2 in macrophages in CD11b/LIF BMT recipients. However, stimulation of BMDMs with LIF reduced *Ccl2* expression and CCL2 protein secretion (Fig. 4e, f), indicating that LIF acts directly on macrophages to negatively regulate *Ccl2*. In addition, F4/80+ macrophages were prominent sources of CCL2 in *mdx* muscle (Fig. 4g), and transplantation of CD11b/LIF BMCs reduced the proportion of F4/80+ macrophages that expressed detectible CCL2 by 15% (Fig. 4h).

Transplanted CD11b/LIF cells reduce muscle fibrosis. Fibrosis of dystrophin-deficient muscle is largely driven by arginine metabolism by arginase expressed by M2-biased macrophages[23]. Arginine hydrolysis by arginase produces metabolites that are utilized to generate substrate molecules necessary for connective tissue production[28]. Because we observed reductions in M2-biased macrophages in muscles of *mdx* mice that were recipients of CD11b/LIF BMT and lower levels of expression of *Arg2*, we assayed whether fibrosis was affected. Transplantation of CD11b/LIF BMCs reduced collagen types 1, 3, and 5 in *mdx* muscle by ~41%, 22%, and 25%, respectively, compared to WT BMT recipients (Fig. 5a–i). However, the anti-fibrotic effect of CD11b/LIF BMT cannot be solely attributed to reductions of arginine metabolism by M2-biased macrophages. QPCR data showed that mRNA levels of collagen types 1 alpha 1 (*Col1a1*), 3 alpha 1 (*Col3a1*), and 5 alpha 3 (*Col5a3*) were reduced by ~57%, 51%, and 30%, respectively, in CD11b/LIF BMC recipients (Fig. 5j), indicating treatment effects on fibrogenic cells, in addition to effects on macrophages that provide substrate for fibrogenesis.

M2-biased macrophages can act directly on fibrogenic cells through TGFβ which activates fibro/adipogenic progenitor cells (FAPs) into fibroblasts and stimulates fibroblasts to produce collagen[29–32]. TGFβ can also activate Wnt-signaling, which increases myogenic-to-fibrogenic conversion of muscle stem cells, further contributing to dystrophic muscle fibrosis[33]. We tested whether the CD11b/LIF BMT affected key transcripts of the Wnt and TGFβ pro-fibrotic pathways. Although there was no effect on the expression of *Tgfb1* or *Axin2*, a Wnt-target gene (Fig. 5k), the expression of downstream TGFβ target genes connective tissue growth factor (*Ctgf*), fibronectin (*Fn1*), and snail family zinc finger 1 (*Snai1*)[34–37] were reduced by ~33%, 43%, and 33%, respectively (Fig. 5k).

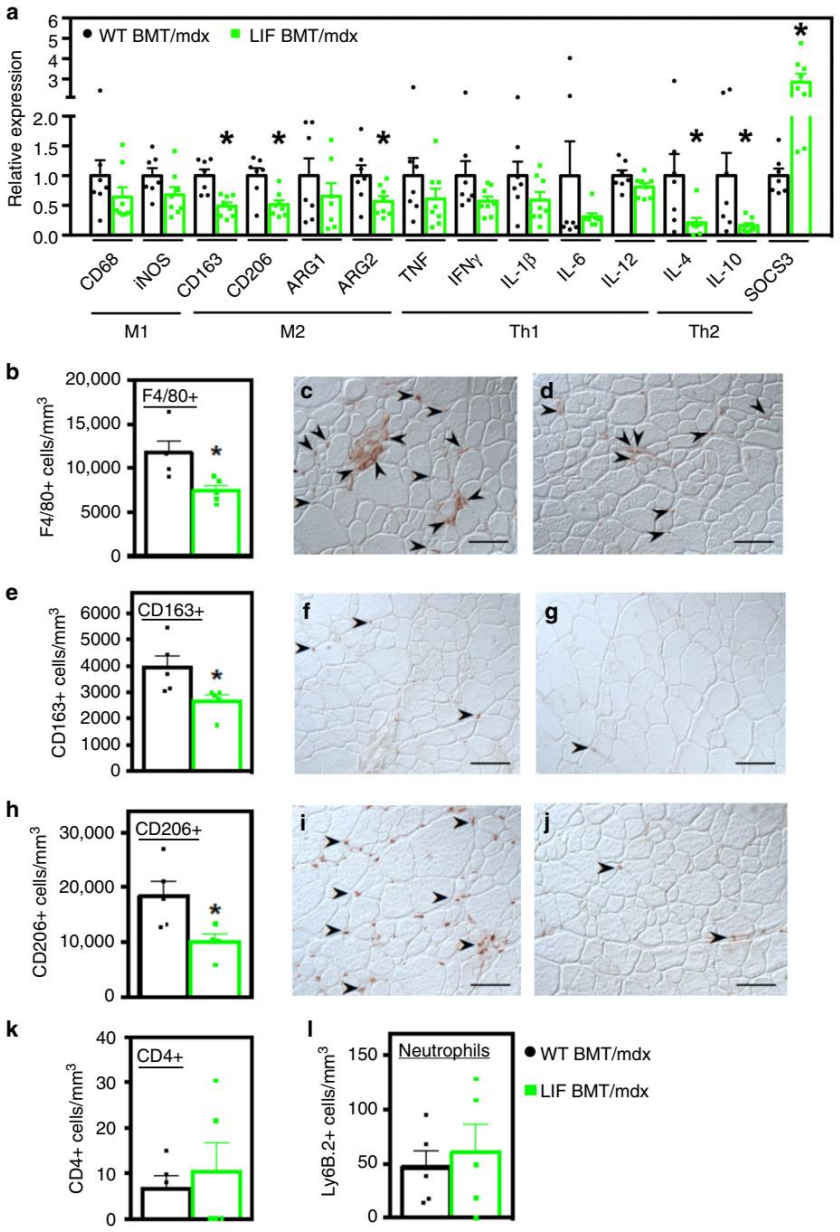

Fig. 3 Transplantation of CD11b/LIF transgenic BMCs into *mdx* mice reduces inflammation in dystrophic muscle. **a** QPCR analysis shows that the transplantation of CD11b/LIF transgenic BMCs into *mdx* recipients (LIF BMT/*mdx*) reduced expression of transcripts associated with M2-biased macrophages (*Cd163*, *Cd206*, and *Arg2*), Th2 cytokines (*Il4* and *Il10*), and increased expression of the negative regulator of cytokine signaling (*Socs3*) compared to WT BMT *mdx* recipients (WT BMT/*mdx*) 4 months post-transplantation. $N = 7$ or 8 for WT BMT/*mdx* and LIF BMT/*mdx* data sets, respectively, except $n = 7$ for LIF BMT/*mdx Arg1* data set. * Indicates significantly different from WT BMT/*mdx* recipients at $P < 0.05$. *F*-test *Ifng* ($P = 0.0145$), *Il6* ($P < 0.0001$), *Il4* ($P = 0.0015$), *Il10* ($P < 0.0001$), and *Socs3* ($P = 0.0061$). For all histograms in the figure, the bars indicate mean ± sem. **b**–**j** Cross-sections of TA muscles from WT BMT/*mdx* (**c**, **f**, **i**) or LIF BMT/*mdx* (**d**, **g**, **j**) mice were immunolabeled with antibodies to F4/80 (**c**, **d**), CD163 (**f**, **g**), and CD206 (**i**, **j**). Bars = 50 µm. The numbers of F4/80+ (**b**), CD163+ (**e**), and CD206+ (**h**) cells normalized to muscle volume were reduced in LIF BMT/*mdx* recipients. Similarly, cross-sections were immunolabeled with antibodies to CD4 and Ly-6B.2 (neutrophils) to test for changes in the concentrations of other populations of immune cells. There was no change in the concentrations of CD4+ (**k**) and Ly-6B.2+ (**l**) cells. $N = 5$ for each data set, except $n = 4$ for CD206 LIF BMT/*mdx* data set. * Indicates significantly different from WT BMT/*mdx* recipients at $P < 0.05$. All *P*-values based on two-tailed *t*-test. Source data are provided as a Source Data file

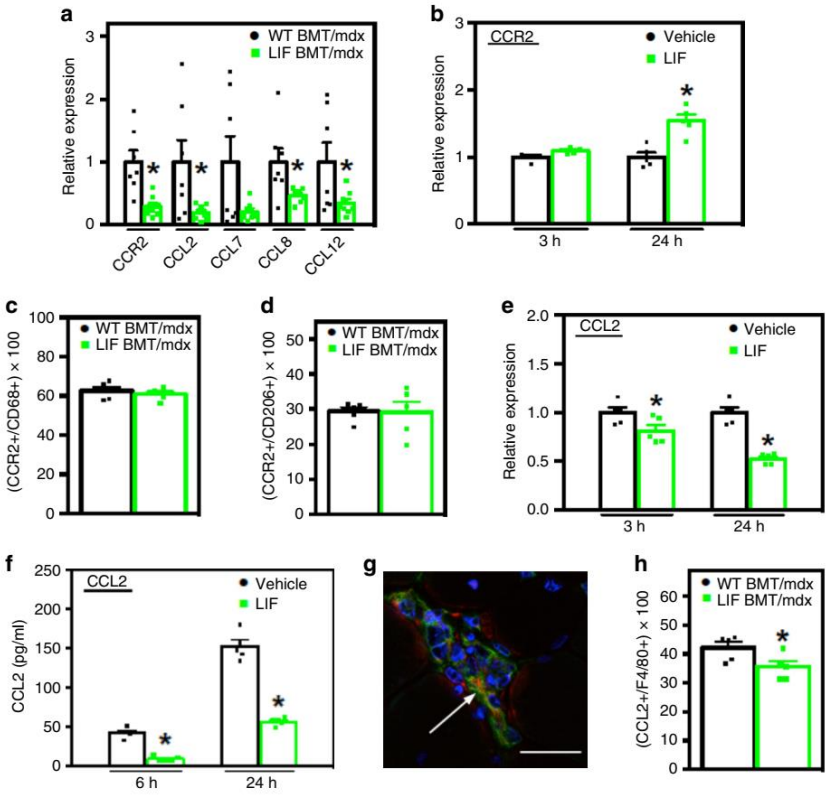

Fig. 4 Transplantation of CD11b/LIF transgenic BMCs disrupts *Ccl2* expression in dystrophic muscles by inhibiting macrophage expression of CCL2. **a** QPCR analysis shows that TA muscles from LIF BMT/*mdx* recipients have reduced expression of *Ccr2* and its ligands *Ccl2*, *Ccl7* ($P = 0.06$), *Ccl8*, and *Ccl12*. $N = 7$ or 8 for WT BMT/*mdx* and LIF BMT/*mdx* data sets, respectively, except $n = 7$ for LIF BMT/*mdx* *Ccl8* data set. * Indicates significantly different from WT BMT/*mdx* recipients at $P < 0.05$. *F*-test *Ccr2* ($P = 0.0087$), *Ccl2* ($P < 0.0001$), *Ccl7* ($P = 0.0001$), *Ccl8* ($P = 0.001$), and *Ccl12* ($P = 0.001$). For all histograms in the figure, the bars indicate mean ± sem. **b** QPCR analysis for *Ccr2* gene expression of BMDMs treated with recombinant LIF (10 ng/ml) for 3- and 24-h. **c**, **d** Muscle sections co-labeled with antibodies to CD68 (**c**) or CD206 (**d**) and CCR2 show no change in the proportions of cells co-expressing CCR2 between transplant recipient groups. $N = 5$ for each data set. **e** QPCR analysis shows reduced *Ccl2* gene expression in BMDMs stimulated with LIF as described in (**b**). **f** ELISA of conditioned media showed less CCL2 secreted into the media of BMDMs stimulated with LIF for 6- and 24-h compared to control cultures. For cell culture experiments, $N = 5$ technical replicates for each data set, cells for each time point were isolated from independent donors. Significant findings were verified with biological replicates of experiments from independent donors. *P*-values based on two-tailed *t*-test. *F*-test CCL2 protein 24 h ($P = 0.0337$). **g**, **h** Cross-sections of TA muscles from WT BMT/*mdx* or LIF BMT/*mdx* mice were immunolabeled with antibodies to F4/80 (green) and CCL2 (red) show that F4/80+ cells express CCL2 (**g**). Nuclei are stained blue with DAPI. Bar = 10 µm. **h** The proportion of F4/80+ cells co-expressing CCL2 was reduced in LIF BMT/*mdx* recipients. $N = 5$ for each data set, * indicates significantly different from WT BMT/*mdx* recipients at $P < 0.05$. *P*-values based on two-tailed *t*-test. Source data are provided as a Source Data file

LIF reduces macrophage TGFβ1 expression. Although we observed no effect of CD11b/LIF BMT on *Tgfb1* mRNA in whole muscle homogenates, we assayed more specifically for effects on TGFβ expression in intramuscular macrophages by assaying the proportion of macrophages that expressed TGFβ. We found that there were 17.7% fewer intramuscular macrophages that expressed detectible TGFβ in CD11b/LIF recipients, compared to WT recipients (Fig. 6a). Interestingly, the greatest reduction of TGFβ expressing macrophages was seen in inflammatory lesions of CD11b/LIF recipients (Fig. 6c) compared to WT recipients (Fig. 6b).

We tested whether reduced TGFβ1 expression in CD11b/LIF BMT recipients reflected direct actions of LIF on macrophages to inhibit TGFβ1 expression. When we treated BMDMs with LIF for 24 h, *Tgfb1* gene expression was reduced by 47% and secreted TGFβ protein expression by 29% (Fig. 6d, e), showing that LIF is a negative regulator of TGFβ1 expression in macrophages. However, *Tgfb1* gene expression was not reduced after 3 h of LIF stimulation, suggesting that LIF-mediated inhibition of *Tgfb1* could be a secondary effect.

LIF reduces fibrogenesis and *Ctgf* mRNA in muscle cells. TGFβ signaling promotes the fibrogenic conversion of myogenic cells in dystrophic muscle, thereby contributing to fibrosis[33]. Because transplantation of CD11b/LIF BMCs into *mdx* mice reduces fibrosis, we tested whether LIF reduces the proportion of myogenic cells acquiring a fibrogenic phenotype. Muscle sections that were double-labeled with anti-Pax7, a marker of satellite cells, and anti-HSP47, a collagen-specific molecular chaperone[38,39] showed that the proportion of Pax7+ cells that expressed HSP47 was reduced by 27.8% in CD11b/LIF recipients (Fig. 7a–c); this

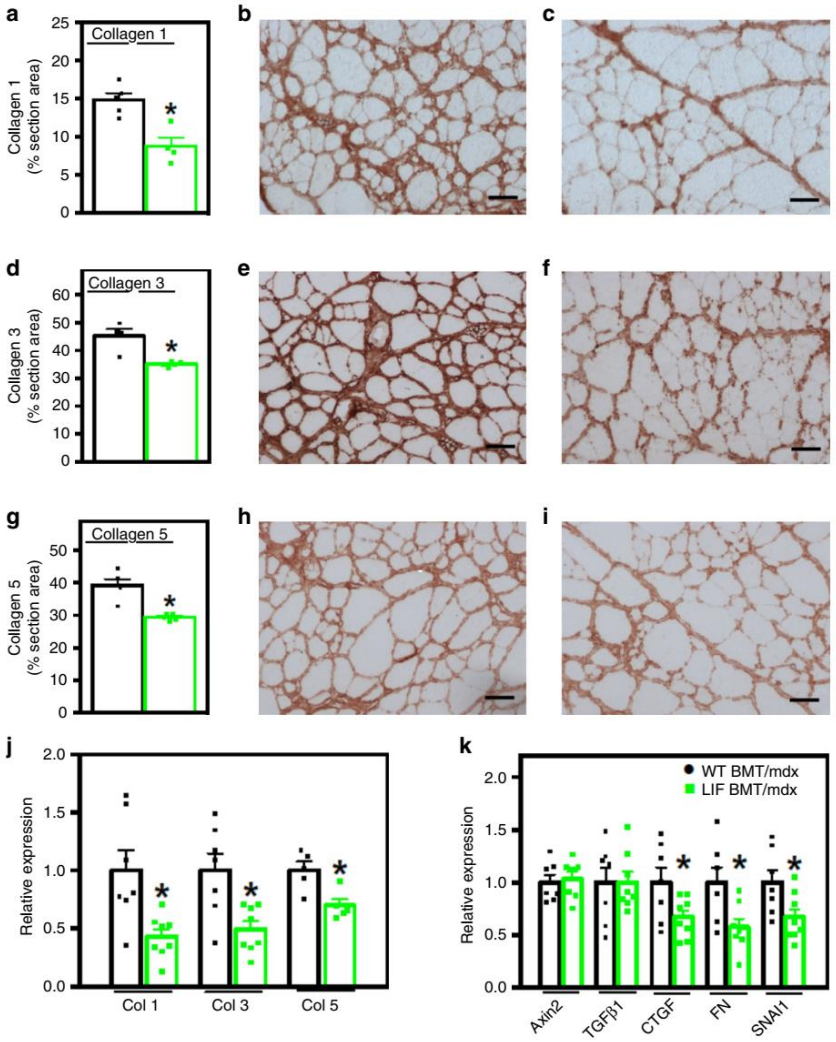

Fig. 5 Transplantation of CD11b/LIF transgenic BMCs into *mdx* mice reduces muscle fibrosis. **a**–**i** TA muscles from WT BMT/*mdx* (**b**, **e**, **h**) and LIF BMT/*mdx* transplant recipients (**c**, **f**, **i**) were immunolabeled for collagen types 1 (**a**–**c**), 3 (**d**–**f**), and 5 (**g**–**i**). Bars = 50 µm. The volume fraction of muscle occupied by collagen types 1 (**a**), 3 (**d**), and 5 (**g**) was reduced in LIF BMT/*mdx* recipients. $N = 5$ for WT BMT/*mdx* and LIF BMT/*mdx* data sets, except $n = 4$ WT BMT/*mdx* collagen type 3 and LIF BMT/*mdx* collagen type 1. * Indicates significantly different from WT BMT/*mdx* recipients at $P < 0.05$. *F*-test collagen type 3 ($P = 0.0055$) and type 5 ($P = 0.0155$). For all histograms in the figure, the bars indicate mean ± sem. **j** QPCR data presented as mean ± sem shows that LIF BMT/*mdx* recipients also had reduced expression of transcripts encoding *Col1a1*, *Col3a1*, and *Col5a3*. $N = 7$ or 8 for WT BMT/*mdx* and LIF BMT/*mdx* data sets, respectively, except $n = 5$ for *Col5a3* data sets. **k** QPCR analysis of transcripts associated with the pro-fibrotic Wnt- (*Axin2*) and TGFβ1-signaling (*Tgfb1*, *Ctgf*, *Fn1*, and *Snai1*) pathways showed reduced expression of *Ctgf*, *Fn1*, and *Snai1* in LIF BMT/*mdx* recipients. $N = 7$ or 8 for WT BMT/*mdx* and LIF BMT/*mdx* data sets, respectively, except $n = 7$ for LIF BMT/*mdx Axin2* group. * Indicates significantly different from WT BMT/*mdx* recipients at $P < 0.05$. *P*-values based on two-tailed *t*-test. *F*-test *Col1a1* ($P = 0.0250$). Source data are provided as a Source Data file

indicates that satellite cells had a less fibrogenic phenotype in CD11b/LIF recipients. Expression of *Serpinh1*, the gene that encodes HSP47, was also reduced 24% in the whole muscle lysate of CD11b/LIF recipients (mean ± sem: WT BMT/*mdx* 1 ± 0.08 and LIF BMT/*mdx* 0.76 ± 0.06, $n = 7$ and 8 per data set, respectively, $P = 0.03$; two-tailed *t*-test). We also assayed whether transplantation of CD11b/LIF BMCs affected the proportion of satellite cells that expressed ERTR7 in vivo. ERTR7 was chosen in addition to HSP47 because satellite cells in injured and aging muscle that display elevated levels of ERTR7 expression have shifted away from a myogenic phenotype, toward a fibrogenic phenotype[40,41]. Our data show that the transgene reduced the proportion of satellite cells that expressed ERTR7 in *mdx* muscle in vivo, similar to the reduction of satellite cells expressing HSP47 (Fig. 7c, d).

We also tested whether the CD11b/LIF transgene affected the phenotype of myogenic progenitor cells (MPCs) in later stages of *mdx* pathology by assaying for changes in the expression of fibrogenic genes in MPCs that were freshly-isolated from muscles of 14-months-old mice. MPCs (CD11b-CD31-CD45-Sca1-α7

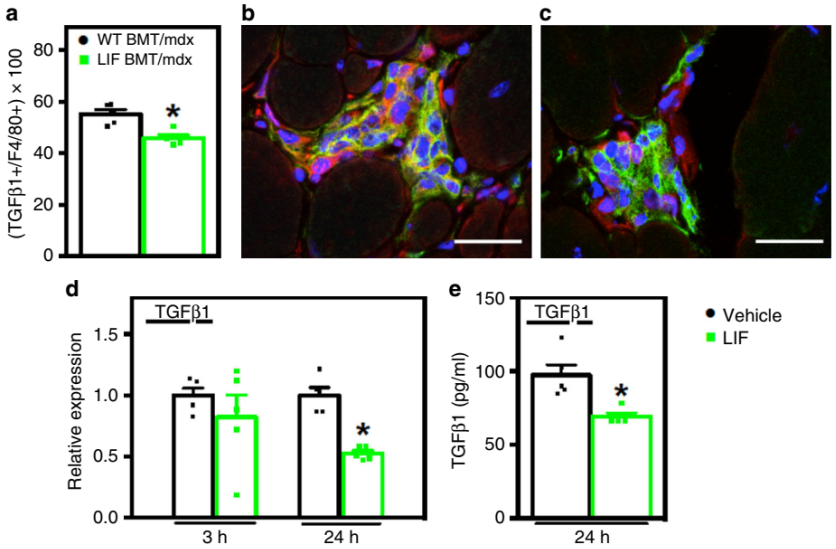

Fig. 6 LIF inhibits macrophage TGFβ1 expression. **a**–**c** Muscle sections were co-labeled with antibodies to pro-fibrotic TGFβ (red) and the pan macrophage marker F4/80 (green) to test for changes in macrophage expression of TGFβ. Nuclei appear blue (DAPI). Bars = 25 µm. **a** The proportion of F4/80+ cells co-expressing TGFβ was reduced in LIF BMT/*mdx* recipients. The greatest reduction in the number of F4/80+ cells positive for TGFβ (orange) was in inflammatory lesions of LIF BMT/*mdx* (**c**) compared to WT BMT/*mdx* recipients (**b**). $N = 5$ for each data set, * indicates significantly different from WT BMT/*mdx* recipients at $P < 0.05$. For all histograms in the figure, the bars indicate mean ± sem. **d** QPCR analysis of BMDMs treated with recombinant LIF (10 ng/ml) for 3- or 24-h shows that *Tgfb1* expression is inhibited by LIF after 24 h of stimulation. **e** The concentration of secreted TGFβ was also reduced in BMDMs stimulated with LIF for 24 h, analyzed by ELISA. $N = 5$ technical replicates for each data set. Significant findings were verified with biological replicates of experiments from independent donors. * Indicates significantly different from control at $P < 0.05$. Source data are provided as a Source Data file

integrin+ cells) from CD11b/LIF transgenic *mdx* mice showed lower expression levels of *Fn1* and *Col3a1* compared to non-transgenic mice (Supplementary Fig. 5). In addition, we observed strong trends for the reduction in expression of *Serpinh1* (HSP47) and *Col1a1* in freshly-isolated MPCs.

We also examined the effects of LIF on TGFβ1-induced muscle cell fibrogenesis in vitro. We assayed myoblasts and myotubes treated with TGFβ1 and/or LIF for changes in expression of fibrogenic genes downregulated in CD11b/LIF BMT recipients (*Ctgf*, *Fn1*, and *Col1a1*; Fig. 5j, k). Co-stimulation with TGFβ1 and LIF inhibited *Ctgf* expression, compared to cells treated with TGFβ1 only (Fig. 7e, h). LIF also reduced basal *Ctgf* expression after 24 h of stimulation in myotubes. *Fn1* expression was stable in myoblasts treated with TGFβ1, LIF, or TGFβ1 + LIF for 3 h (Fig. 7f). After 24 h, TGFβ1-induced *Fn1* expression, but co-stimulation with LIF had no effect (Fig. 7i). TGFβ1 stimulation for 3 h induced the expression of *Col1a1* in myotubes, and LIF attenuated TGFβ1-induced expression *of Col1a1* in myotubes (Fig. 7g). LIF stimulation for 24 h reduced basal *Col1a1* expression in myoblasts, but not TGFβ1-induced expression of *Col1a1* (Fig. 7j).

LIF reduces the prevalence of FAPs in dystrophic muscle. Because FAP-derived fibroblasts are important sources of connective tissue proteins, we assayed whether CD11b/LIF BMT affected FAP numbers in vivo or whether LIF affected the expression of fibrogenic proteins by FAP-derived fibroblasts in vitro. QPCR analysis showed that CD11b/LIF BMT recipients had a 47% reduction in *Pdgfra* expression (Fig. 8a) which could reflect fewer FAPs. Recipients of CD11b/LIF BMT had fewer cells that expressed PDGFRα and were double-negative for CD31 and CD45, which are FAPs[42] (Fig. 8b, c), although the proportion of PDGFRα+ cells that expressed HSP47 was unaffected by the transgene (Fig. 8d). The findings indicate that reductions in numbers of FAPs in the muscles of *mdx* mice receiving CD11b/LIF BMT may contribute to reduced muscle fibrosis.

We then tested whether LIF influenced the fibrogenic activity of FAP-derived fibroblasts in vitro. We sorted FAPs (CD11b/31/45- PDGFRα+) from WT muscles (Fig. 8e) and subcultured them prior to stimulation with TGFβ1, LIF, or TGFβ1 + LIF[41,42]. We used fibroblasts derived from FAPs rather than freshly-isolated FAPs because fibroblasts differentiated from FAPs are the primary source of connective tissue proteins in muscle[32]. We tested if LIF affected *Pdgfra* expression in fibroblasts in vitro because enhanced PDGFRα signaling can cause pathological fibrosis[43]. However, LIF did not affect *Pdgfra* expression in fibroblasts (mean ± sem: control cells 1 ± 0.04 and LIF-treated cells 1.13 ± 0.23, $n = 4$ per data set, $P = 0.61$; two-tailed *t*-test). Treatments for 3 h with TGFβ1-induced *Ctgf* expression in fibroblasts, but LIF had no effect on basal or TGFβ1-induced *Ctgf* (Fig. 8f). The magnitude of TGFβ1-induced *Ctgf* expression in fibroblasts (1.9-fold) was less than in myoblasts (~11.6-fold) and myotubes (~7.1-fold) (Fig. 7e). TGFβ1, LIF or TGFβ1 + LIF had no effect on *Fn1* or *Col1a1* expression in fibroblasts (Fig. 8g, h). We then tested whether prolonged stimulation of fibroblasts with TGFβ1, LIF, or TGFβ1 + LIF affected *Ctgf*, *Fn1*, or *Col1a1* expression. Similar to effects of brief stimulations, *Ctgf* expression was induced ~2.0-fold by TGFβ1 but the induction was not affected by LIF. There was also no effect of prolonged stimulation with TGFβ1 on the expression of *Fn1* or *Col1a1* (Fig. 8i–k).

Transplanted CD11b/LIF cells do not affect muscle growth. Because changes in macrophage phenotype and numbers influence muscle regeneration and myogenesis[14,44–47], we assayed

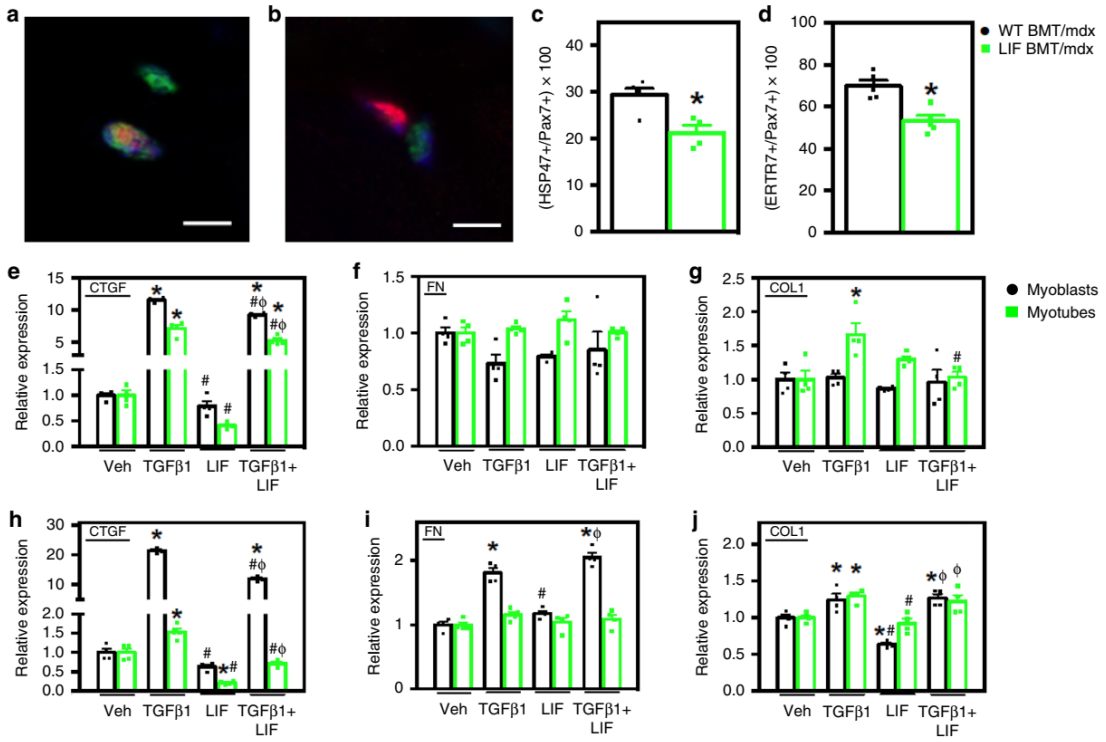

Fig. 7 LIF inhibits fibrogenesis and TGFβ1-induced *Ctgf* expression in muscle cells. **a** TA muscle sections were co-labeled with antibodies to Pax7 (red) and HSP47 (green) in WT BMT/*mdx* (**a**) and LIF BMT/*mdx* (**b**) recipients. Nuclei appear blue (DAPI). Bars = 5 µm. **c** Fewer Pax7+ cells co-expressed HSP47 in LIF BMT/*mdx* recipients (green symbols) compared to WT BMT/*mdx* recipients (black symbols). **d** Muscle sections were also co-labeled with antibodies to Pax7 and fibrogenic marker Ertr7 to confirm that fewer Pax7+ cell acquired a fibrogenic phenotype in LIF BMT/*mdx* recipients. $N = 5$ for each data set, except $n = 4$ for WT BMT/*mdx* Pax7/HSP47 data set, * indicates significantly different from WT BMT/*mdx* at $P < 0.05$. *P*-values based on two-tailed *t*-test. For all histograms in the figure, the bars indicate mean ± sem. **e**–**j** Myoblasts (black symbols) and myotubes (green symbols) were stimulated with LIF (10 ng/ml) and TGFβ1 (10 ng/ml) for 3- (**e**–**g**) or 24-h (**h**–**j**). **e**, **h** LIF inhibited TGFβ1-induced *Ctgf* mRNA in myoblasts and myotubes after 3- and 24-h of stimulation. LIF inhibited basal *Ctgf* expression in myotubes at 24 h (**h**). **f**, **i** LIF did not affect *Fn1* expression in myoblasts or myotubes after 3- or 24-h. Additionally, LIF attenuated TGFβ1-induced *Col1a1* expression in myotubes, but not myoblasts after 3 h of stimulation (**g**). Myoblasts stimulated with LIF for 24 h had reduced *Col1a1* expression (**j**). $N = 4$ technical replicates per group. Significant findings were verified with biological replicates of experiments from independent cultures. * Indicates significantly different from control, # indicates significantly different from TGFβ1-stimulated, and Φ indicates significantly different from LIF-stimulated at $P < 0.05$. *P*-values based on ANOVA with Tukey's multiple comparison test. Source data are provided as a Source Data file

whether regeneration was affected in CD11b/LIF BMT recipients. There were no significant differences in TA muscle weight, total muscle fiber number, proportions of regenerating fibers or muscle fiber size (Fig. 9a–d). No muscle fibers expressed dMHC in WT BMT/*mdx* or LIF BMT/*mdx* mice. Additionally, QPCR assays showed no effect of CD11b/LIF on expression of the myogenic transcription factors: *Pax7*, *Myod1*, *Myog*, or *Mrf4* (Fig. 9e). These data indicate that the CD11b/LIF transgene did not influence processes through which immune cells modulate regeneration in *mdx* muscle.

Discussion

The results of our investigation demonstrate that transplantation of genetically-modified BMCs provides a means to deliver therapeutic molecules to dystrophic muscle. In addition, by regulating the expression of the therapeutic transgene with the CD11b promoter, LIF delivery can be modified by the stages of maturation and activation of innate immune cells that differentiate from BMCs. This strategy provides a mechanism for the endogenous regulation of transgene expression by the transplant recipients that is responsive to the magnitude and site of inflammation. This system also permits long-term delivery of therapeutic molecules following a single therapeutic intervention. Although tissues were analyzed 4 months following transplantation in the present investigation, at that time circulating leukocyte populations were nearly 87% donor-derived. However, in humans experiencing BMT, stable mixed chimerism can persist for years in peripheral blood cell populations[48,49], showing that long-term benefits to humans can result from a single transplantation.

The potential therapeutic advantage of targeting therapeutic molecules to diseased tissue by using transgenes under control of the CD11b promoter is emphasized by comparing our findings with the outcomes of previous strategies to deliver LIF via hematopoietic cell transplantation. Transplantation of a hematopoietic cell line in which the cells were multiply-transduced with a retroviral construct containing cDNA encoding LIF produced high systemic levels of LIF and killed the recipient mice[50,51]. In those experiments the retrovirus-transplant recipients reached serum LIF concentrations at 1400 units/ml, although serum LIF was undetectable in mice transplanted with cells that did not contain the LIF expressing retrovirus[50,51]. This

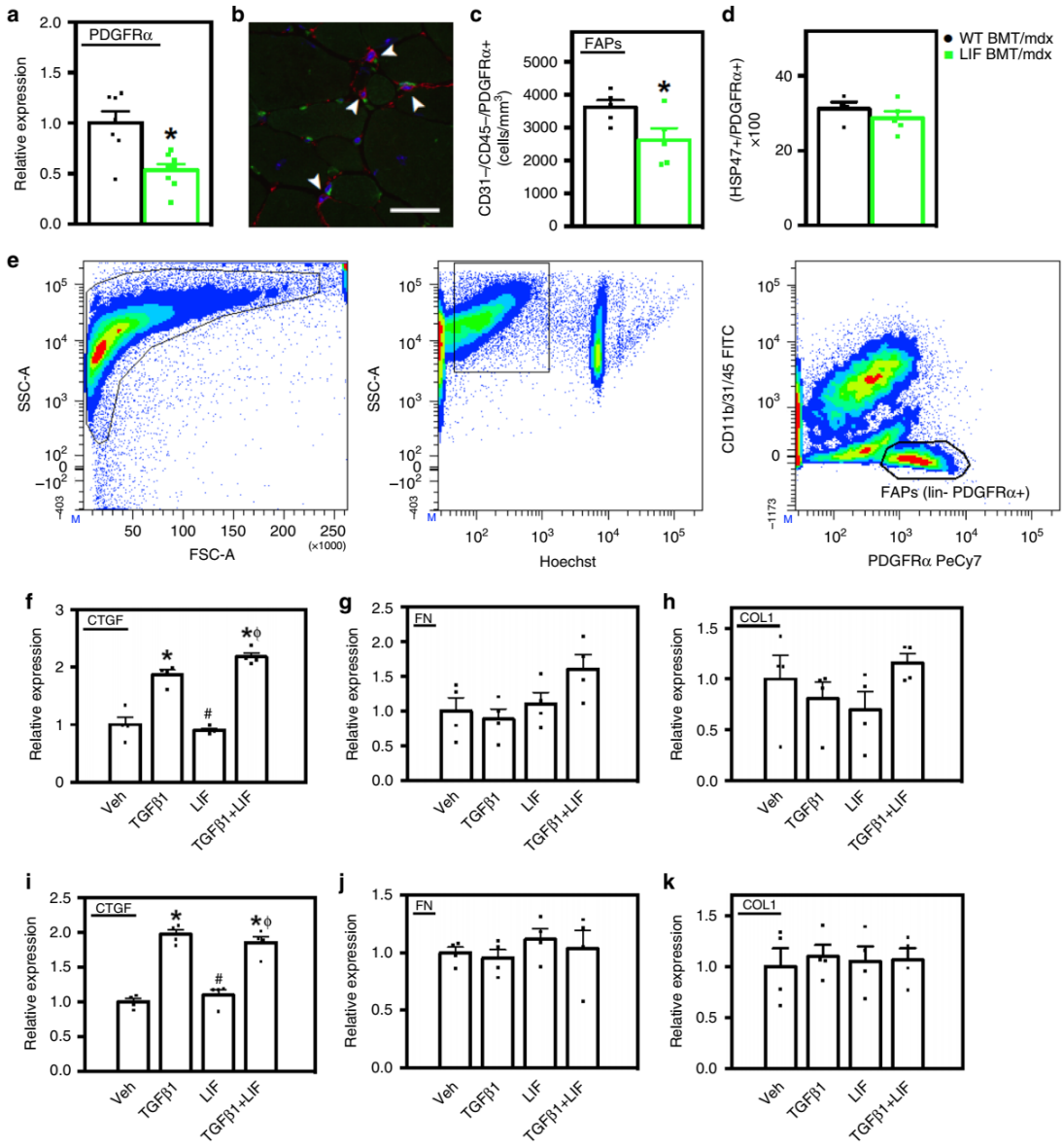

Fig. 8 Transplantation of CD11b/LIF transgenic BMCs reduces the numbers of FAPs in dystrophic muscle but does not affect phenotype. **a** QPCR analysis shows that TA muscles from LIF BMT/*mdx* recipients have reduced *Pdgfra* gene expression. $N = 7$ or 8 for WT BMT/*mdx* and LIF BMT/*mdx* data sets, respectively, * indicates significantly different from WT BMT/*mdx* recipients at $P < 0.05$. *P*-values based on two-tailed *t*-test. For all histograms in the figure, the bars indicate mean ± sem. **b** To quantify the number of FAPs, muscle sections were co-labeled with antibodies to PDGFRα (red) and CD31, CD45 (green). Arrowheads indicate FAPs (CD31-CD45-PDGFRα+). Bar = 50 µm. **c** Fewer FAPs (CD31-CD45-PDGFRα+) in TA cross-sections of LIF BMT/*mdx* recipients compared to WT BMT/*mdx* recipients. $N = 5$ for each data set. **d** There was no detectible change in phenotype of PDGFRα+ cells assayed for co-expression of the fibrogenic marker HSP47. **e** FACS plots demonstrating strategy for sorting FAPs (Hoechst + CD11b-CD31-CD45-PDGFRα+). Fibroblasts derived from FAPs were stimulated with LIF (10 ng/ml) and/or TGFβ1 (10 ng/ml) for 3 h (**f**–**h**) or 3 days (**i**–**k**) and assayed by QPCR for *Ctgf* (**f**, **i**), *Fn1* (**g**, **j**), and *Col1a1* (**h**, **k**). $N = 4$ technical replicates for each data set. Significant findings were verified with biological replicates of cells sorted from independent donors. * Indicates significantly different from control cultures, # indicates significantly different from TGFβ1 treated cultures, and Φ indicates significantly different from LIF-treated cultures at $P < 0.05$. *P*-values based on ANOVA with Tukey's multiple comparison test. Source data are provided as a Source Data file

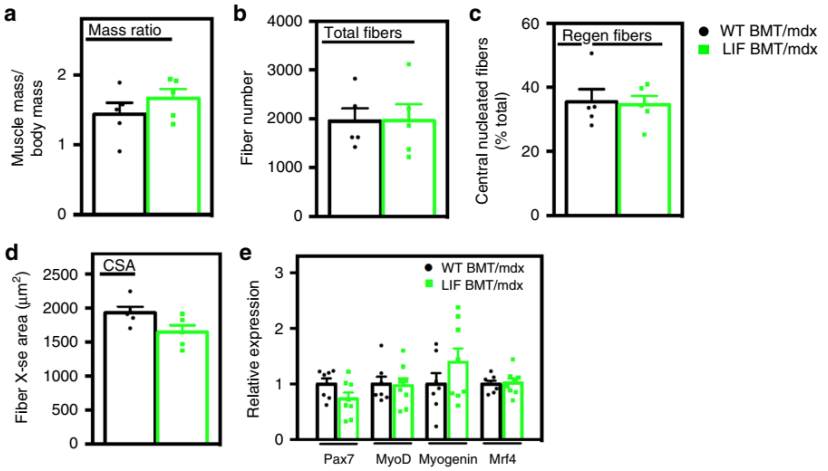

Fig. 9 Transplantation of CD11b/LIF transgenic BMCs does not affect muscle growth or regeneration. Assays of muscle mass to body mass ratio (**a**), fiber number (**b**), proportion of centrally-nucleated regenerating fibers (**c**), and muscle fiber cross-sectional area (**d**) indicate no difference in muscle growth or regeneration between WT BMT/*mdx* and LIF BMT/*mdx* recipients. $N = 5$ per group. For all histograms in the figure, the bars indicate mean ± sem. **e** QPCR analysis shows no difference in the expression of myogenic transcription factors (*Pax7*, *Myod1*, *Myog*, and *Mrf4*) in WT BMT/*mdx* versus LIF BMT/*mdx* recipients. $N = 7$ or 8 for WT BMT/*mdx* and LIF BMT/*mdx* data sets, respectively. No significant differences were identified between groups at $P < 0.05$, determined by two-tailed *t*-test. Source data are provided as a Source Data file

contrasts with the delivery system we employ, in which elevated LIF production was detectible within inflammatory lesions in dystrophic muscle and pathology was reduced, but LIF remained undetectable in the sera. This indicates that more precise temporal and spatial delivery of LIF is necessary for safe and beneficial therapeutic application.

Exogenous LIF has been reported previously to increase the growth of dystrophic muscle fibers[19,20], but we did not observe an effect of the CD11b/LIF transgene on muscle mass or fiber size in transgenic mice or in CD11b/LIF BMT recipients. These differences in outcome may reflect the different modes of LIF delivery, in which increased fiber size resulted from continuous delivery of high concentrations of exogenous LIF[19,20]. However, we found that transplantation of CD11b/LIF transgenic BMCs affected *mdx* muscle by decreasing muscle fibrosis, consistent with the treatment effect achieved by delivery of exogenous LIF[19,20,52]. In part, the anti-fibrotic influences of the CD11b/LIF transgene were attributable to modifying the phenotype of satellite cells, reflected in the reduced proportion of satellite cells that expressed detectible levels of the collagen chaperone, HSP47, and expressed ERTR7, a connective tissue protein expressed by pro-fibrotic satellite cells[40]. This is functionally important in the context of DMD pathology because the transition of satellite cells from an HSP47−/ERTR7− to an HSP47+/ERTR7+ phenotype reflects a reduction in their myogenic capacity and an increase in their production of connective tissue proteins that may exacerbate the pathology of muscular dystrophy[33] and lead to a reduction in the regenerative capacity of muscle over time[40].

Although the CD11b/LIF transgene reduced the expression of pro-fibrotic molecules by muscle cells in CD11b/LIF BMT recipients in vivo, LIF did not reduce the basal level of expression of genes encoding connective tissue proteins by muscle cells in vitro. Instead, we found that LIF reduced the activation of pro-fibrotic genes in myoblasts that was induced by the cytokine TGFβ. TGFβ has broad, profibrotic effects by increasing the expression of major, connective tissue proteins, including collagen and fibronectin[53,54], and reductions in TGFβ can significantly decrease fibrosis of dystrophin-deficient muscle, at least at early stages of the disease[1,2,29]. In addition to increasing the production of connective tissue proteins, TGFβ can also influence muscle fibrosis by promoting the differentiation of myofibroblasts from muscle[55,56] and by increasing the expression of other profibrotic growth factors, especially CTGF[53,54]. Our finding that LIF reduced or prevented the TGFβ-mediated induction of *Ctgf* expression in muscle cells may be particularly significant in *mdx* pathology because reductions in *Ctgf* expression can significantly slow pathology[57]. Thus, our in vitro and in vivo data collectively indicate that increases in LIF diminish fibrosis of dystrophic muscle by opposing the profibrotic influence of TGFβ on muscle cells.

The observation that the CD11b/LIF BMT reduced TGFβ1 expression in intramuscular macrophages without causing reductions in total TGFβ1 expression in whole muscle also indicates the specificity of targeting treatment effects that are achieved by the CD11b/LIF transgene. This may provide advantages over other experimental and therapeutic approaches that have been explored previously to reduce fibrosis of dystrophic muscle by inhibiting TGFβ1 expression or activity through pharmacological approaches[1,3,58,59]. While those pharmacological approaches are technically straight-forward and effective at reducing fibrosis in dystrophic muscle, their systemic administration does not provide delivery specifically to sites of inflammation, and increases the risks of off-target effects.

Although CD11b/LIF BMT reduced pathological changes in satellite cells, we found that some beneficial effects of CD11b/LIF transgenic cells are attributable to modulation of the inflammatory response, rather than direct actions on muscle (Fig. 10). Despite the fact that DMD and *mdx* dystrophy result from mutations that cause loss of the membrane-associated structural protein, dystrophin, and lead to a mechanically-weaker muscle cell membrane[60,61], most muscle fiber damage results from lysis caused by myeloid cells, especially macrophages expressing inducible nitric oxide synthase (iNOS) that are biased toward the M1, pro-inflammatory phenotype[7,26]. However, as the disease progresses, macrophages in dystrophic muscle shift to a CD163+/CD206+ phenotype that increases muscle fibrosis[23] and is

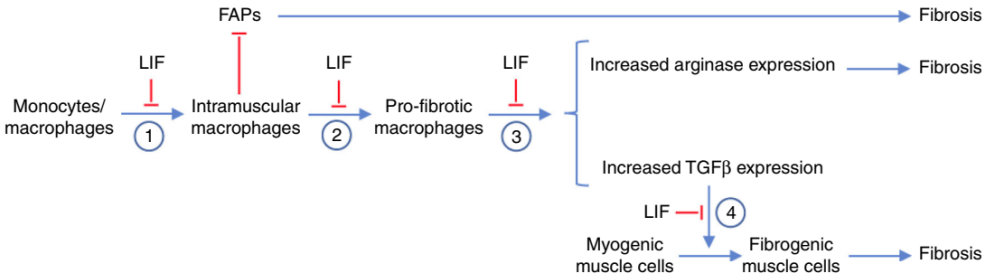

Fig. 10 Potential immunomodulatory and anti-fibrotic actions of LIF expressed by the CD11b/LIF transgene in muscular dystrophy. (1) LIF can serve an immunomodulatory role by reducing the expression of *Ccl2* in macrophages, which is associated with reduced recruitment of monocytes/macrophages into dystrophic muscle. (2) LIF can serve an immunomodulatory role by reducing the activation of monocytes/macrophages to a CD163+, M2-biased phenotype that can increase fibrosis of dystrophic muscle. (3) LIF can reduce the expression of the pro-fibrotic molecules *Arg1* and *Tgfb1* in macrophages. (4) LIF can reduce the TGFβ1-mediated induction of pro-fibrotic genes in muscle cells, including *Ctgf* and *Col1a1*

characteristic of type 2 immunity; much of the lethality of DMD is attributable to fibrosis of cardiac and respiratory muscles. Thus, by modulating the numbers and phenotype of macrophages in dystrophic muscle, LIF can produce broad effects on muscle pathology.

Some of the immunomodulatory effects achieved by transplantation of CD11b/LIF transgenic cells reflect the effects of transgene expression within the diseased muscle. For example, *Socs3* expression was significantly elevated in muscles of mice that received CD11b/LIF BMT, although expression of the transgene in macrophages in vitro did not affect the expression of *Socs3*. LIF can increase *Socs3* expression in multiple cell types[62] and elevated expression or activity of *Socs3* in macrophages can strongly influence their phenotype and cytokine production. In vivo models of inflammation show that siRNA-silencing of SOCS3 or targeted deletion of SOCS3 in macrophages can either promote[63] or oppose[64] the M1-biased phenotype. In experimental peritonitis, SOCS3 mRNA silencing in macrophages caused elevated expression of the M2 phenotypic markers *Il10*, *Mrc1*, and *Arg1*[64], which is consistent with the inverse relationship we observed between elevated *Socs3* expression in CD11b/LIF BMT recipients and reduced expression of *Il10*, *Arg2*, and *Mrc1*. Together, these observations suggest that the shift of CD11b/LIF macrophages away from an M2-biased phenotype in *mdx* BMT recipients may result, in part, from LIF induction of *Socs3* after the transgenic macrophages enter the diseased muscle. However, some of the treatment effects that we observed may have resulted from immunomodulatory roles of the transgene that occurred before their invasion into the pathological muscle. Our finding that isolated BMCs from CD11b/LIF mice showed greatly reduced levels of *Cd163* and *Arg1* expression as they differentiated to macrophages in vitro shows that some autocrine influences of the transgene on macrophage gene expression do not require localization of the cells in the dystrophic muscle. This contrasts with the reduced expression of TGFβ in intramuscular macrophages of CD11b/LIF BMT recipients that did not occur in transgenic macrophages in vitro. The reduction in arginase expression in CD11b/LIF transgenic macrophages may be particularly important in the pathophysiology of muscular dystrophy because arginine metabolism by arginase increases proline production which is necessary for collagen synthesis and contributes significantly to increased fibrosis in *mdx* muscles during progressive stages of pathology[23].

The immunomodulatory influences of the transgene extend beyond autocrine effects on macrophage phenotype, because the muscles of CD11b/LIF BMC recipients showed large reductions in the expression of ligands for CCR2. Previous investigators established that signaling through CCR2 is a primary mechanism for recruiting macrophages to diseased or injured muscle by showing that blockade or deletion of CCR2 greatly reduces macrophage entry into injured muscle[27,45,47]. We found that CD11b/LIF BMT decreased expression of CCR2 ligands in muscle and reduced the numbers of macrophages that expressed CCL2. Those reductions were also associated with large reductions in total numbers of F4/80+ intramuscular macrophages, including CD206+ and CD163+ macrophages. Thus, much of the anti-inflammatory effect of the transgene may occur through disruption of CCR2-mediated signaling, leading to reduced numbers of intramuscular macrophages and impairing their activation to a pro-fibrotic, M2-biased phenotype.

Collectively, our findings show that expression of a CD11b/LIF transgene in BMDCs can disrupt multiple processes that contribute to fibrosis of dystrophic muscle, including affecting macrophage recruitment, phenotype and production of pro-fibrotic cytokines and enzymes, in addition to preventing the fibrogenic conversion of satellite cells and reducing numbers of FAPs (Fig. 10). However, we believe that the more broadly-significant finding in our investigation is that our data show that genetically-modified BMCs can be used as vectors to deliver therapeutic genes to dystrophic muscle. This approach is applicable not only to LIF, but may provide a more specific targeting strategy for the numerous gene products that have been previously identified as potentially-useful, therapeutic molecules for DMD.

Methods

Mice. All experimentation complied with all relevant ethical regulations for animal testing and research, and the study protocol was approved by the Chancellor's Animal Research Committee at the University of California, Los Angeles. C57BL/10ScSn-Dmd^{mdx}/J *mice* (*mdx* mice) were purchased from The Jackson Laboratory (Bar Harbor, ME) and bred in pathogen-free vivaria. *Mdx* mice were selected for use in these experiments instead of more rapidly progressive models of DMD because the goal of our investigation is to test our hypothesis that transplantation of genetically-modified BMCs provides a novel therapeutic strategy for muscular dystrophy. If we used a rapidly, progressive mouse model, such as the *mdx/utr*− mouse line in which the mice die at 2–3 months of age, we would be unable to assay for treatment effects achieved by bone marrow transplantation because the mice would die before enough time passed for sufficient BMC engraftment and then for the transplanted cells to mediate their therapeutic effects.

In preparation for generating CD11b/LIF mice, the complete *Mus musculus* LIF cDNA sequence (611-bp; NM_008501) was amplified by PCR and ligated into a pGL3-Basic vector (Promega) at the Nco I/Xba I sites. The pGL3-Basic vector contained a 550-bp fragment of the human CD11b promoter at the Hind III site, upstream of the LIF insertion site. The 1215-bp, hCD11b/LIF fragment was isolated from pGL3-Basic by restriction endonuclease digestion with Xho I/Xba I and used for pronuclear injection into CB6F1 eggs to generate transgenic mice. Positive founders were identified by PCR screening for presence of the hCD11b/LIF construct and backcrossed with *C57BL/6J* mice for 7 generations. The hCD11b/LIF

line is maintained as hemizygous to produce transgenic mice and wild-type, littermate controls for experimentation. Mice were randomly allocated to experimental groups. WT or CD11b/LIF BMCs were transplanted into *mdx* mice assigned non-sequential identification numbers. Investigators collecting data and performing analysis were aware of animal numbers only and were blinded to treatment groups.

CD11b/LIF *mdx* transgenic mice were produced by crossing CD11b/LIF hemizygous males with *mdx* females to generate CD11b/LIF hemizygous, transgenic mice that were also dystrophin-deficient (CD11b/LIF *mdx*). Dystrophin-deficient status was verified by ARMS PCR screening[65] and presence of the hCD11b/LIF construct was determined as described above. The CD11b/LIF *mdx* mice were backcrossed with wild-type *mdx* mice for 7 generations to produce CD11b/LIF *mdx* mice that were dystrophin-deficient and either hemizygous or wild-type controls for the CD11b/LIF transgene.

Bone marrow transplantation. Beginning 1 week prior to BMT, mouse drinking water was supplemented with trimethoprim/sulfamethoxazole (80 µg/ml trimethoprim and 400 µg/ml sulfamethoxazole) and continued for 3 weeks. Two-month-old female *mdx* mice underwent myeloablative preconditioning via intraperitoneal injections of 1,4-butanediol dimethanesulfonate (Sigma-Aldrich) (20 mg/kg body weight) 72-, 48-, and 24-h prior to BMT. On the day of transplantation, male WT and CD11b/LIF donor mice were euthanized and their femur and tibia bones were sterilely dissected and flushed of BMCs. BMCs were isolated and recipient mice received 10^7 donor BMCs by tail-vein injection. At 4 months post-BMT, tissues and BMCs were collected from recipient mice. BMCs were used for chimerism analysis by fluorescent in situ hybridization of the Y-chromosome (Kreatech FISH Probes).

RNA isolation and QPCR. RNA was isolated from muscle homogenates and reverse transcribed to produce cDNA[24]. QPCR experiments were designed using established guidelines for experimental design, data normalization and data analysis to maximize the rigor of quantifying the relative levels of mRNA[13,66,67]. The expression for each gene in control samples was set to 1 and the other expression values were then scaled to that value. PCR primers are listed in Supplementary Table 1.

Cultured cells were washed twice with ice-cold DPBS and collected in Trizol (Invitrogen). RNA was extracted and isolated with chloroform extraction and isopropyl alcohol precipitation, followed by clean-up with an RNA Clean and Concentrator Kit (Zymo Research). Total RNA was quantified, reverse transcribed, and used for QPCR[13].

RNA was isolated from FACS sorted cells by first sorting cells directly into Buffer RLT RNA lysis buffer (Qiagen). RNA was isolated using a Qiagen RNeasy Micro Kit according to the manufacturer's protocol. RNA yield was quantified using a BioDrop µLite. RNA (50 ng/reaction) was reverse transcribed using a qScript XLT cDNA Supermix (QuantaBio). QPCR experiments were performed on a QuantStudio 5 Real-Time PCR System (Thermo Fisher) with PerfeCTa SYBR Green Supermix, Low Rox (QuantaBio)[13].

Immunohistochemistry. Muscles dissected from euthanized mice were frozen in liquid nitrogen-cooled isopentane. Cross-sections 10-µm thick were taken from the mid-belly of muscles and fixed in ice-cold acetone or 2% paraformaldehyde for 10 min. Endogenous peroxidase activity in the sections was quenched by immersion in 0.3% H_2O_2. Most sections were blocked for 1 h with blocking buffer (3% bovine serum albumin (BSA), 2% gelatin, and 0.05% Tween-20 in 50 mM Tris–HCl pH 7.6 containing 150 mM NaCl). Alternatively, sections were incubated with 10% horse serum in PBS with 0.1% Tween-20 or mouse-on-mouse blocking reagent (M.O.M. kit; Vector) for sections to be incubated with primary antibodies from goat or mouse origin, respectively. Sections were then incubated with: rat anti-mouse F4/80 (1:100, overnight at 4 °C, eBioscience, clone BM8), rat anti-mouse CD68 (1:100, 3 h at room temperature (RT), AbD Serotec, clone FA-11), rabbit anti-mouse CD163 (1:100, 3 h at RT, Santa Cruz Biotech, clone M-96), rat anti-mouse CD206 (1:50, 3 h at RT, AbD Serotec, clone MR5D3), rat anti-CD4 (1:25, overnight at 4 °C, Biolegend, clone GK1.5), rat anti-Ly-6B.2 (1:25, 2 h at RT, Bio-Rad, clone 7/4), rabbit anti-collagen type 1 (1:50, 3 h at RT, Chemicon, #AB745), goat anti-collagen type 3 (1:50, 3 h at RT, Southern Biotech #1330-01), goat anti-collagen type 5 (1:50, overnight at 4 °C, Southern Biotech, #1350-01), goat anti-LIF (1:66, overnight at 4 °C, R&D Systems, #AB-449), and mouse anti-developmental myosin heavy chain (1:100, overnight at 4 °C, Novacastra, #106304). The sections were washed with phosphate buffered saline (PBS) and probed with biotin-conjugated secondary antibodies (1:200, 30 min at RT, Vector Laboratories). Sections were then washed with PBS and incubated with avidin D-conjugated HRP (1:1000, 30 min at RT, Vector). Staining was visualized with the peroxidase substrate, 3-amino-9-ethylcarbazole (Vector).

Immunofluorescence. For co-labeling of macrophages, sections were fixed in ice-cold acetone for 10 min and then incubated in blocking buffer for 1 h. Sections were then incubated with rat anti-F4/80 and goat anti-CCL2 (1:50, R&D Systems, AB-479-NA) or rabbit anti-TGFβ1 (1:100, Abcam, #ab92486) overnight at 4 °C. Sections were washed with PBS and then incubated with donkey anti-rat Dylight 488 (1:200, 30 min at RT, Abcam, #ab102260) and horse anti-rabbit IgG Dylight 594 (1:200, 30 min at RT, Vector, #DI-1094) or horse anti-goat IgG Dylight 594 (1:200, 30 min at RT, Vector, #DI-3094). Sections were then washed with PBS and mounted with Prolong Gold mounting media (Invitrogen).

For identification of CCR2+ macrophages, sections were fixed with 4% PFA for 10 min and then incubated with blocking buffer for 1 h. Sections were then labeled with rabbit anti-mouse CCR2 (1:50, Abcam, clone E68) and rat anti-mouse CD68 or rat anti-mouse CD206 at 4 °C overnight. Sections were washed with PBS and then incubated with donkey anti-rat IgG Dylight 594 (1:200, 30 min at RT, Abcam, #ab102262) and horse anti-rabbit IgG Dylight 488 (1:200, 30 min at RT, Vector, #DI-1088).

For identification of fibrogenic satellite cells, sections were fixed in 2% paraformaldehyde for 10 min. Slides were then immersed in antigen retrieval buffer (10 mM sodium citrate, 0.05% Tween-20, pH 6) at 95–100 °C for 40 min, except for sections undergoing Pax7/Ertr7 co-labeling this step was omitted. Sections were then treated with blocking buffer from a mouse-on-mouse immunohistochemistry kit (M.O.M. kit; Vector) for 1 h and immunolabeled with mouse anti-Pax7 and rabbit anti-HSP47 (1:200, Abcam, #77609) or anti-Ertr7 (1:1000, SCBT, #SC-73355) overnight at 4 °C. Anti-Pax7 was purified from hybridoma cell supernatant (Developmental Studies Hybridoma Bank, Iowa City, Iowa)[68]. Sections were washed with PBS and then incubated with horse anti-mouse IgG Dylight 594 (1:200, 30 min at RT, Vector, DI-2594) and horse anti-rabbit IgG Dylight 488 (1:200, 30 min at RT).

For identification of FAPs, sections were fixed in ice-cold acetone for 10 min and then incubated with blocking buffer for 1 h. Sections were then labeled with rat anti-mouse CD31 conjugated with FITC (1:50, eBioscience, clone 390), rat anti-mouse CD45 conjugated with FITC (1:100, eBioscience, clone 30-F11), and goat anti-PDGFRα (1:100, R&D Systems, #AF1062) at 4 °C overnight. Sections were washed with PBS and then incubated with horse anti-goat IgG Dylight 594 (1:200, 30 min at RT, Vector).

For identification of fibrogenic PDGFRα+ cells, sections were fixed in ice-cold acetone for 10 min and then incubated with blocking buffer for 1 h. Sections were then labeled with rabbit anti-mouse HSP47 (1:100, ABcam, clone EPR4217) and goat anti-PDGFRα at 4 °C overnight. Sections were washed with PBS and then incubated with horse anti-goat IgG Dylight 594 (1:200, 30 min at RT) and horse anti-rabbit IgG Dylight 488 (1:200, 30 min at RT).

Stereology. The number of cells per volume of muscle was determined by measuring the total volume of each section using a stereological, point-counting technique to determine section area and then multiplying that value by the section thickness (10 µm)[7]. The numbers of immunolabeled cells in each section were counted and expressed as the number of cells per unit volume of each section.

Assays for fiber number, central nucleation, and size. TA muscles were sectioned at the midbelly of muscles and used for fiber cross-sectional area measurements[5]. The proportion of fibers containing central nuclei, an indicator of fiber regeneration, was also determined. Central-nucleation was expressed as the ratio of central nucleated fibers relative to the entire population of fibers sampled for each muscle. The cross-sectional areas of >300 muscle fibers were measured using a digital imaging system (BioQuant).

Assay of muscle connective tissue content. The volume fraction of muscle that was occupied by collagen types 1, 3, and 5 was determined by overlaying a 10 × 10 eye-piece grid on microscopic images of cross-sections of entire muscle that were immunolabeled with antibodies to collagen types 1, 3, or 5.

Preparation of BMMCs and BMDMs. BMMCs were separated from whole BMC preparations flushed from WT or CD11b/LIF femurs and tibiae and separated using a histopaque-1077 gradient (Sigma). The freshly-isolated BMMCs were then used for RNA isolation and analysis. For preparation of BMDMs, BMCs were aseptically flushed from WT or CD11b/LIF femurs and tibiae and differentiated in vitro to BMDMs[24]. BMDMs were stimulated for 24 h with activation media consisting of Dulbecco's Modified Eagle Medium (DMEM) with 0.25% heat-inactivated fetal bovine serum (FBS; Omega), 100 U/ml penicillin, 100 µg/ml streptomycin (1% P/S), and 10 ng/ml macrophage colony stimulating factor (MCSF; R&D).

ELISA analysis of BMDM conditioned media. Cultures of BMDM from WT mice were established as described above. On the 6th day of culture, the BMDMs were switched to DMEM containing 1% P/S, 0.25% heat-inactivated FBS, and M-CSF or media containing 10 ng/ml recombinant mouse LIF (eBioscience) (stimulation media). After 24 h of stimulation, conditioned media (CM) were collected, briefly centrifuged to remove particulates and then frozen at −20 °C. Separate aliquots of BMDM CM from each sample were analyzed for expression of CCL2 (Duoset ELISA, R&D Systems, #DY479) and TGFβ (Emax immunoassay; Promega, #G7590), according to manufacturer's instructions. Following an HRP-based reaction, a colored product was formed in proportion to the amount of cytokine present, which was analyzed by a spectrophotometer (Bio-Rad Benchmark Microplate Reader) at a wavelength of 450 nm with a 540 nm correction. The

concentration of each cytokine was determined by comparing the optical density of the samples to the standard curve.

ELISA analysis of serum. Whole blood was collected from the femoral artery and allowed to clot on ice for at least 30 min. The whole blood was spun for 10 min at 2000×*g* at 4 °C. The serum was collected and stored in liquid nitrogen until analyzed for circulating LIF, TNFα, IFNγ, IL-4, and IL-10 by ELISA, according to manufacturer's instructions (R&D Systems, Quantikine ELISAs, #MLF00, MTA00B, MIF00, M4000B, and M1000B). Each group contained 3 replicates.

Assays for LIF effects on muscle cell fibrogenesis. The C2C12 cell line was purchased from American Type Culture Collection (ATCC CRL-1772 cell line). The cells were authenticated as myoblasts by confirming their differentiation into contractile myotubes that express characteristic muscle proteins. Cells were seeded in six-well plates at 6×10^4 cells per well and cultured in DMEM containing 10% FBS, 1% P/S at 37 °C in 5% CO_2 for 24 h and then serum-starved overnight prior to stimulation. To generate myotubes, myoblasts were grown to 90% confluence and then differentiated in serum-free DMEM for 24 h. The cells were then returned to DMEM containing 10% FBS for 5 days. Myoblast and myotube cultures were stimulated with vehicle, TGFβ1 (10 ng/ml), LIF (10 ng/ml), or TGFβ1 + LIF for 3- or 24-h.

FAPs and myogenic progenitor cell preparation and isolation. FAPs were isolated from 6-month-old WT mice. Hindlimb and forelimb muscles were dissected and rinsed in DMEM. Muscles were minced and digested in 5 ml of enzyme buffer (DMEM, 25 mM HEPES (Sigma), 5 mM $MgCl_2$ (Fisher), 2% P/S, 12.5 U dispase, type II, 12.5 U collagenase B, and 20 µg/ml DNase I (Roche)) for 60 min at 37 °C with gentle trituration. The digestion was neutralized with 2 volumes of staining buffer (DMEM, 10 mM $NaHCO_3$ (EMD Millipore), 25 mM HEPES, 5 mM EDTA, 5 mM $MgCl_2$, 1 mM L-glutamine, 2% BSA, and 2% P/S). The digestate was passed through 100 µm mesh filters and cells were pelleted at 350*g* for 5 min. Cells were resuspended in ACK lysis buffer (Lonza) for 5 min followed by the addition of an equal volume of staining buffer and cells were pelleted at 350*g* for 5 min. Cells were resuspended in staining buffer with CD16/32 (eBioscience #14-0161-85; 0.5 µg/test) for 10 min to block Fc receptor binding. Cells were labeled with Hoechst (Sigma #14533) and antibodies against CD11b (eBioscience #11-0112; 0.25 µg/test), CD31 (eBioscience #11-0311; 0.5 µg/test) and CD45 (eBioscience #11-0451; 0.1 µg/test) conjugated with FITC and PDGFRα conjugated with PE-Cy7 (eBioscience #25-1401; 0.2 µg/test). FAPs (Hoechst + CD11b/31/45-PDGFRα+) were sorted into collection buffer (DMEM, 10 mM $NaHCO_3$ and 20% FBS) using a BD SORP FACSAriaII cell sorter.

MPCs were isolated from 14-months-old CD11b/LIF *mdx* mice and littermate controls. Hindlimb and forelimb muscles were dissected and digested as described for FAPs isolation. Isolated cells were resuspended in staining buffer with CD16/32 for 10 min to block Fc receptor binding. Cells were labeled with cell impermeant dye DAPI (Sigma) to distinguish live cells and antibodies against CD11b, CD31, and CD45 conjugated with FITC and Sca-1 conjugated with PE-Cy5 (eBioscience #15-5981; 0.2 µg/test), integrin α7 conjugated with PE (Medical and Biological Laboratories #K0046-5; 15 µl/test). Live MPCs (DAPI-CD11b/31/45-Sca1-α7int+) were sorted into Buffer RLT RNA lysis buffer (Qiagen) using a FACSAriaIII high speed cell sorter.

Primary fibroblast cell culture. Sorted FAPs were cultured in growth medium (DMEM, 20% FBS, 10% heat-inactivated horse serum, 1% P/S and 2.5 ng/ml bFGF) on tissue culture plates coated with Matrigel[41]. After plating, cells were cultured for 3 days and half the medium was changed. Cells were expanded and subcultured. Prior to stimulation, cells were cultured in reduced serum media overnight (DMEM, 2% FBS, 1% P/S, and 2.5 ng/ml bFGF). Fibrogenic cell cultures were stimulated with vehicle, TGFβ1 (10 ng/ml), LIF (10 ng/ml), or TGFβ1 + LIF for 3 h or 3 days (with media changes at 24- and 48-h).

Physiological analysis. We assayed muscle stiffness and viscoelasticity at 14 months of age because connective tissue accumulation in *mdx* muscle is progressive between 3 and 24 months of age. We expected that if we sampled for effects of the transgene on muscle stiffness during the late, progressive stage of the disease, the magnitude of the effect would be greater, which would enable us to address more definitively the question of whether the transgene influenced muscle stiffness. Male WT/*mdx* and LIF/*mdx* mice were anesthetized by the intraperitoneal (i.p.) injection of ketamine (40 mg/kg body weight). Anesthesia was checked by testing mice for a positive reflex response to a hind foot pinch and by monitoring respiration. Additional i.p. injections of ketamine were given throughout the study, as needed. For in-situ analysis of the TA muscle the knee was immobilized to the heated (37 °C) platform of an 809C in-situ mouse apparatus (Aurora Scientific). Silk sutures (5-0; Ethicon) were knotted to the distal, severed tendon and then secured to the lever arm of a dual-mode force transducer-servomotor (Aurora Scientific, Model 305C-5N). After placing platinum-tipped electrodes into the leg above the knee, flanking the sciatic nerve, the TA muscle was stimulated by pulses and manipulated on three axes to find the optimal muscle length (L_o). L_o was multiplied by the pennation of 0.6 for the TA muscle[69] to determine optimal fiber length (L_f). To measure elasticity, the muscle was left unstimulated while the lever arm oscillated at ±20% of the L_f for 20 s. Muscles were allowed to rest for 60 s before subsequent oscillation series. Muscles were allowed to rest for 60 s before a series of oscillations at 3 Hz, which provides a physiological strain and strain rate[70]. Dynamic Muscle Control and Dynamic Muscle Analysis (Aurora Scientific) software was used to conduct experiments and record data. Force measurements were normalized to muscle cross-sectional area, and position measurements were normalized to percent of L_f.

Statistical analyses. All data are presented as mean ± sem. Statistical significance was calculated using unpaired Student's *t*-tests or ordinary one-way ANOVA with Tukey's multiple comparison test to determine differences among multiple groups. Differences with a P-value < 0.05 were considered statistically significant. The equality of variance between the groups that are being compared was tested with an F test, experiments with a P-value < 0.05 are denoted in the figure legend. Additionally, for immunohistochemistry and immunofluorescence experiments, slides were only included if concurrently immunolabeled. Statistical analysis was performed using GraphPad Prism.

Reporting summary. Further information on research design is available in the Nature Research Reporting Summary linked to this article.

Data availability

The authors declare that the data supporting the findings of this study are available within the paper and its Supplementary Information files. The source data pertaining to Figs. 1a–c, 2a, d, f, g, i, j, m, p–r, 3a, b, e, h, k, l, 4a–f, h, 5g, j, k, 6a, d, e, 7c–f, 9a–d, f and Supplementary Figs. 1a, 1b, 1c, 1d, 2a, 2b, 3a, 3b, 3c, 3d, 4a, 4b, 4c, 5b, 5c, 5d, 5e, and 5f are provided as a Source Data file.

Received: 22 June 2018 Accepted: 22 May 2019
Published online: 26 June 2019

References

1. Nelson, C. A. et al. Inhibiting TGF-β activity improves respiratory function in mdx mice. *Am. J. Pathol.* **178**, 2611–2621 (2011).
2. Andreetta, F. et al. Immunomodulation of TGF-beta 1 in mdx mouse inhibits connective tissue proliferation in diaphragm but increases inflammatory response: implications for antifibrotic therapy. *J. Neuroimmunol.* **175**, 77–86 (2006).
3. Taniguti, A. P. T., Pertille, A., Matsumura, C. Y., Santo Neto, H. & Marques, M. J. Prevention of muscle fibrosis and myonecrosis in mdx mice by suramin, a TGF-β1 blocker. *Muscle Nerve* **43**, 82–87 (2011).
4. Bogdanovich, S. et al. Functional improvement of dystrophic muscle by myostatin blockade. *Nature* **420**, 418–421 (2002).
5. Wehling-Henricks, M. et al. Klotho gene silencing promotes pathology in the mdx mouse model of Duchenne muscular dystrophy. *Hum. Mol. Genet.* **25**, 2465–2482 (2016).
6. Straub, V., Rafael, J. A., Chamberlain, J. S. & Campbell, K. P. Animal models for muscular dystrophy show different patterns of sarcolemmal disruption. *J. Cell Biol.* **139**, 375–385 (1997).
7. Wehling, M., Spencer, M. J. & Tidball, J. G. A nitric oxide synthase transgene ameliorates muscular dystrophy in mdx mice. *J. Cell Biol.* **155**, 123–131 (2001).
8. Spencer, M. J., Walsh, C. M., Dorshkind, K. A., Rodriguez, E. M. & Tidball, J. G. Myonuclear apoptosis in dystrophic mdx muscle occurs by perforin-mediated cytotoxicity. *J. Clin. Invest.* **99**, 2745–2751 (1997).
9. Spencer, M. J., Montecino-Rodriguez, E., Dorshkind, K. & Tidball, J. G. Helper (CD4(+)) and cytotoxic (CD8(+)) T cells promote the pathology of dystrophin-deficient muscle. *Clin. Immunol.* **98**, 235–243 (2001).
10. Cai, B., Spencer, M. J., Nakamura, G., Tseng-Ong, L. & Tidball, J. G. Eosinophilia of dystrophin-deficient muscle is promoted by perforin-mediated cytotoxicity by T cell effectors. *Am. J. Pathol.* **156**, 1789–1796 (2000).
11. Hodgetts, S., Radley, H., Davies, M. & Grounds, M. D. Reduced necrosis of dystrophic muscle by depletion of host neutrophils, or blocking TNFalpha function with Etanercept in mdx mice. *Neuromuscul. Disord.* **16**, 591–602 (2006).
12. Gorospe, J. R., Nishikawa, B. K. & Hoffman, E. P. Recruitment of mast cells to muscle after mild damage. *J. Neurol. Sci.* **135**, 10–17 (1996).
13. Villalta, S. A., Deng, B., Rinaldi, C., Wehling-Henricks, M. & Tidball, J. G. IFN-γ promotes muscle damage in the mdx mouse model of Duchenne muscular dystrophy by suppressing M2 macrophage activation and inhibiting muscle cell proliferation. *J. Immunol.* **187**, 5419–5428 (2011).
14. Villalta, S. A. et al. Interleukin-10 reduces the pathology of mdx muscular dystrophy by deactivating M1 macrophages and modulating macrophage phenotype. *Hum. Mol. Genet.* **20**, 790–805 (2011).

15. Todd, R. F., Nadler, L. M. & Schlossman, S. F. Antigens on human monocytes identified by monoclonal antibodies. *J. Immunol.* **126**, 1435–1442 (1981).
16. Griffin, J. D., Ritz, J., Nadler, L. M. & Schlossman, S. F. Expression of myeloid differentiation antigens on normal and malignant myeloid cells. *J. Clin. Invest.* **68**, 932–941 (1981).
17. Rosmarin, A. G. et al. Differential expression of CD11b/CD18 (Mo1) and myeloperoxidase genes during myeloid differentiation. *Blood* **73**, 131–136 (1989).
18. Robertson, T. A., Maley, M. A., Grounds, M. D. & Papadimitriou, J. M. The role of macrophages in skeletal muscle regeneration with particular reference to chemotaxis. *Exp. Cell Res.* **207**, 321–331 (1993).
19. Kurek, J., Bower, J., Romanella, M. & Austin, L. Leukaemia inhibitory factor treatment stimulates muscle regeneration in the mdx mouse. *Neurosci. Lett.* **212**, 167–170 (1996).
20. Austin, L. et al. Leukemia inhibitory factor ameliorates muscle fiber degeneration in the mdx mouse. *Muscle Nerve* **23**, 1700–1705 (2000).
21. Hunt, L. C., Upadhyay, A., Jazayeri, J. A., Tudor, E. M. & White, J. D. An anti-inflammatory role for leukemia inhibitory factor receptor signaling in regenerating skeletal muscle. *Histochem. Cell Biol.* **139**, 13–34 (2013).
22. Sica, A. & Mantovani, A. Macrophage plasticity and polarization: in vivo veritas. *J. Clin. Invest.* **122**, 787–795 (2012).
23. Wehling-Henricks, M. et al. Arginine metabolism by macrophages promotes cardiac and muscle fibrosis in mdx muscular dystrophy. *PLoS ONE* **5**, e10763 (2010).
24. Wehling-Henricks, M. et al. Macrophages escape Klotho gene silencing in the mdx mouse model of Duchenne muscular dystrophy and promote muscle growth and increase satellite cell numbers through a Klotho-mediated pathway. *Hum. Mol. Genet.* **27**, 14–29 (2018).
25. Adams, T. E. et al. Growth hormone preferentially induces the rapid, transient expression of SOCS-3, a novel inhibitor of cytokine receptor signaling. *J. Biol. Chem.* **273**, 1285–1287 (1998).
26. Villalta, S. A., Nguyen, H. X., Deng, B., Gotoh, T. & Tidball, J. G. Shifts in macrophage phenotypes and macrophage competition for arginine metabolism affect the severity of muscle pathology in muscular dystrophy. *Hum. Mol. Genet.* **18**, 482–496 (2009).
27. Mojumdar, K. et al. Inflammatory monocytes promote progression of Duchenne muscular dystrophy and can be therapeutically targeted via CCR2. *EMBO Mol. Med.* **6**, 1476–1492 (2014).
28. Curran, J. N., Winter, D. C. & Bouchier-Hayes, D. Biological fate and clinical implications of arginine metabolism in tissue healing. *Wound Repair Regen.* **14**, 376–386 (2006).
29. Vidal, B. et al. Fibrinogen drives dystrophic muscle fibrosis via a TGFbeta/alternative macrophage activation pathway. *Genes Dev.* **22**, 1747–1752 (2008).
30. Zhou, L. et al. Temporal and spatial mRNA expression patterns of TGF-beta1, 2, 3 and TbetaRI, II, III in skeletal muscles of mdx mice. *Neuromuscul. Disord.* **16**, 32–38 (2006).
31. Lemos, D. R. et al. Nilotinib reduces muscle fibrosis in chronic muscle injury by promoting TNF-mediated apoptosis of fibro/adipogenic progenitors. *Nat. Med.* **21**, 786–794 (2015).
32. Uezumi, A. et al. Fibrosis and adipogenesis originate from a common mesenchymal progenitor in skeletal muscle. *J. Cell Sci.* **124**, 3654–3664 (2011).
33. Biressi, S., Miyabara, E. H., Gopinath, S. D., Carlig, P. M. M. & Rando, T. A. A Wnt-TGFβ2 axis induces a fibrogenic program in muscle stem cells from dystrophic mice. *Sci. Transl. Med.* **6**, 267ra176 (2014).
34. Peinado, H., Quintanilla, M. & Cano, A. Transforming growth factor beta-1 induces snail transcription factor in epithelial cell lines: mechanisms for epithelial mesenchymal transitions. *J. Biol. Chem.* **278**, 21113–21123 (2003).
35. Liu, Y. et al. Transforming growth factor-β (TGF-β)-mediated connective tissue growth factor (CTGF) expression in hepatic stellate cells requires Stat3 signaling activation. *J. Biol. Chem.* **288**, 30708–30719 (2013).
36. Ignotz, R. A. & Massagué, J. Transforming growth factor-beta stimulates the expression of fibronectin and collagen and their incorporation into the extracellular matrix. *J. Biol. Chem.* **261**, 4337–4345 (1986).
37. Lustig, B. et al. Negative feedback loop of Wnt signaling through upregulation of Conductin/Axin2 in colorectal and liver tumors. *Mol. Cell. Biol.* **22**, 1184–1193 (2002).
38. Ishida, Y. & Nagata, K. Hsp47 as a collagen-specific molecular chaperone. *Methods Enzymol.* **499**, 167–182 (2011).
39. Taguchi, T., Nazneen, A., Al-Shihri, A. A., Turkistani, K. A. & Razzaque, M. S. Heat shock protein 47: a novel biomarker of phenotypically altered collagen-producing cells. *Acta Histochem. Cytochem.* **44**, 35–41 (2011).
40. Brack, A. S. et al. Increased Wnt signaling during aging alters muscle stem cell fate and increases fibrosis. *Science* **317**, 807–810 (2007).
41. Joe, A. W. B. et al. Muscle injury activates resident fibro/adipogenic progenitors that facilitate myogenesis. *Nat. Cell Biol.* **12**, 153–163 (2010).
42. Uezumi, A., Fukada, S., Yamamoto, N., Takeda, S. & Tsuchida, K. Mesenchymal progenitors distinct from satellite cells contribute to ectopic fat cell formation in skeletal muscle. *Nat. Cell Biol.* **12**, 143–152 (2010).
43. Mueller, A. A., van Velthoven, C. T., Fukumoto, K. D., Cheung, T. H. & Rando, T. A. Intronic polyadenylation of PDGFRα in resident stem cells attenuates muscle fibrosis. *Nature* **540**, 276–279 (2016).
44. Tidball, J. G. & Wehling-Henricks, M. Macrophages promote muscle membrane repair and muscle fibre growth and regeneration during modified muscle loading in mice in vivo. *J. Physiol.* **578**, 327–336 (2007).
45. Shireman, P. K. et al. MCP-1 deficiency causes altered inflammation with impaired skeletal muscle regeneration. *J. Leukoc. Biol.* **81**, 775–785 (2007).
46. Segawa, M. et al. Suppression of macrophage functions impairs skeletal muscle regeneration with severe fibrosis. *Exp. Cell Res.* **314**, 3232–3244 (2008).
47. Martinez, C. O. et al. Regulation of skeletal muscle regeneration by CCR2-activating chemokines is directly related to macrophage recruitment. *Am. J. Physiol. Regul. Integr. Comp. Physiol.* **299**, R832–R842 (2010).
48. Ball, L. M. et al. Paediatric allogeneic bone marrow transplantation for homozygous beta-thalassaemia, the Dutch experience. *Bone Marrow Transpl.* **31**, 1081–1087 (2003).
49. Reuter, U. et al. Correction of complete interferon-gamma receptor 1 deficiency by bone marrow transplantation. *Blood* **100**, 4234–4235 (2002).
50. Metcalf, D. & Gearing, D. P. Fatal syndrome in mice engrafted with cells producing high levels of the leukemia inhibitory factor. *Proc. Natl. Acad. Sci. USA* **86**, 5948–5952 (1989).
51. Metcalf, D. & Gearing, D. P. A myelosclerotic syndrome in mice engrafted with cells producing high levels of leukemia inhibitory factor (LIF). *Leukemia* **3**, 847–852 (1989).
52. White, J. D., Davies, M., McGeachie, J. & Grounds, M. D. An evaluation of leukaemia inhibitory factor as a potential therapeutic agent in the treatment of muscle disease. *Neuromuscul. Disord.* **12**, 909–916 (2002).
53. Igarashi, A., Okochi, H., Bradham, D. M. & Grotendorst, G. R. Regulation of connective tissue growth factor gene expression in human skin fibroblasts and during wound repair. *Mol. Biol. Cell* **4**, 637–645 (1993).
54. Frazier, K., Williams, S., Kothapalli, D., Klapper, H. & Grotendorst, G. R. Stimulation of fibroblast cell growth, matrix production, and granulation tissue formation by connective tissue growth factor. *J. Invest. Dermatol.* **107**, 404–411 (1996).
55. Zanotti, S., Gibertini, S. & Mora, M. Altered production of extra-cellular matrix components by muscle-derived Duchenne muscular dystrophy fibroblasts before and after TGF-beta1 treatment. *Cell Tissue Res.* **339**, 397–410 (2010).
56. Cencetti, F., Bernacchioni, C., Nincheri, P., Donati, C. & Bruni, P. Transforming growth factor-beta1 induces transdifferentiation of myoblasts into myofibroblasts via up-regulation of sphingosine kinase-1/S1P3 axis. *Mol. Biol. Cell* **21**, 1111–1124 (2010).
57. Morales, M. G. et al. Reducing CTGF/CCN2 slows down mdx muscle dystrophy and improves cell therapy. *Hum. Mol. Genet.* **22**, 4938–4951 (2013).
58. Gosselin, L. E. et al. Localization and early time course of TGF-beta 1 mRNA expression in dystrophic muscle. *Muscle Nerve* **30**, 645–653 (2004).
59. Cohn, R. D. et al. Angiotensin II type 1 receptor blockade attenuates TGF-β-induced failure of muscle regeneration in multiple myopathic states. *Nat. Med.* **13**, 204–210 (2007).
60. Hoffman, E. P., Brown, R. H. & Kunkel, L. M. Dystrophin: the protein product of the Duchenne muscular dystrophy locus. *Cell* **51**, 919–928 (1987).
61. Petrof, B. J., Shrager, J. B., Stedman, H. H., Kelly, A. M. & Sweeney, H. L. Dystrophin protects the sarcolemma from stresses developed during muscle contraction. *Proc. Natl. Acad. Sci. USA* **90**, 3710–3714 (1993).
62. Laszlo, G. S. & Nathanson, N. M. Src family kinase-independent signal transduction and gene induction by leukemia inhibitory factor. *J. Biol. Chem.* **278**, 27750–27757 (2003).
63. Qin, H. et al. SOCS3 deficiency promotes M1 macrophage polarization and inflammation. *J. Immunol.* **189**, 3439–3448 (2012).
64. Arnold, C. E. et al. A critical role for suppressor of cytokine signalling 3 in promoting M1 macrophage activation and function in vitro and in vivo. *Immunology* **141**, 96–110 (2014).
65. Amalfitano, A. & Chamberlain, J. S. The mdx-amplification-resistant mutation system assay, a simple and rapid polymerase chain reaction-based detection of the mdx allele. *Muscle Nerve* **19**, 1549–1553 (1996).
66. Nolan, T., Hands, R. E. & Bustin, S. A. Quantification of mRNA using real-time RT-PCR. *Nat. Protoc.* **1**, 1559–1582 (2006).
67. Bustin, S. A. et al. The MIQE guidelines: minimum information for publication of quantitative real-time PCR experiments. *Clin. Chem.* **55**, 611–622 (2009).
68. Wang, Y., Wehling-Henricks, M., Samengo, G. & Tidball, J. G. Increases of M2a macrophages and fibrosis in aging muscle are influenced by bone marrow aging and negatively regulated by muscle-derived nitric oxide. *Aging Cell* **14**, 678–688 (2015).
69. Burkholder, T. J., Fingado, B., Baron, S. & Lieber, R. L. Relationship between muscle fiber types and sizes and muscle architectural properties in the mouse hindlimb. *J. Morphol.* **221**, 177–190 (1994).

70. Bellardita, C. & Kiehn, O. Phenotypic characterization of speed-associated gait changes in mice reveals modular organization of locomotor networks. *Curr. Biol.* **25**, 1426–1436 (2015).

Acknowledgements

Research reported in this publication was supported by the National Institute of Arthritis and Musculoskeletal and Skin Diseases of the National Institutes of Health under Award Numbers F32AR065845 (to S.S.W.), F31AR071783 (to I.F.), F32AR071233 (to J.R.), and RO1AR066036, RO1AR062579, and R21AR066817 (to J.G.T.). The content is solely the responsibility of the authors and does not necessarily represent the official views of the National Institutes of Health. Flow cytometry was performed in the UCLA Jonsson Comprehensive Cancer Center (JCCC) and Center for AIDS Research Flow Cytometry Core Facility that is supported by National Institutes of Health awards P30 CA016042 and 5P30 AI028697, and by the JCCC, the UCLA AIDS Institute, the David Geffen School of Medicine at UCLA, the UCLA Chancellor's Office, and the UCLA Vice Chancellor's Office of Research. Confocal laser scanning microscopy was performed at the California NanoSystems Institute Advanced Light Microscopy/Spectroscopy Shared Resource Facility at UCLA. DNA microinjections for the production of the CD11b/LIF transgenic mice were performed at the University of California, Irvine Transgenic Mouse Facility. The Pax7 hybridoma developed by T.M. Jessell, Columbia University, was obtained from the Developmental Studies Hybridoma Bank, created by the NICHD of the NIH and maintained at The University of Iowa, Department of Biology, Iowa City, IA 52242, USA.

Author contributions

S.S.W., M.W.-H., I.F., and J.G.T. conceived and designed the experiments. S.S.W., M.W.-H., I.F., C.B., J.R., and Y.W. performed the experiments. S.S.W., I.F., and J.G.T. analyzed the data and wrote the manuscript.

Additional information

Supplementary Information accompanies this paper at https://doi.org/10.1038/s41467-019-10614-1.

Competing interests: The authors declare no competing interests.

Reprints and permission information is available online at http://npg.nature.com/reprintsandpermissions/

Peer review information: *Nature Communications* thanks the anonymous reviewers for their contribution to the peer review of this work.

Publisher's note: Springer Nature remains neutral with regard to jurisdictional claims in published maps and institutional affiliations.

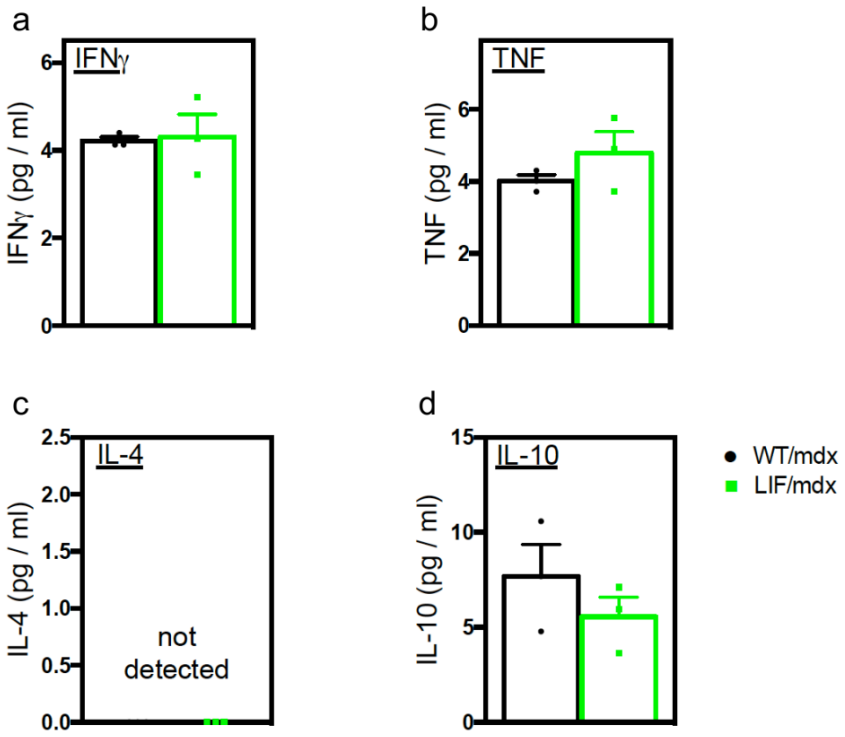

Supplementary figure 1: Expression of a CD11b/LIF transgene in *mdx mice* does not affect systemic pro-inflammatory or anti-inflammatory cytokine expression in *mdx mice*. Serum ELISA for circulating levels of IFNγ (A), TNF (B), IL-4 (C) and IL-10 (D) showed no significant change in serum cytokine concentrations of 3-months old WT/*mdx* and LIF/*mdx mice*. For all histograms in the figure, the bars indicate mean ± *sem*. N = 3 for each data set. No significant differences were identified between groups using *P*-values < 0.05, determined by two-tailed *t*-test. Source data are provided as a Source Data file.

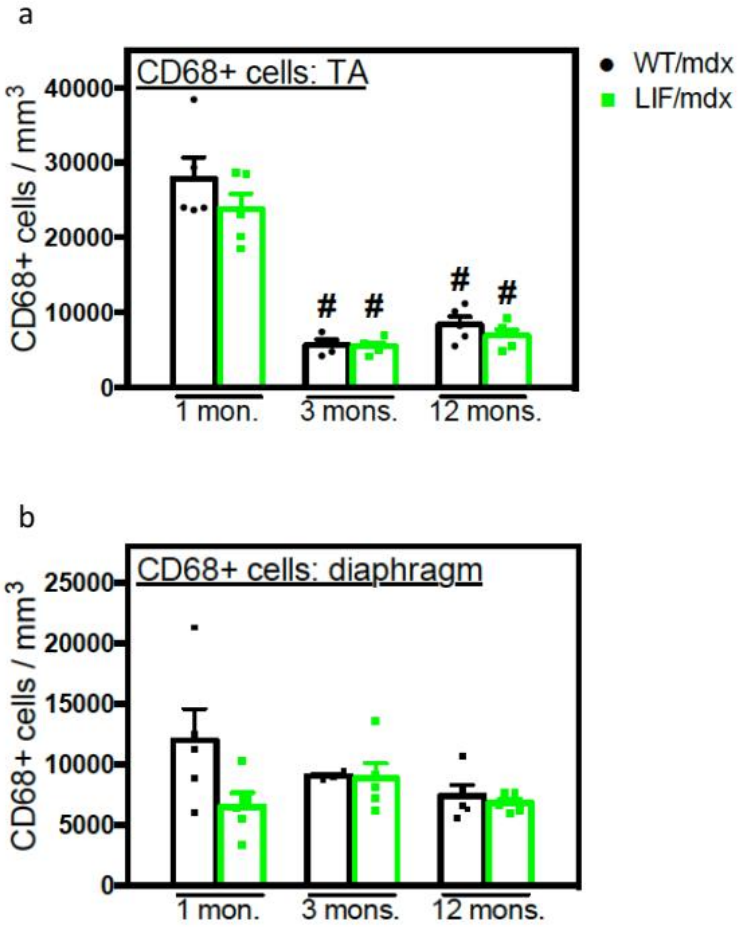

Supplementary figure 2: Expression of a CD11b/LIF transgene in *mdx mice* does not affect CD68+ cell numbers in TA or diaphragm muscle. TA (A) and diaphragm (B) muscles of WT/*mdx* and LIF/*mdx* transgenic *mice* were immunolabeled and the numbers of CD68+ cells at the ages of 1-, 3- and 12-months were quantified. No significant differences in the number of CD68+ cells were found between genotypes at the ages tested. For all histograms in the figure, the bars indicate mean ± *sem*. N = 5 for each data set, except n = 4 for 3-months WT/*mdx mice*. # indicates significant difference versus 1-month *mice* of the same genotype at $P < 0.05$. *P*-values based on two-tailed *t*-test. Source data are provided as a Source Data file.

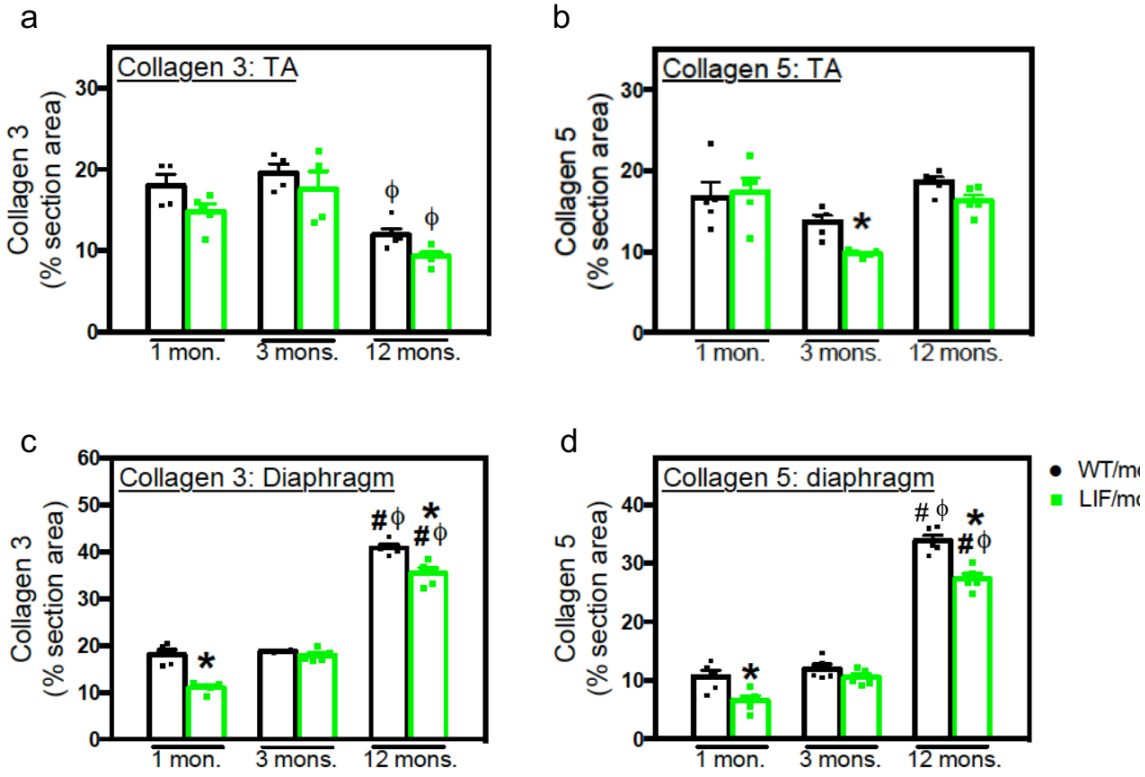

Supplementary figure 3: Expression of a CD11b/LIF transgene in *mdx mice* reduces collagen types 3 and 5 accumulation in TA and diaphragm muscles. (A-D) TA and diaphragm muscles of WT/*mdx* and LIF/*mdx mice* were immunolabeled for collagen types 3 (A, C) or 5 (B, D) at the ages of 1-, 3- and 12-months. The volume fraction of area occupied by each collagen type was quantified in the TA (A, B) and diaphragm (C, D). The accumulation of collagen type 3 was reduced in 1- and 12-months diaphragms of LIF/*mdx mice*. Collagen type 5 accumulation was also reduced in 3-months TAs, 1- and 12-months diaphragms of LIF/*mdx mice*. For all histograms in the figure, the bars indicate mean ± *sem*. N = 5 for each data set, except n = 4 for collagen type 3 WT/*mdx* 1- and 3-month TA, LIF/*mdx* 3-month TA, WT/*mdx* 3-month diaphragm data sets. * indicates significant difference versus WT/*mdx mice* of the same age at $P < 0.05$. # indicates significant difference versus 1-month *mice* of the same genotype at $P < 0.05$. Φ indicates significant difference versus 3-months-old *mice* of the same genotype at $P < 0.05$. *P*-values based on two-tailed *t*-test. *F*-test collagen type 3 3-month diaphragm ($P = 0.0242$) and collagen type 5 3-month TA ($P = 0.0139$). Source data are provided as a Source Data file.

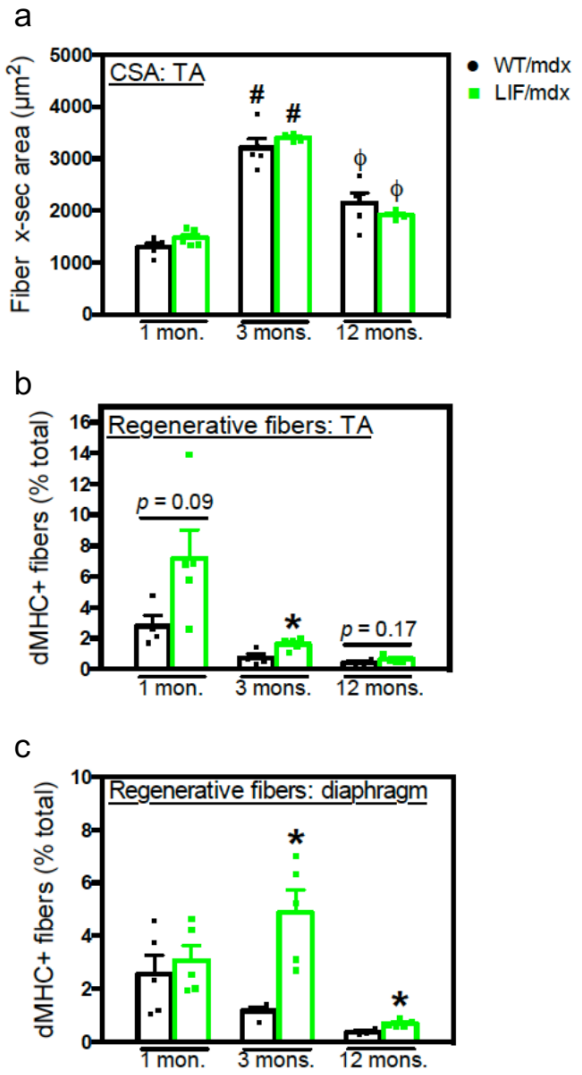

Supplementary figure 4: Expression of a CD11b/LIF transgene in *mdx mice* does not affect muscle fiber growth but increases the formation of regenerating fibers. (A) The average fiber cross-sectional area of WT/*mdx* and LIF/*mdx* TAs was quantified at 1-, 3- and 12-months. No significant differences were detected between the two genotypes at the ages tested. For all histograms in the figure, the bars indicate mean ± *sem*. N = 5 for each data set, except n = 4 for 3- and 12-months LIF/*mdx* TA muscles. # indicates significant difference versus 1-month *mice* of the same genotype at $P < 0.05$. Φ indicates significant difference versus 3-months-old *mice* of the same genotype at $P < 0.05$. *P*-values based on two-tailed *t*-test. *F*-test TA muscle fiber cross-sectional area 3- ($P = 0.0222$) and 12-months TA ($P = 0.0230$). (B-C) TA and diaphragm muscles of WT/*mdx* and LIF/*mdx mice* were immunolabeled with antibodies to developmental myosin heavy chain (dMHC) at 1-, 3- and 12-months. The proportion of dMHC+ to total muscle fibers was quantified. The proportion of dMHC+ fibers increased in TA muscles at 3-months (B) and diaphragm muscles at 3- and 12-months (C). Data are presented as mean ± *sem*, n = 5 for each data set, except n = 4 for 1-, 3- and 12-months WT/*mdx* TA muscles and 3- and 12-months WT/*mdx* diaphragm muscles. * indicates significant difference versus WT/*mdx mice* of the same age at $P < 0.05$. *P*-values based on two-tailed *t*-test. *F*-test diaphragm muscle fiber cross-sectional area 3-months ($P = 0.0113$). Source data are provided as a Source Data file.

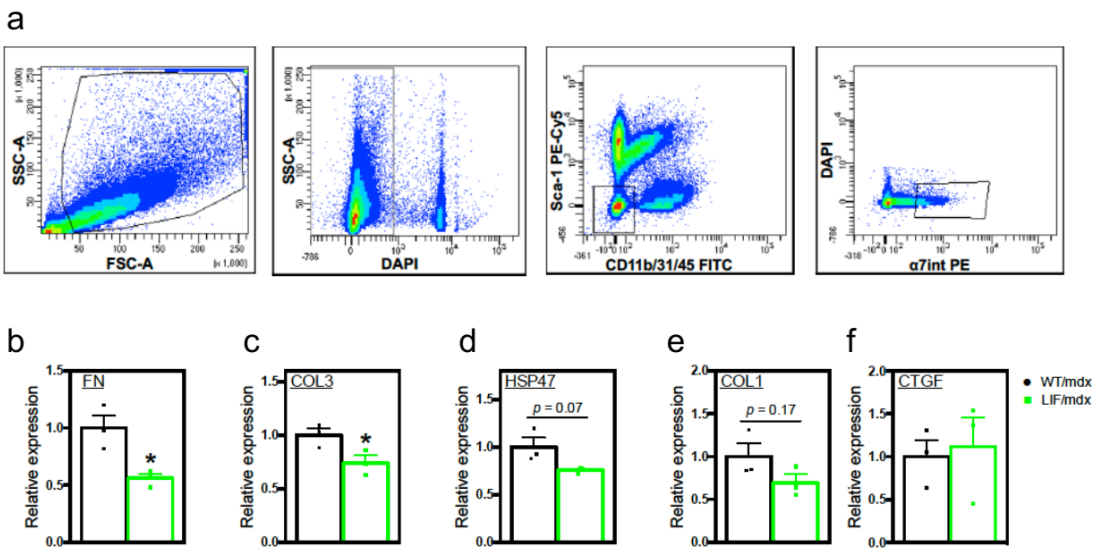

Supplementary figure 5: Expression of a CD11b/LIF transgene in *mdx mice* attenuates expression of fibrogenic genes in myogenic progenitor cells. (A) FACS plots demonstrating strategy for sorting myogenic progenitor cells (DAPI-CD11b-CD31-CD45-Sca1-Intα7+) from 14-months old WT/*mdx* and LIF/*mdx mice*. (B-F) RNA was collected from sorted myogenic progenitor cells and used for QPCR analysis of *Fn* (B), *Col3a1* (C), *Hsp47* (D), *Col1a1* (E) and *Ctgf* (F). For all histograms in the figure, the bars indicate mean ± *sem*. N = 3 for each data set. * indicates significant difference versus WT/*mdx mice* at $P < 0.05$. *P*-values based on two-tailed *t*-test. Source data are provided as a Source Data file.

Gene	Forward	Reverse
Cd11b	CATGAATGATGCTTACCTGGGTTATG	CCCAAAATAAGAGCCAATCTGG
Lif	GTCTTGGCCGCAGGGATTG	GCACAGGTGGCATTTACAGG
Serpinh1	GACCCATGACCTGCAGAAAC	GAAGGCAGTGGCATGGAAC
Cd68	CAAAGCTTCTGCTGTGGAAAT	GACTGGTCACGGTTGCAAG
iNOS	CAGCACAGGAAATGTTTCAGC	TAGCCAGCGTACCGGATGA
Cd163	GCAAAAACTGGCAGTGGG	GTCAAAATCACAGACGGAG
Cd206	GGATTGTGGAGCAGATGGAAG	CTTGAATGGAAATGCACAGAC
Arg1	CAATGAAGAGCTGGCTGGTGT	GTGTGAGCATCCACCCAAATG
Arg2	GAAGTGGTTAGTAGAGCTGTGTC	GGTGAGAGGTGTATTAATGTCCG
Tnf	CTTCTGTCTACTGAACTTCGGG	CACTTGGTGGTTTGCTACGAC
Ifng	GACAATCAGGCCATCAGCAAC	CGGATGAGCTCATTGAATGCTT
Il1b	GTAATGAAAGACGGCACACC	CTCTGCAGACTCAAACTCC
Il6	GAACAACGATGATGCACTTGC	CTTCATGTACTCCAGGTAGCTATGGT
Il12a	TGCCTTGGTAGCATCTATGAG	TTCAGGCGGAGCTCAGATAG
Il4	GGATGTGCCAAACGTCCTC	GAGTTCTTCTTCAAGCATGGAG
Il10	CAAGGAGCATTTGAATTCCC	GGCCTTGTAGACACCTTGGTC
Tgfb1	CTCCACCTGCAAGACCAT	CTTAGTTTGGACAGGATCTGG
Socs3	CTTTCTTATCCGCGACAGCTC	CACTGGATGCGTAGGTTCTTG
Ccr2	CCTGTAAATGCCATGCAAGTTC	GTATGCCGTGGATGAACTGAG
Ccl2	GCTCAGCCAGATGCAGTTAAC	CTCTCTCTTGAGCTTGGTGAC
Ccl7	CAACCAGATGGGCCCAATG	GATAACAGCTTCCCAGGGACAC
Ccl8	GATAAGGCTCCAGTCACCTGC	CCCTGCTTGGTCTGGAAAAC
Ccl12	CTGGACCAGATGCGGTGAG	AAGATCACAGCTTCCCGGG
Col1a1	TGTGTGCGATGACGTGCAAT	GGGTCCCTCGACTCCTACA
Col3a1	ATCCCATTTGGAGAATGTTGTGC	GGACATGATTCACAGATTCCAGG
Col5a3	CGGGGTACTCCTGGTCCTAC	GCATCCCTACTTCCCCCTTG
Axin2	GACGCACTGACCGACGATTC	CTGCGATGCATCTCTCTCTGG
Ctgf	GGACACCTAAAATCGCCAAGC	GGCACAGGTCTTGATGAACATC
Fn	GCTCAGCAAATCGTGCAGC	CTAGGTAGGTCCGTTCCCACTG
Snai1	CTTGTGTCTGCACGACCTGTG	GTCAGCAAAAGCACGGTTG
Tpt1	GGAGGGCAAGATGGTCAGTAG	CGGTGACTACTGTGCTTTCG
Rnps1	AGGCTCACCAGGAATGTGAC	CTTGGCCATCAATTTGTCCT
Rpl13a	CCTGCTGCTCTCAAGGTTGTT	CGATAGTGCATCTTGGCCTTT
Srp14	AGAGCGAGCAGTTCCTGAC	CGGTGCTGATCTTCCTTTTC
Rplp0	GGACCCGAGAAGACCTCCTT	GCTGCCGTTGTCAAACACC

Supplementary Table 1: Primer sequences.

Chapter 3:

Myeloid cell-mediated targeting of LIF to dystrophic muscle causes transient increases in muscle fiber lesions by disrupting the recruitment and dispersion of macrophages in muscle

OXFORD

Human Molecular Genetics, 2021, Vol. 00, No. 00

https://doi.org/10.1093/hmg/ddab230
General Article

GENERAL ARTICLE

Myeloid cell-mediated targeting of LIF to dystrophic muscle causes transient increases in muscle fiber lesions by disrupting the recruitment and dispersion of macrophages in muscle

Ivan Flores[1], Steven S. Welc[2,3], Michelle Wehling-Henricks[4] and James G. Tidball[1,4,5]

[1]Molecular, Cellular & Integrative Physiology Program, University of California, Los Angeles, CA 90095-1606, USA, [2]Department of Anatomy, Cell Biology & Physiology, Indiana University School of Medicine, Indianapolis, IN 46402, USA, [3]Indiana Center for Musculoskeletal Health, Indiana University School of Medicine, Indianapolis, IN 46202, USA, [4]Department of Integrative Biology and Physiology, University of California, Los Angeles, CA 90095-1606, USA and [5]Department of Pathology and Laboratory Medicine, David Geffen School of Medicine at UCLA, University of California, Los Angeles, CA 90095, USA

*To whom correspondence should be addressed at: James G. Tidball, Molecular, Cellular & Integrative Physiology Program, University of California, Los Angeles, CA 90095-1606, USA. Tel: 310-206-3395; Fax: 310-825-8489; Email: jtidball@physci.ucla.edu

Abstract

Leukemia inhibitory factor (LIF) can influence development by increasing cell proliferation and inhibiting differentiation. Because of its potency for expanding stem cell populations, delivery of exogenous LIF to diseased tissue could have therapeutic value. However, systemic elevations of LIF can have negative, off-target effects. We tested whether inflammatory cells expressing an LIF transgene under control of a leukocyte-specific, CD11b promoter provide a strategy to target LIF to sites of damage in the *mdx* mouse model of Duchenne muscular dystrophy, leading to increased numbers of muscle stem cells and improved muscle regeneration. However, transgene expression in inflammatory cells did not increase muscle growth or increase numbers of stem cells required for regeneration. Instead, transgene expression disrupted the normal dispersion of macrophages in dystrophic muscles, leading to transient increases in muscle damage in foci where macrophages were highly concentrated during early stages of pathology. The defect in inflammatory cell dispersion reflected impaired chemotaxis of macrophages to C-C motif chemokine ligand-2 and local increases of LIF production that produced large aggregations of cytolytic macrophages. Transgene expression also induced a shift in macrophage phenotype away from a CD206+, M2-biased phenotype that supports regeneration. However, at later stages of the disease when macrophage numbers declined, they dispersed in the muscle, leading to reductions in muscle fiber damage, compared to non-transgenic *mdx* mice. Together, the findings show that macrophage-mediated delivery of transgenic LIF exerts differential effects on macrophage dispersion and muscle damage depending on the stage of dystrophic pathology.

Received: May 10, 2021. **Revised:** August 4, 2021. **Accepted:** August 5, 2021

Introduction

A recently developed strategy for targeting therapeutic molecules to dystrophic muscle exploits inflammatory cells as natural vectors to selectively express and deliver potentially beneficial proteins to diseased muscle (1). Because inflammatory cells rapidly invade dystrophic muscle specifically at the times and locations where pathology is active, and afterwards they naturally reduce in numbers and activity when pathology attenuates, they provide a rapidly responsive, intrinsic system to target disease. This targeting approach is especially valuable in diseases such as Duchenne muscular dystrophy (DMD) which is unpredictably 'asynchronous' (2), in which different muscles and even different groups of muscle fibers in the same muscle occur at different stages of injury and repair. As a consequence, foci of muscle damage and necrosis can exist hundreds of micrometers from sites where muscle fibers are experiencing regeneration or hundreds of micrometers from sites where muscle fibers have not experienced damage.

Leukemia inhibitory factor (LIF) has long been expected to have potential therapeutic benefits in treating muscular dystrophy, attributable to its numerous influences on myogenesis. For example, LIF stimulates myoblast proliferation *in vitro* (3–5), which is mediated through the Jak2-Stat3 pathway (6) and may also expand their numbers *in vitro* by reducing their frequency of apoptosis (7). In addition, LIF can inhibit the formation of post-mitotic, multinucleated myotubes *in vitro* by inhibiting myoblast differentiation, which may also lead to expansion of myoblast numbers (7). LIF can also affect growth of myotubes at later stages of myogenesis *in vitro* by increasing their protein synthesis via an Akt-mediated mechanism (8). These pro-myogenic, anabolic influences of LIF on muscle cells *in vitro* are reflected in the responses of muscle to changes in LIF expression or delivery following muscle injury or in muscle disease. Elevations of systemic LIF levels in mice experiencing acute muscle injury or denervation cause faster growth of regenerative muscles (9,10) and muscle regeneration following acute injury is slower in LIF-null mutant mice (11). Similarly, increased delivery of LIF to diaphragm muscles in the *mdx* mouse model of DMD produced larger muscle fibers (12).

Although those *in vitro* and *in vivo* effects of LIF on myogenesis support its potentially beneficial role in the treatment of injured and diseased muscle, increased delivery of LIF can also cause negative, off-target effects. For example, prolonged, systemic elevations of LIF in cancer can significantly increase wasting of non-diseased muscle fibers (13–15), emphasizing the importance of targeting LIF specifically to sites of active muscle pathology, to enhance myogenesis at those sites. We previously addressed this obstacle to targeting LIF specifically to sites of pathological muscle damage by transplanting transgenic bone marrow cells (BMCs) that expressed an LIF transgene under control of the leukocyte-specific, CD11b promoter (CD11b/LIF transgene) (1). Because the transplanted cells subsequently differentiated into inflammatory cells in which the LIF transgene was expressed at high levels at sites of muscle damage, the system provided a targeted delivery of LIF to sites of pathology. The primary beneficial outcome of that therapeutic intervention was a reduction in fibrosis, which is a debilitating feature of muscular dystrophy (1).

Expression of the CD11b/LIF transgene in *mdx* mice also produced a significant increase in the number of regenerating fibers in dystrophic muscle, which could represent either a beneficial or a detrimental effect of targeted delivery of LIF. On one hand, the outcome could reflect improved muscle regeneration, which would be consistent with many of the influences of LIF on muscle cells *in vitro*. Alternatively, the increase in muscle regeneration could also result from amplification of muscle fiber damage, which would lead to more repair. In either scenario, the LIF-induced changes in the extent of regeneration of dystrophic muscle could be caused by perturbations of the immune response to muscular dystrophy, because LIF can modulate the inflammatory response to injury or disease (16,17) and perturbations of the immune response to muscular dystrophy can either worsen muscle damage (18–21) or improve repair (1,21–26).

In the present investigation, we test whether expression of the CD11b/LIF transgene in inflammatory cells leads to changes in the function of inflammatory cells that can influence injury or growth of dystrophic muscles. In particular, we assess whether the CD11b/LIF transgene influences the numbers, distribution or phenotype of innate immune cells or specific macrophage subpopulations in dystrophic, *mdx* muscle and whether their cytotoxicity or chemotactic response is affected. We also test whether expression of the transgene amplifies muscle fiber damage *in vivo* or influences the regeneration or growth of dystrophic muscles over the course of *mdx* dystrophy. Together, the findings will contribute to the assessment of whether targeted delivery of the CD11b/LIF transgene to dystrophic muscle has promising therapeutic potential.

Results

We confirmed that LIF expression was elevated in macrophages located in muscles of LIF/*mdx* mice by isolating macrophages from pooled limb muscles obtained from LIF/*mdx* and WT/*mdx* mice and assaying for LIF expression by QPCR (Fig. 1a). We next investigated whether LIF protein occurred at elevated levels where macrophages accumulated in transgenic muscles. Labeling of adjacent muscle cross-sections for CD68+ macrophages (Fig. 1b), LIF protein (Fig. 1c) and CD206+ macrophages (Fig. 1d) showed that LIF protein content was increased at sites enriched with CD68+ macrophages but with fewer CD206+ macrophages. Our previous findings demonstrated that LIF protein content was greater in inflammatory lesions of LIF/*mdx* muscles compared to WT/*mdx* muscles (1). We also assayed whether there were higher levels of LIF protein in muscle fibers of LIF/*mdx* mice compared to fibers in WT/*mdx* mice, which would indicate ectopic expression of the gene in muscle, but found no significant difference between the two genotypes (Suppl. Fig. 1). These data validate that the overexpression of LIF in whole muscles of LIF/*mdx* mice results from LIF expression by transgenic macrophages.

We then tested whether the greater co-localization of LIF with M1-biased macrophages was attributable to greater expression of LIF mRNA by M1-biased macrophages compared to M2-biased macrophages. First, we validated that unstimulated (Th0), bone marrow-derived macrophages (BMDMs) isolated from LIF/*mdx* mice (CD11b/LIF+ BMDMs) expressed significantly higher levels of LIF than BMDMs from WT/*mdx* mice (CD11b/LIF- BMDMs) (Fig. 1e). We then assayed whether expression levels of LIF were affected by whether CD11b/LIF+ BMDMs were stimulated with Th1 (TNFα and IFNγ) or Th2 cytokines (IL4 and IL10). Th1 cytokines are expressed during pro-inflammatory responses and activate macrophages toward an M1 phenotype (27–31). Th2 cytokines downregulate inflammation and activate an M2 phenotype in macrophages (20,21,23,27,29,30,32–35). Our results show that stimulation of CD11b/LIF+ BMDMs with Th1 cytokines approximately doubled their production of LIF (Fig. 1e). However, stimulation of CD11b/LIF+ BMDMs with Th2 cytokines

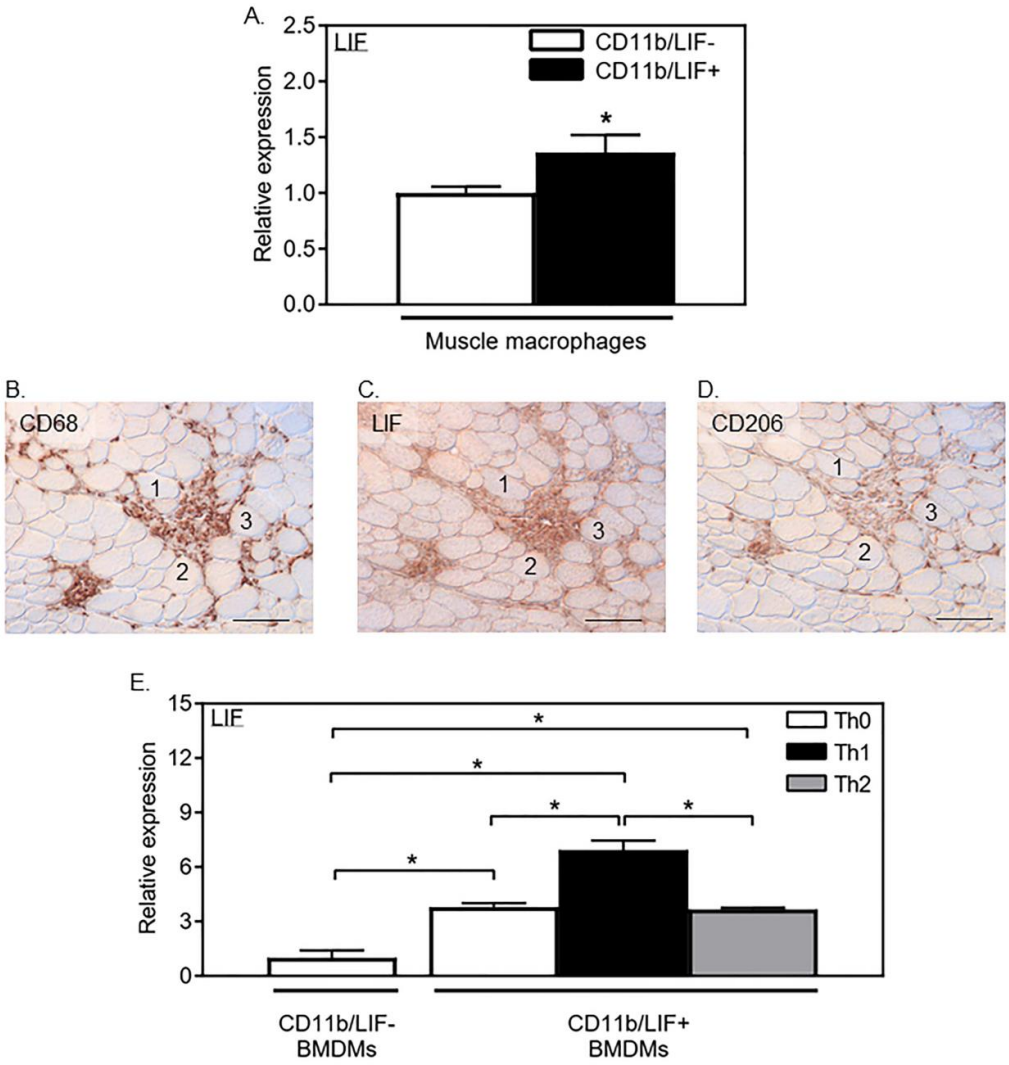

Figure 1. LIF expression is elevated in intramuscular macrophages of LIF/*mdx* mice. Histogram of LIF expression in macrophages isolated from the hind limb muscles of WT/*mdx* and LIF/*mdx* mice. **(A)**. * indicates significant difference compared to CD11b/LIF- muscle macrophages ($P < 0.05$). *P*-values are based on a two-tailed t-test. $N = 5$ for WT/*mdx* and $n = 3$ for LIF/*mdx* mice. Bars = SEM. Immunolabeling of adjacent cross-sections with anti-CD68 **(B)**, anti-LIF **(C)** and anti-CD206 **(D)** shows local, elevated LIF protein content at sites that are most highly enriched with CD68+ macrophages in LIF/*mdx* muscles. Fibers that are numbered '1,' '2' or '3' are individual fibers that appear in adjacent sections, to provide reference points in the sections. Scale bars = 50 µm. QPCR analysis of CD11b/LIF- and CD11b/LIF+ BMDMs that were unstimulated (Th0) or stimulated with Th1 or Th2 cytokines show increased expression of *lif* in M1-biased BMDMs **(E)**. * indicates significant difference between the two groups indicated by the ends of the horizontal brackets ($P < 0.05$). N = 3 for all groups. *P*-values are based on two-way ANOVA with Tukey's multiple comparisons test. Bars = SEM.

did not affect LIF expression relative to Th0 transgenic BMDMs (Fig. 1e). These findings show that expression of LIF in LIF/*mdx* mice is highest in M1-biased macrophages, which indicates that LIF is delivered to muscles in LIF/*mdx* mice primarily by pro-inflammatory macrophages.

CD11b/LIF transgene expression reduces CD206+ macrophage numbers

We assessed the effects of CD11b/LIF transgene expression on muscle inflammation in *mdx* mice during the acute onset of pathology (1-month-old), successful regeneration (3-months-old) and during the period of progressive degeneration (12-months-old) that includes progressive reductions of satellite cell numbers and function, progressive reductions in muscle fiber size, progressive increases in fibrosis and progressive reductions in muscle strength (36–38). Although the total number of CD11b+innate immune cells in *mdx* muscle declined following the acute peak of pathology (Fig. 2 a-f; m), transgene expression did not affect CD11b+cell numbers at any stage (Fig. 2m). This negative result resembles the absence of treatment effect of CD11b/LIF transgene expression on CD68+ macrophages in *mdx* muscle (1). However, when we assayed whether the transgene affected the numbers of CD206+,

M2-biased macrophages (Fig. 2 g-l, n), we observed a transgene-mediated reduction in the numbers of CD206+ macrophages at 1-month and 3-months of age, although their numbers returned to non-transgenic *mdx* levels by 12-months of age (Fig. 2n). These findings indicate that CD11b/LIF transgene expression selectively reduces the numbers of CD206+ macrophages in dystrophic muscles at early stages of the disease.

Macrophage-mediated delivery of transgenic LIF reduces macrophage dispersion

Although we found no effect of the CD11b/LIF transgene on total numbers of CD11b + innate immune cells in *mdx* muscle, the transgene dramatically influenced the dispersion of immune cells in muscle. At the 1-month time-point, CD11b + (Fig. 3a), CD68+ (Fig. 3b) and CD206+ (Fig. 3c) macrophages were broadly dispersed throughout the muscles of WT/*mdx* mice. In contrast, CD11b + (Fig. 3d) and CD68+ (Fig. 3e) showed clumped population dispersions in LIF/*mdx* muscles, despite no effect of the transgene on the total numbers in muscle of either cell population (Fig. 2m) (1). CD206+ macrophages also exhibited a clumped population dispersion in inflammatory lesions of LIF/*mdx* mice (Fig. 3f), although the effect was not as apparent as it was for CD68+ macrophages. The transgene did not affect macrophage dispersion at the 3-month (Fig. 3 g-l) or 12-month (data not shown) time-points.

CD11b/LIF+ macrophages have reduced chemotactic potential

The reduced numbers and dispersion of macrophages in LIF/*mdx* muscles suggest that elevated levels of LIF can affect macrophage chemotaxis within dystrophic muscles. We assayed whether LIF could affect C-C motif chemokine ligand-2 (CCL2) production in BMDMs because CCL2 is a potent chemoattractant that plays a dominant role in recruiting macrophages to injured tissues, including muscle (39–49). Analysis of the proportion of F4/80+ macrophages that express CCL2 (F4/80 + CCL2+ cells) showed that macrophages are an *in vivo* source of CCL2 in LIF/*mdx* muscles (Fig. 4 a–d). We observed a reduction of more than 20% in the proportion of macrophages expression CCL2 in muscles of 1-month-old LIF/mdx mice and observed a strong trend for the same effect at the 3-month time-point (Fig. 4e). We confirmed that the reduction in CCL2 expression was attributable to direct effects of LIF on macrophages by stimulating BMDMs generated from wild-type C57 mice (WT BMDMs) with recombinant LIF (rLIF), which reduced CCL2 secretion into the medium, relative to vehicle-stimulated BMDMs (Fig. 4f). Similarly, BMDMs generated from LIF/mdx mice (CD11b/LIF+ BMDMs) secreted less CCL2 than BMDMs generated from WT/*mdx* mice (CD11b/LIF- BMDMs) in the absence of rLIF stimulation (Fig. 4g). QPCR analysis confirmed decreased expression of *ccl2* by CD11b/LIF+ BMDMs (Fig. 4h).

In addition to reducing available CCL2, transgene expression may also reduce the chemotactic response of macrophages to CCL2. We used a chemotaxis assay to test whether CD11b/LIF transgene expression could reduce the migration of BMDMs in response to CCL2 and found that Th0 and M2-biased, CD11b/LIF- BMDMs were responsive to CCL2 (Fig. 4i). However, expression of the transgene by BMDMs eliminated their chemotactic response to CCL2 (Fig. 4i). Collectively, our results show that elevated expression of LIF by transgenic macrophages reduces their expression of CCL2 and their chemotactic response to CCL2, which may contribute to the disruption of normal dispersion of macrophages in *mdx* muscles.

Muscle fiber damage is increased at sites of increased macrophage accumulation

Prolonged activation of M1-biased macrophages in *mdx* muscles can exacerbate fiber damage through muscle membrane lysis (22,50,51). We assayed whether the localized increase in CD68+ macrophages could affect fiber damage in LIF/*mdx* muscles. Labeling of injured (albumin+) fibers (52) in 1-month muscles of WT/*mdx* (Fig. 5a) and LIF/*mdx* (Fig. 5b) mice showed albumin+ fiber clusters that resembled CD68+ macrophage clusters at the same time-point (Fig. 3). Labeling of adjacent cross-sections of LIF/*mdx* muscles for CD68+ macrophages (Fig. 5c), albumin+ fibers (Fig. 5d) and CD206+ macrophages (Fig. 5e) confirmed co-localization of injured fibers to areas enriched with CD68+ macrophages and relatively few CD206+ macrophages. Quantification of albumin+ fibers at each stage of the pathology showed a transient increase in fiber damage of LIF/*mdx* muscles at 1- and 3-months of age (Fig. 5f). However, at 12-months of age when macrophages are broadly dispersed in muscles, LIF/*mdx* muscles showed significantly less fiber damage (Fig. 5f). We also assayed whether transgene expression affected variance of muscle fiber cross-sectional area, which is also an indicator of muscle pathology (53,54), and found a transient increase in fiber area variance at the 1-month time-point (Fig. 5g). Increased variance occurs when there is increased damage because there are more injured fibers and each injured fiber can be at a different stage of repair and growth, which increases size variance in the population.

In addition to increasing muscle damage by increasing the numbers of M1-biased macrophages at sites of injury, the transgene may also increase the cytotoxic potential of individual macrophages. To test this possibility, we performed a fluorescence microscopy-based cytotoxicity assay to measure macrophage-mediated lysis of myoblasts. In this approach, non-labeled BMDMs were co-cultured with muscle cells that were pre-labeled with the fluorescent marker, CFSE (488 nm emission). Following the cytotoxicity period, lysed cells were labeled using GelRed (594 nm emission), a cell membrane-impermeable DNA-binding dye. The proportion of lysed muscle cells (CFSE+GelRed+ cells) out of total muscle cells (CFSE+ cells) was quantified using fluorescence microscopy (Fig. 6 a–f). We validated the sensitivity of this assay by showing a positive correlation between numbers of lysed muscle cells and numbers of wild-type BMDMs present in the co-cultures (Fig. 6g). We used this approach to test the cytotoxic potential of CD11b/LIF- and CD11b/LIF+ BMDMs. The BMDMs were polarized to a cytolytic phenotype using Th1 cytokines or left in an unpolarized state prior to co-culturing the BMDMs with muscle cells. Although Th1-stimulated BMDMs of both genotypes showed increased cytotoxicity compared to genotype-matched, unpolarized BMDMs, transgene expression had no effect on the cytotoxic potential of Th1-stimulated or unstimulated BMDMs (Fig. 6h). Our results indicate that increased muscle damage observed in LIF/*mdx* mice is caused by increased, localized accumulation of M1-biased macrophages at inflammatory lesions and not by increased cytotoxic potential of CD11b/LIF+ macrophages.

LIF transgenic macrophages accumulate at sites of *mdx* muscle growth and repair

Our previous work showed an increase in the numbers of regenerating, developmental myosin heavy chain-positive (dMHC+) fibers in LIF/*mdx* muscles (1), which suggested the possibility that those sites of repair could be associated with elevated numbers of transgenic macrophages. We tested

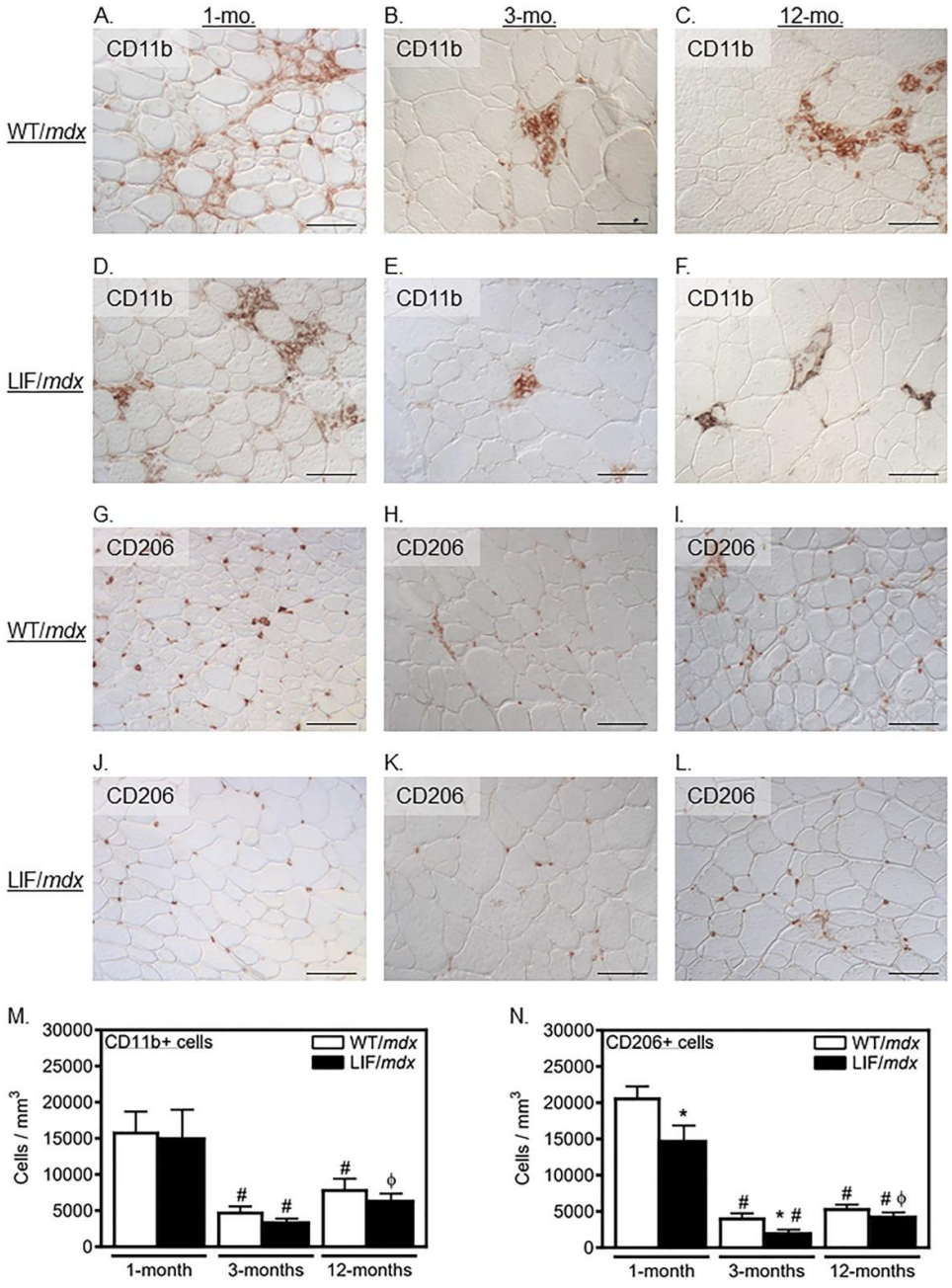

Figure 2. CD11b/LIF transgene expression does not affect total numbers of leukocytes in dystrophic muscle, but specifically reduces numbers of CD206+ macrophages. Cross-sections of WT/*mdx* **(A-C, G-I)** and LIF/*mdx* **(D-F, J-L)** muscles were immunolabeled with anti-CD11b **(A–F)** and anti-CD206 **(G–L)** to identify innate immune cells and M2-biased macrophages, respectively. Muscle sections were labeled at the 1- **(A, D G, J)**, 3- **(B, E, H, K)** and 12-month **(C, F, I, L)** time-points. Scale bars = 50 μm. Numbers of CD11b + **(M)** and CD206+ **(N)** cells were normalized to muscle volume in mice of both genotypes along the course of pathology and show a reduction of CD206+ macrophages in LIF/*mdx* muscles. * indicates significant difference compared to age-matched, WT/*mdx* mice ($P < 0.05$). # and Φ indicate significant difference compared to 1- and 3-month mice of the same genotype, respectively. *P*-values are based on two-tailed t-tests. CD11b + cell data: $n = 5$ for all groups. CD206+ cell data: $n = 7$ for both groups at the 1-month time-point and $n = 5$ for all groups at the 3- and 12-month time-points. Bars = SEM.

whether high densities of macrophages were associated with elevated numbers of dMHC+ fibers by labeling adjacent muscle sections for CD68+ macrophages (Fig. 7a, d), dMHC+ fibers (Fig. 7b, e) and CD206+ macrophages (Fig. 7c, f), which showed that regions of muscle regeneration were most-enriched with CD68+ macrophages. We then assayed whether the proportion

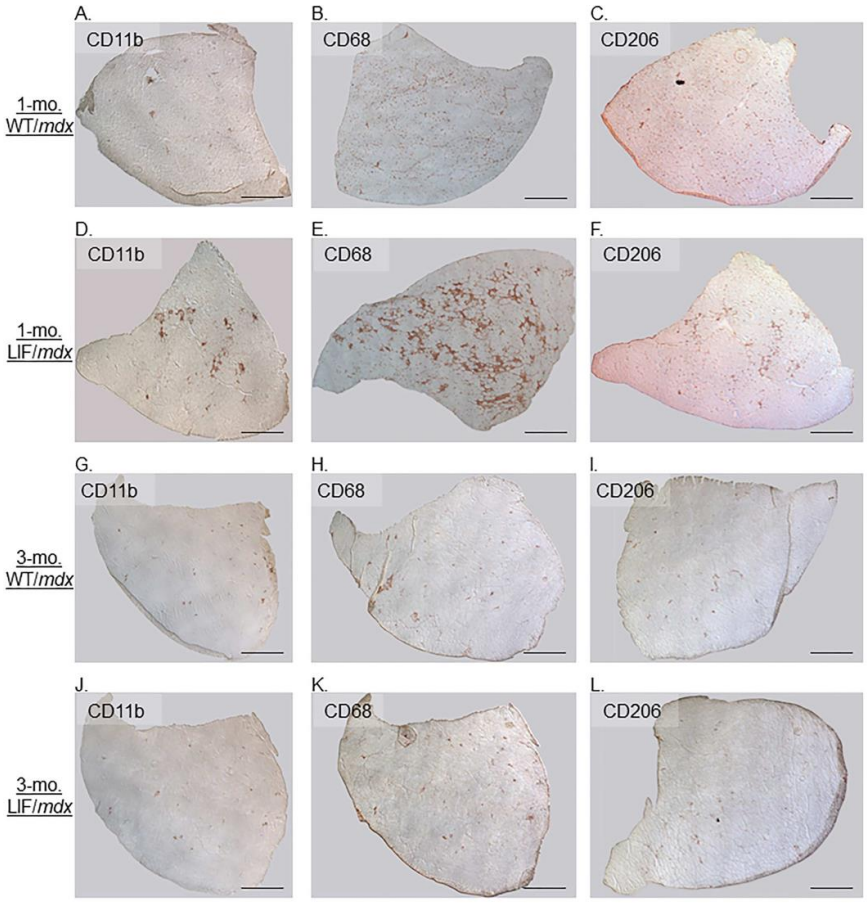

Figure 3. The LIF/transgene inhibits dispersal of macrophages in dystrophic muscles. Muscle cross-sections of 1- **(A–F)** and 3-month-old **(G–L)** TA muscles from WT/*mdx* **(A-C, G–I)** and LIF/*mdx* **(D–F, J–L)** mice were immunolabeled for macrophage markers to assess immune cell localization. Labeling with anti-CD11b **(A, D, G, J)**, anti-CD68 **(B, E, H, K)** and anti-CD206 **(C, F, I, L)** shows that transgene expression modifies macrophage dispersion in LIF/*mdx* mice at 1-month, but not at 3-months of age. Scale bars = 500 μm.

of CD68+ macrophages that were located at sites of muscle regeneration was greater in LIF/*mdx* muscles and observed a nearly 2-fold increase in the density of CD68+ cells at areas of regeneration in LIF/*mdx* muscles compared to WT/*mdx* muscles and found that CD68+ macrophages in LIF/*mdx* muscles were 3.7-fold more concentrated at regenerating areas than non-regenerating areas (Fig. 7g–k). Thus, CD11b/LIF transgene expression increased the density of CD68+ macrophages at sites of muscle regeneration.

CD11b/LIF expression does not affect *mdx* muscle growth or repair

The observation that LIF transgenic macrophages were present at high numbers at sites of dMHC+ fibers suggested two interpretations of the findings. First, the transgenic macrophages may promote muscle growth and regeneration or the elevated numbers of dMHC+ fibers may occur at sites where macrophages induced cytolysis, leading to subsequent repair. We tested whether transgenic macrophages promoted growth of *mdx* muscles by assaying for treatment effects on muscle mass or muscle fiber size. However, LIF/*mdx* mice showed no significant differences in muscle mass (Fig. 8a, b), fiber size (Fig. 8 c–f) or number of fibers per muscle (Fig. 8g) at the 1-, 3- and 12-month time-points. In addition, expression of the transgene did not affect the numbers of Pax7+, MyoD+ or myogenin+ cells in *mdx* muscle (Fig. 9 a–d). Our results indicate that macrophage-mediated delivery of transgenic LIF does not have a significant effect on muscle growth or regeneration during the course of *mdx* dystrophy.

Discussion

The primary finding in our investigation is that expression of a CD11b/LIF transgene by inflammatory cells in dystrophic muscle amplifies muscle fiber damage during the early peak of *mdx* muscle pathology. However, as inflammatory cell numbers diminished and their dispersal increased during progressive stages of the pathology, the detrimental effect of the transgene declined. By 12 months of age, expression of the transgene produced a significant reduction of fiber damage. The amplification of fiber damage early in the disease is attributable to high local concentrations of CD68+ macrophages, which can lyse *mdx* muscle fibers through a free-radical-mediated mechanism (22,51).

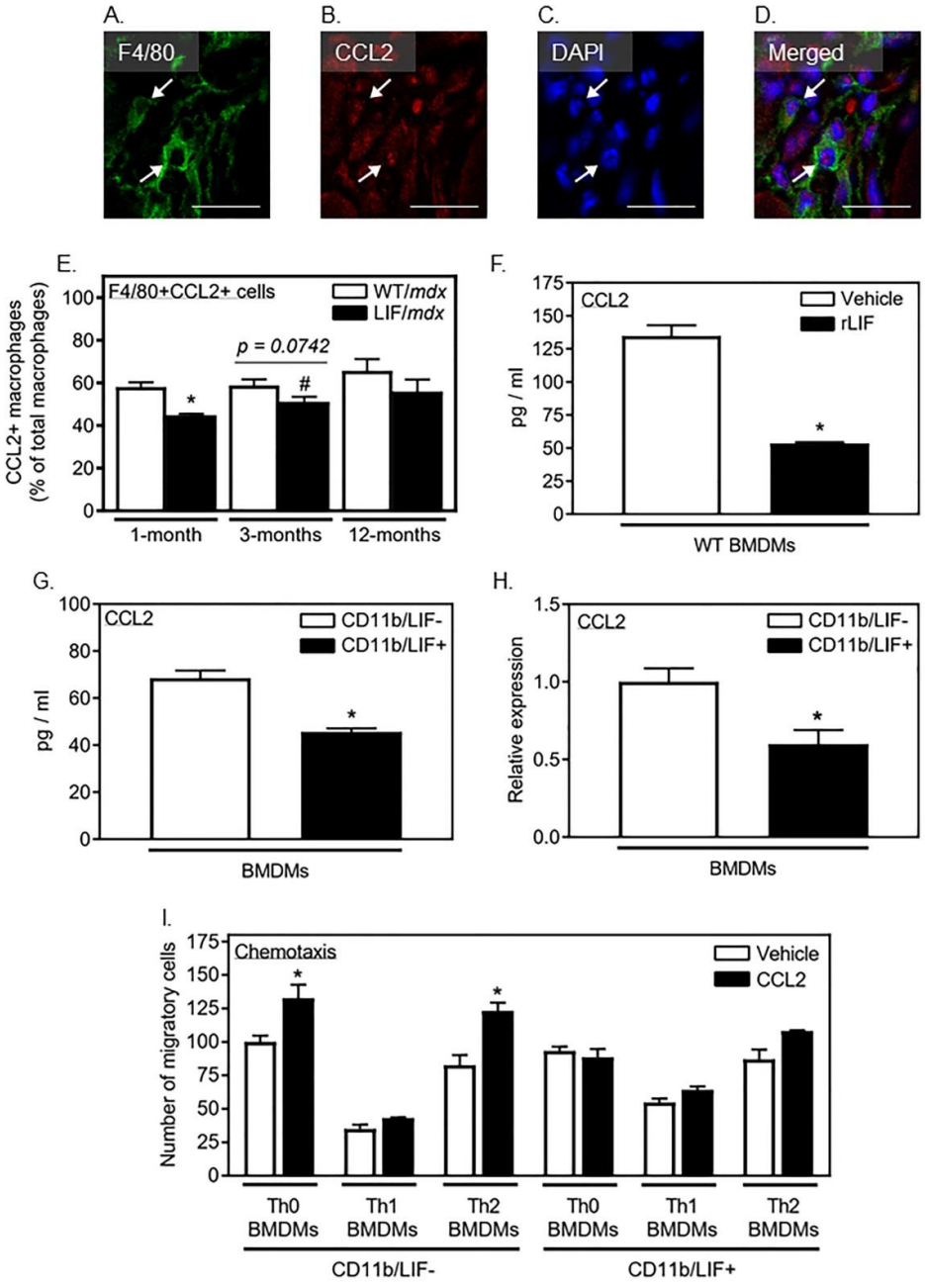

Figure 4. The CD11b/LIF transgene reduces CCL2 expression in CD11b/LIF+ macrophages and reduces chemotaxis to CCL2. Cross-sections labeled with anti-F4/80 **(A)** and anti-CCL2 **(B)** show that macrophages are a source of CCL2 in *mdx* muscles **(A–D)**. The arrows point to F4/80 and CCL2 double-positive cells. Scale bars = 20 μm. The proportion of F4/80+ macrophages that express CCL2 (F4/80 + CCL2+) is reduced in the muscles of LIF/*mdx* mice **(E)**. * indicates significant difference compared to age-matched, WT/*mdx* mice ($P < 0.05$). # indicates significant difference compared to 1-month-old mice of the same genotype ($P < 0.05$). $N = 5$ for all groups except WT/*mdx* muscles at the 3-month time-point ($n = 4$). ELISA of conditioned media shows reduced secretion of CCL2 from WT BMDMs treated with rLIF **(F)**. * indicates significant difference compared to vehicle-treated BMDMs ($P < 0.05$). $N = 5$ for both groups. ELISA of conditioned media from CD11b/LIF- and CD11b/LIF+ BMDMs shows reduced secretion of CCL2 mediated by transgene expression **(G)**. * indicates significant difference compared to CD11b/LIF- BMDMs ($P < 0.05$). $N = 5$ for both groups. QPCR analysis of CD11b/LIF- and CD11b/LIF+ BMDMs confirms the reduced secretion of CCL2 shown in **(G)** is caused by reduced expression of *ccl2* in CD11b/LIF+ BMDMs **(H)**. * indicates significant difference compared to CD11b/LIF- BMDMs ($P < 0.05$). $N = 5$ for CD11b/LIF- BMDMs and $n = 4$ for CD11b/LIF+ BMDMs. *In vitro* analysis of the chemotactic response of Th0-, Th1- and Th2-stimulated BMDMs shows reduced response to CCL2 from CD11b/LIF+ BMDMs **(I)**. * indicates significant difference compared to genotype-matched BMDMs receiving the same stimulation ($P < 0.05$). $N = 3$ for all groups except CD11b/LIF+ BMDMs with a Th0 and Th2 activation ($n = 2$). *P*-values are based on two-tailed t-test for all data. Bars = SEM.

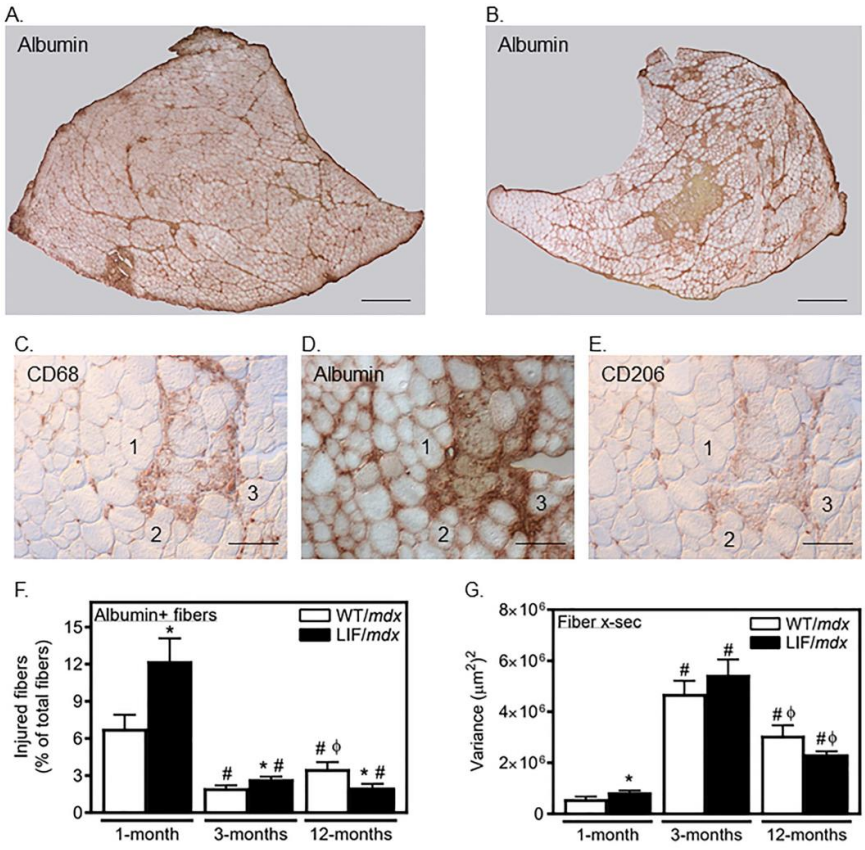

Figure 5. Muscle fiber damage is more extensive in LIF/*mdx* muscles at sites of macrophage accumulation. Cross-sections from 1-month-old WT/*mdx* **(A)** and LIF/*mdx* **(B)** muscles labeled with anti-albumin show injured fiber clusters that resemble CD68+ macrophage dispersion (Fig. 3B and 3E). Scale bars = 500 μm. Immunolabeling of adjacent cross-sections from LIF/*mdx* muscles with anti-CD68 **(C)**, anti-albumin **(D)** and anti-CD206 **(E)** shows greater co-localization of injured fibers with CD68+ macrophages relative to CD206+ macrophages. Fibers that are numbered '1,' '2' or '3' are individual fibers that appear in adjacent sections, to provide reference points in the sections. Scale bars = 50 μm. Transgene expression transiently increases the dystrophic pathology, as shown by an increase in the proportion of albumin+ fibers **(F)** and muscle fiber CSA variance **(G)** in LIF/*mdx* mice. * indicates significant difference compared to age-matched, WT/*mdx* mice ($P < 0.05$). # and Φ indicate significant difference compared to 1- and 3-month mice of the same genotype, respectively. *P*-values are based on two-tailed t-tests. Albumin+ fibers: $n = 5$ for all groups. Fiber variance: $n = 5$ for all groups except LIF/*mdx* samples at the 12-month time-point ($n = 4$). Bars = SEM.

Although the cytotoxicity of the transgenic macrophages did not differ from wild-type macrophages, the extent of muscle membrane lysis increased as numbers of macrophages increased *in vitro* or in inflammatory lesions *in vivo*; thus, the defect in CD68+ macrophage dispersal in the muscle produced high densities of cytolytic cells at foci of muscle fiber damage.

The high, local concentrations of muscle macrophages that were caused by the CD11b/LIF transgene occurred despite previous findings which showed that elevated LIF expression reduced total numbers of F4/80+ monocytes/macrophages that were recruited to *mdx* muscles at early stages of the pathology (1). This inhibitory effect on recruitment of monocytes/macrophages reflects some specificity of the influence of transgenic LIF on specific leukocyte populations because we found no effect of transgene expression on the numbers of CD11b + innate immune cells in *mdx* muscle. CD11b is expressed by monocytes and macrophages, but it is also expressed by basophils, neutrophils, eosinophils and NK cells, all of which are present in elevated numbers in *mdx* muscles (55–58). This tells us that elevated LIF expression does not reduce the aggregate numbers of innate immune cells in dystrophic muscle, but is more specifically inhibitory for monocytes/macrophages.

The selective reduction in monocytes/macrophage caused by elevated LIF is contrary to expectations based on other investigations. For example, *in vivo* observations have shown that the recruitment of macrophages to sites of tissue injury in the peripheral or central nervous system is reduced in LIF-null mutant mice (59) and *in vitro* findings have demonstrated that LIF is directly chemoattractive to macrophages and other myeloid cells (59,60). Our findings indicate that the reduction in macrophage recruitment caused by increased LIF is attributable to inhibition of powerful chemotactic signaling by CCL2 by elevated LIF expression. CCL2 plays a central role in regulating the traffic of immune cells to sites of muscle injury (61,62), intramuscular macrophages that express CCL2 play a major role in recruiting leukocytes to acutely injured muscles (63) and *mdx* muscle cells and inflammatory cells can release CCL2 to promote inflammation (64). Expression of the CD11b/LIF transgene reduced the production of CCL2 in macrophages and reduced the chemotactic response of macrophages to CCL2, both of which

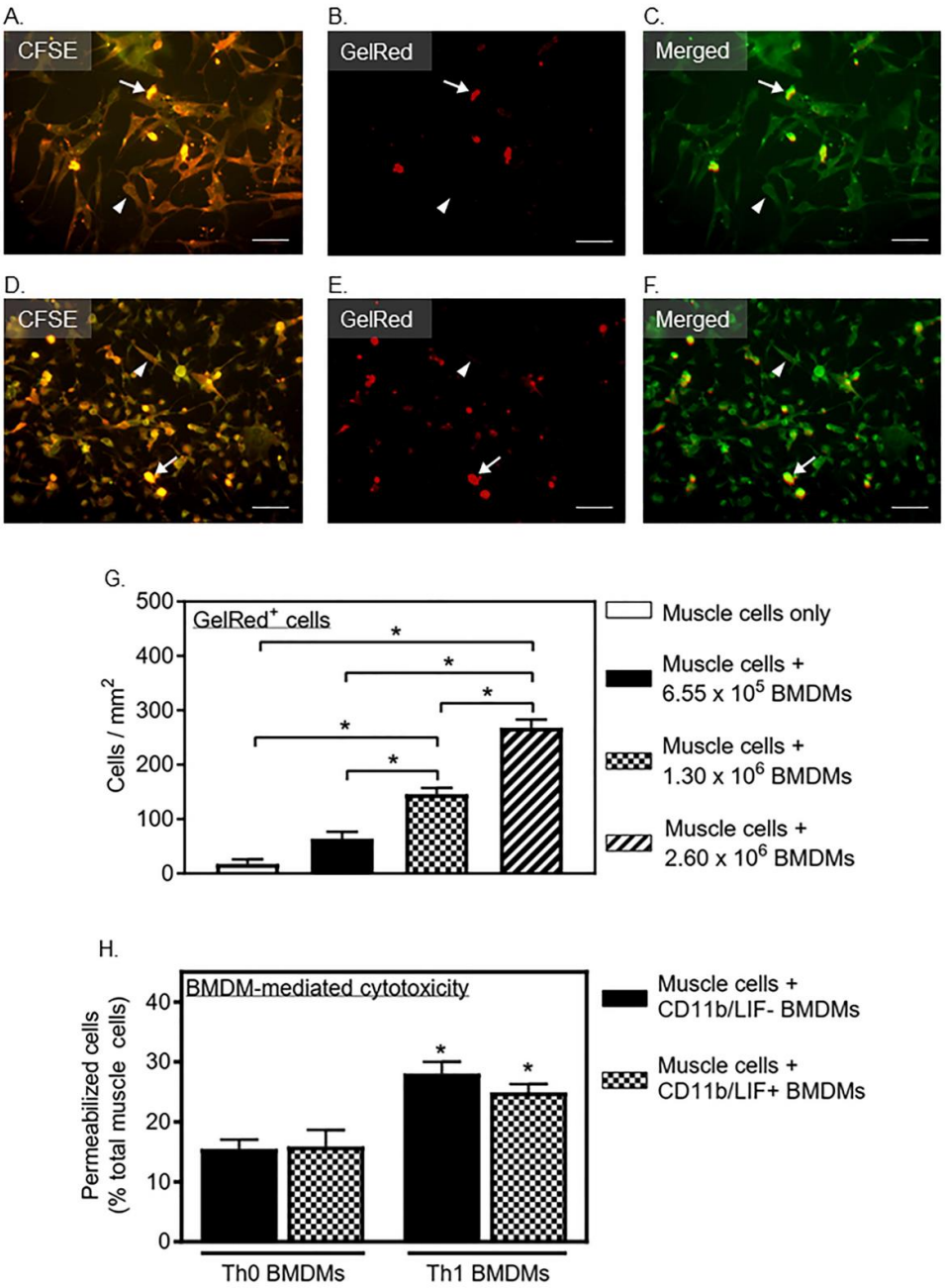

Figure 6. Expression of the CD11b/LIF transgene does not affect macrophage cytotoxic potential. Muscle cells were cultured in the absence **(A–C)** and presence of Th1-activated BMDMs **(D–F)**. Images of CFSE+ **(A, D)** and GelRed+ **(B, E)** muscle cells show an increase in the number of permeabilized muscle cells (CFSE+GelRed+; **C, F**) in the presence of Th1-activated BMDMs. The arrowheads indicate examples of non-permeabilized muscle cells (CFSE+GelRed-). The arrows indicate examples of permeabilized muscle cells (CFSE+GelRed+). Scale bars = 20 µm. Quantification of permeabilized cells shows an increase in muscle cell permeabilization with increasing numbers of Th1-stimulated BMDMs present in the co-cultures **(G)**. * indicates significant difference between the two groups indicated by the ends of the horizontal brackets ($P < 0.05$). *P*-values are based on one-way ANOVA with Tukey's multiple comparisons test. $N = 3$ for all groups except muscle cells only ($n = 2$). The proportion of permeabilized muscle cells is increased in co-cultures with Th1-stimulated BMDMs, but transgene expression does not affect BMDM-mediated permeabilization **(H)**. * indicates significant difference compared to genotype-matched, unstimulated BMDMs ($P < 0.05$). *P*-values are based on two-tailed t-tests. $N = 3$ for all groups. Bars = SEM for all data graphs.

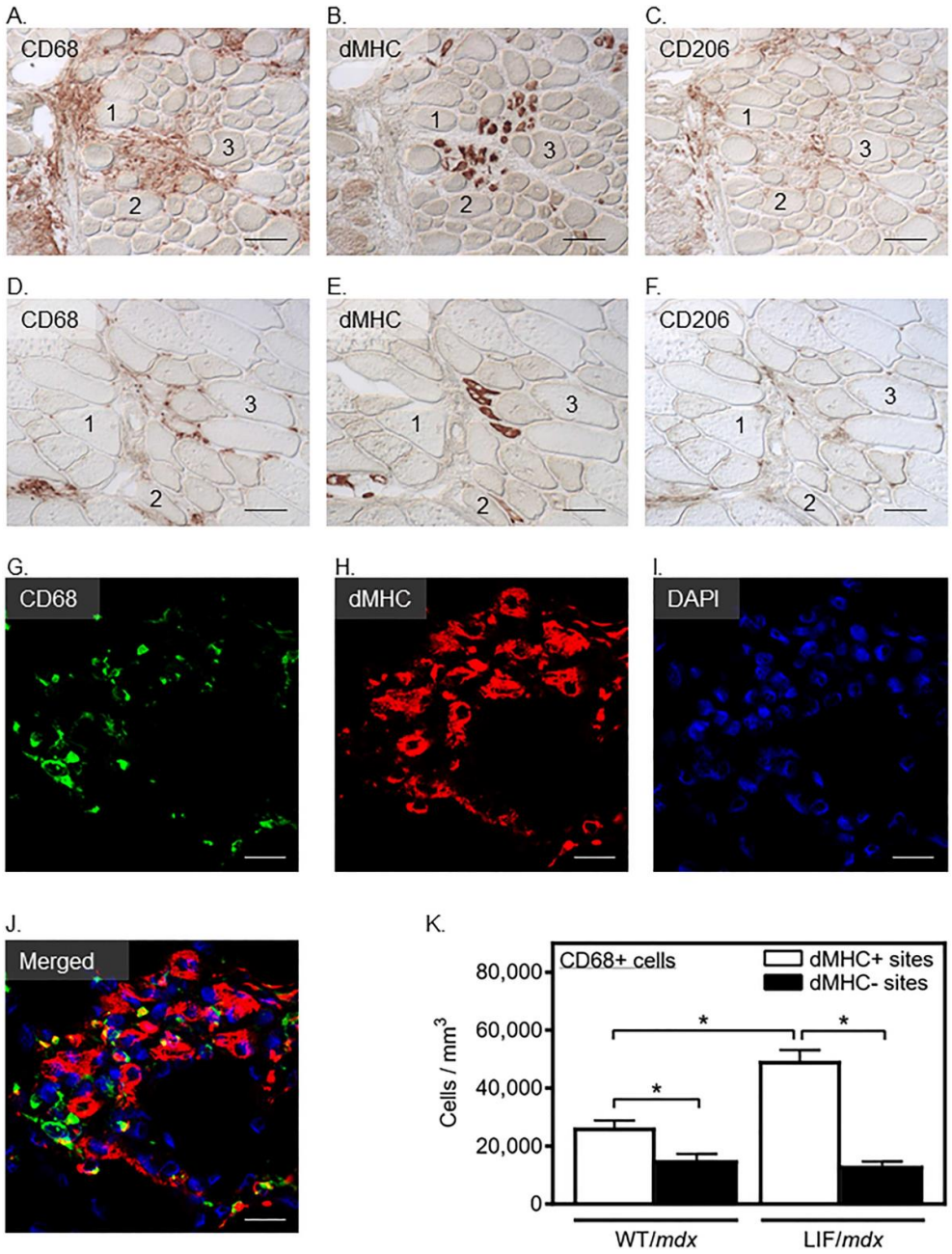

Figure 7. Macrophages accumulate at sites of muscle growth and repair in LIF/*mdx* muscles. Labeling of adjacent cross-sections from 1- **(A–C)** and 3-month **(D–F)** LIF/*mdx* muscles with anti-CD68 **(A, D)**, anti-dMHC **(B, E)** and anti-CD206 **(C, F)** show increased numbers of dMHC+ fibers in areas enriched with CD68+ macrophages. Fibers that are numbered '1,' '2' or '3' are individual fibers that appear in adjacent sections, to provide reference points in the sections. Scale bars = 50 µm. Cross-sections immunolabeled with anti-CD68 **(G)** and anti-dMHC **(H)** show clumped distributions of CD68+ macrophages at sites containing dMHC+ fibers **(G–J)**. Scale bars = 20 µm. Histogram showing increased numbers of CD68+ macrophages located at sites of dMHC+ regenerative areas relative to dMHC- areas in muscles of WT/*mdx* and LIF/*mdx* mice **(K)**. * indicates significant difference between the two groups indicated by the ends of the horizontal brackets ($P < 0.05$). *P*-values are based on two-tailed t-test for all groups. N = 5 for all groups. Bars = SEM.

may underlie the reduction in monocyte/macrophage recruitment and dispersion in LIF/*mdx* muscles.

The reduction in numbers of CD206+ macrophages, an M2-biased phenotype that can promote muscle fibrosis and regener-

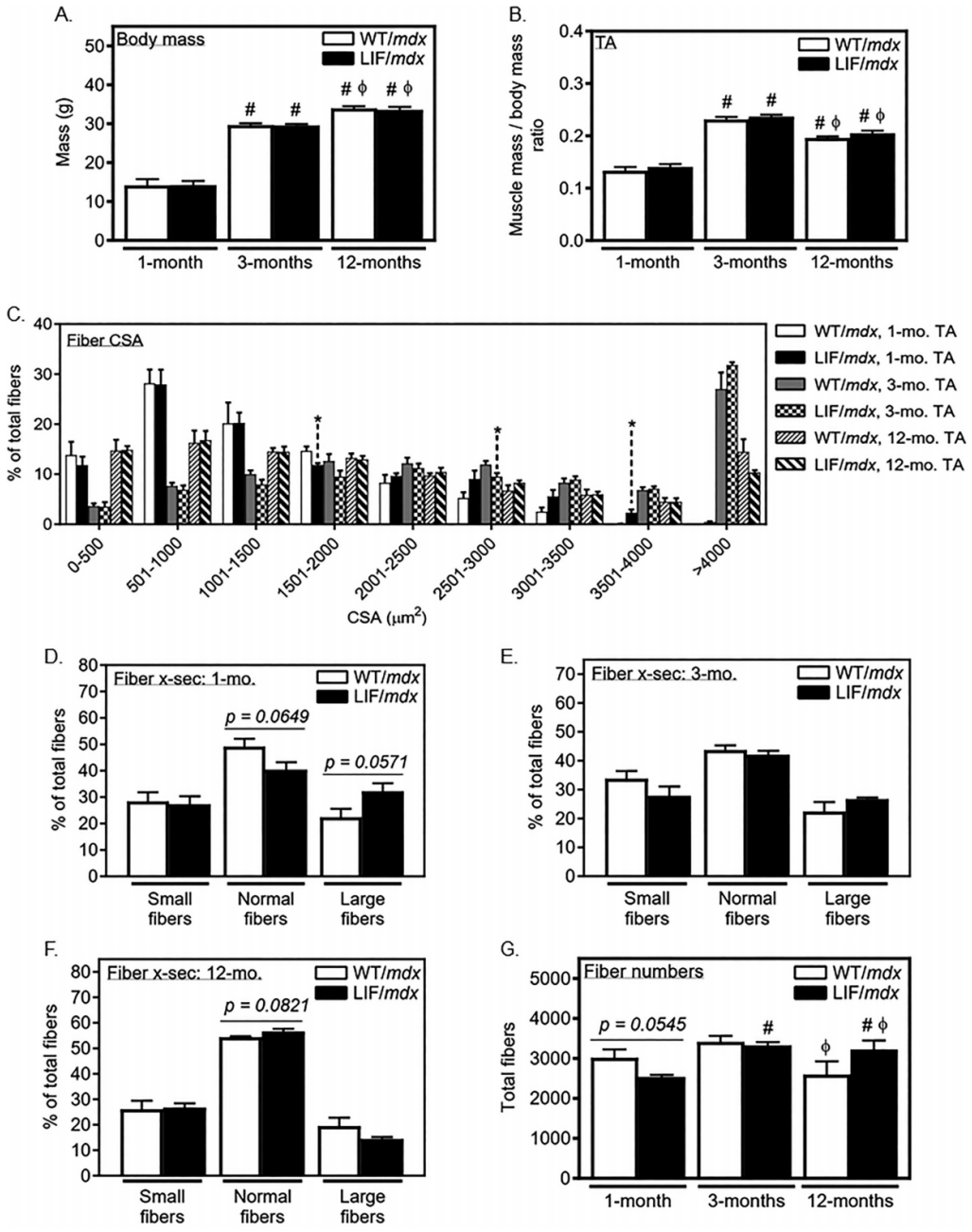

Figure 8. The transgene has little influence on muscle fiber size or growth. Measurements of body mass **(A)**, TA muscle mass to body mass ratio **(B)**, fiber CSA **(C–F)** and fiber numbers **(G)** show no significant difference between WT/*mdx* and LIF/*mdx* mice. * indicates significant difference compared to age-matched, WT/*mdx* mice at the same CSA bin ($P < 0.05$). # and Φ indicate significant difference compared to 1- and 3-month mice of the same genotype, respectively. *P*-values are based on two-tailed t-tests. $N =$ at least 6 for all groups shown in each data graph. Bars = SEM.

ation (18,19,22,65), indicates that elevated expression of LIF may influence macrophage phenotype, shifting them toward a pro-inflammatory, cytolytic M1-biased phenotype. That possibility is supported by previous findings which showed that elevated expression of LIF in inflammatory cells in *mdx* muscles reduced the expression of IL-4 and IL-10 (1), which can be produced by M2-biased macrophages and promote the M2 phenotype (21–23,29,30,32,34,35). However, this differs from the role of LIF in regulating macrophage phenotype in some other diseases. For example, blockade of LIF signaling in tumors in which LIF is expressed at high levels produced a reduction in the expression of M2 phenotypic markers in tumor-associated macrophages,

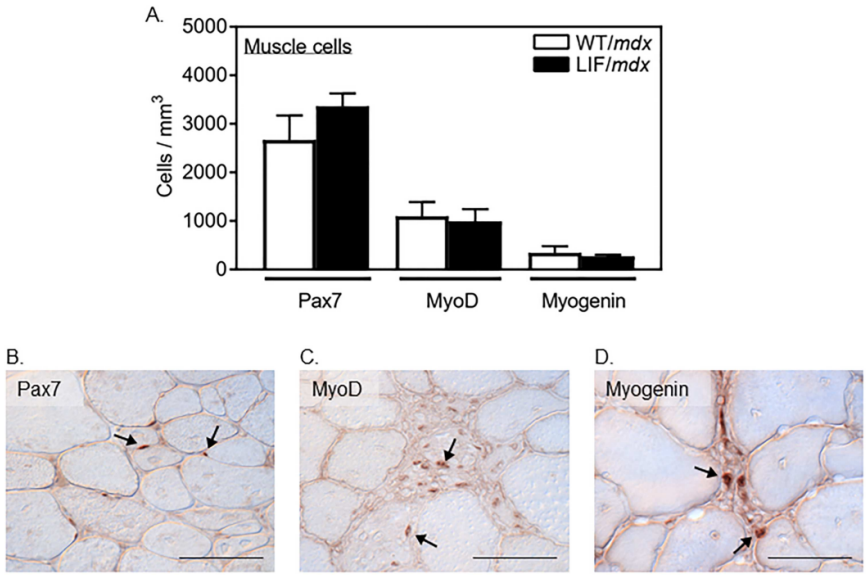

Figure 9. CD11b/LIF expression does not affect myogenesis in dystrophic muscle. Numbers of muscle cells expressing Pax7, MyoD or myogenin are unaffected by transgene expression in the muscles of *mdx* mice **(A)** ($P < 0.05$). *P*-values are based on two-tailed t-tests. $N = 4$ for all groups except WT/mdx mice used to quantify MyoD+ cells ($n = 5$). Bars = SEM. Representative images of Pax7+ **(B)**, MyoD+ **(C)** and myogenin+ **(D)** cells in LIF/*mdx* muscles. Examples of positively labeled cells are indicated with arrows. Scale bars = 50 µm.

including CD206 and CD163 (66). In addition, peripheral blood monocytes from human donors that were directly stimulated with LIF *in vitro* exhibited an M2-biased phenotype (17).

Our finding that expression of the CD11b/LIF transgene did not amplify the number of satellite cells in *mdx* muscles contrasts with previous observations which showed that LIF could increase numbers of C2C12 myoblasts *in vitro* by increasing their proliferation, reducing their apoptosis and delaying their differentiation into post-mitotic myotubes (3,4,6,7,67). However, whether elevations in LIF delivery to injured or diseased muscle affects satellite cell numbers *in vivo* has not been previously tested. The lack of effect of CD11b/LIF transgene expression on satellite cell numbers is therapeutically relevant because reductions in satellite cell numbers over the course of *mdx* muscular dystrophy contribute significantly to the decline of regenerative potential of dystrophic muscle (68–71). Similarly, expression of the CD11b/LIF transgene did not affect muscle fiber size in *mdx* mice. This differs from the increase in *mdx* muscle fiber size that resulted from suturing alginate rods that were infused with recombinant LIF to dystrophic muscles, allowing LIF to diffuse into the muscle for 3 months, leading to an increase in muscle fiber size (12). These differing treatment outcomes may reflect differences in the concentration, location and timing of LIF delivery to the *mdx* muscles, as indicated in investigations of the effects of LIF administration to acutely injured muscle. For example, continuous delivery of recombinant LIF to acutely injured muscle by a mini-osmotic pump increased muscle fiber growth (9) but systemic elevations of recombinant LIF using three intraperitoneal injections per week did not affect the growth of muscle fibers following acute injury (72).

Collectively, our current findings and previous work (1) show that the therapeutic value of inflammatory cell-mediated delivery of a CD11b/LIF transgene to dystrophic muscle may result primarily from its reduction of muscle fibrosis, and not from improving the growth or regenerative capacity of dystrophic muscle. Expression of the transgene produced long-term reductions in the expression and accumulation of connective tissue proteins in dystrophic muscle (1), which diminished muscle stiffness, which is a debilitating feature of muscular dystrophy (73–75). However, the potential for expression of the transgene to cause transient increases in muscle fiber damage early in the pathology, while reducing damage at later stages, indicates that this therapeutic approach would be best administered at later stages of the pathology, when progressive fibrosis is a prominent feature of the disease.

Materials and methods

Mice

All experimentation complied with relevant ethical regulations for animal testing and research, and experimental study protocols were approved by the Chancellor's Animal Research Committee at the University of California, Los Angeles. C57BL/10ScSn-Dmd*mdx*/J mice (*mdx* mice) were purchased from The Jackson Laboratory (Bar Harbor, ME) and bred in specific pathogen-free vivaria.

The CD11b/LIF *mdx* mouse line was generated using the following strategy. The complete *Mus musculus* LIF cDNA sequence (611-bp; NM_008501) was amplified by PCR and ligated into a pGL3-Basic vector (Promega) at the Nco I/Xba I sites. The pGL3-Basic vector also contained a 550-bp fragment of the human CD11b promoter at the Hind III site, upstream of the LIF insertion site. The 1215-bp, hCD11b/LIF fragment was isolated from pGL3-Basic by restriction endonuclease digestion with Xho I/Xba I and used for pronuclear injection into CB6F1 eggs to generate transgenic mice. Positive founders were identified by PCR screening for the hCD11b/LIF construct. Founder mice were backcrossed with C57BL/6 J mice for at least seven generations to generate hemizygous, transgenic (CD11b/LIF.Tg+) mice.

CD11b/LIF *mdx* transgenic mice were produced by crossing CD11b/LIF.Tg+, hemizygous males with *mdx* females to generate CD11b/LIF.Tg+ hemizygous, transgenic mice that were dystrophin-deficient. Dystrophin deficiency was verified by ARMS PCR screening and presence of the hCD11b/LIF construct was determined by PCR screening. The CD11b/LIF *mdx* mice were backcrossed with wild-type *mdx* mice for seven generations to produce hemizygous CD11b/LIF *mdx* mice. The CD11b/LIF *mdx* line is maintained as hemizygous to produce transgenic (LIF/*mdx*) mice and wild-type (WT/*mdx*) littermate controls for experimentation. We showed in previous work that muscle tissue from this transgenic mouse line has more than 60% greater expression of LIF than WT/*mdx* mice (1).

LIF/*mdx* and WT/*mdx* mice were euthanized by inhalation of 32% isoflurane (Zoetis) at 1-, 3- or 12-months of age. Body mass was recorded prior to tissue collection. Both tibialis anterior (TA) muscles were dissected from each mouse and the individual muscle masses were recorded. Investigators collecting data and performing analysis were aware of animal numbers only and were blinded to treatment groups.

Immunohistochemistry

The right TA muscle from each male mouse was dissected and immediately frozen in O.C.T. compound (Tissue-Tek) in liquid nitrogen-cooled isopentane. Muscle cross-sections were cut at a thickness of 10 µm at −20°C and mounted onto glass slides. Cross-sections were fixed for 10 min in acetone cooled to −80°C (for sections to be labeled with anti-CD11b, anti-CD206, anti-CD68, anti-developmental myosin heavy chain (dMHC) or anti-MyoD) or 2% paraformaldehyde (PFA) cooled to 4°C (for sections to be labeled with anti-LIF) or 4% PFA cooled to 4°C (for sections to be labeled with anti-Pax7 or anti-myogenin), or methanol cooled to 4°C (for sections to be labeled with anti-albumin). Endogenous peroxidase activity was quenched using 0.3% H_2O_2 for 10 min. Sections to be labeled for Pax7, MyoD and myogenin were immersed in antigen retrieval buffer (10 mM sodium citrate, 0.05% Tween-20, pH 6) at 95–100°C for 40 min prior to the peroxidase quench step. Sections to be labeled with anti-CD11b, anti-CD206 or anti-CD68 were blocked at room temperature (RT) in bovine serum albumin (BSA) buffer (3% BSA, 0.05% Tween-20, 0.2% gelatin, 0.15 M NaCl, 0.05 M Tris–HCl; 30 min). Sections to be labeled with anti-LIF were blocked in 3% ovalbumin buffer (3% ovalbumin, 0.05% Tween-20, 0.2% gelatin, 0.15 M NaCl, 0.05 M Tris–HCl; 30 min). Sections to be labeled with anti-Pax7, anti-MyoD or anti-myogenin were blocked with M.O.M. blocking buffer (Vector #PK-2200). Sections to be labeled with anti-albumin were blocked with 1% gelatin buffer (1% gelatin, 0.05% Tween-20, 0.15 M NaCl, 0.05 M Tris–HCl; 45 min). Sections were then incubated with rat anti-CD11b (1:100; overnight at 4°C; BioLegend #101202), rat anti-CD68 (1:100; 3 h at RT; AbD Serotec #MCA1957), rat anti-CD206 (1:50; 3 h at RT; AbD Serotec #MCA2235), goat anti-LIF (1:66; overnight at 4°C; R&D Systems #AB-449), rabbit anti-albumin (1:20; overnight at 4°C; Accurate Chemical #YNRRAALBP), mouse anti-dMHC (1:100; overnight at 4°C; Novocastra #NCL-MHCd), mouse anti-Pax7 (1:300; overnight at 4°; Developmental Studies Hybridoma Bank), mouse anti-MyoD (1:50; overnight at 4°C; BD Pharmingen #554130) or mouse anti-myogenin (1:50; overnight at 4°C; BD Pharmingen #556358). The sections were incubated with an appropriate biotinylated secondary antibody for 30 min at RT and then incubated with avidin D-conjugated horseradish peroxidase (1:1000; 30 min at RT; Vector #A-2004). The blocking reagent, secondary antibody and peroxidase reagent used for sections labeled for anti-dMHC, anti-Pax7, anti-MyoD and anti-myogenin were part of a M.O.M. detection kit (Vector #PK-2200). Positive signal was visualized in all slides with the peroxidase substrate, 3-amino-9-ethylcarbazole (AEC, Vector #SK-4200). The sections were washed in phosphate buffered saline (PBS) after each step, beginning with the fixation.

Stereology

The number of cells per volume of muscle was determined by measuring the total volume of each section using a stereological, point-counting technique to determine section area and then multiplying that value by the section thickness (10 µm). The numbers of immunolabeled cells in each section were counted and expressed as the number of cells per volume of each section ([total cells]/[mm^3]). Cell counts were performed on an Olympus BX50 microscope equipped with Nomarski optics.

Immunofluorescence

Macrophages expressing CCL2 were identified in tissue sections that were fixed in acetone cooled to −80°C. The sections were first blocked in 3% ovalbumin buffer for 30 min. The sections were then incubated with rat anti-F4/80 (1:50; Affimatrix eBioscience #14–8011) and goat anti-CCL2 (1:75; R&D Systems #AB-479-NA) overnight at 4°C and then incubated with a biotinylated anti-goat secondary antibody (1:200; Vector BA-9500) for 30 min at RT. The sections were then incubated with anti-rat fluorescent secondary antibody (1:200; DyLight 488; Abcam #ab102260) and DyLight 594 streptavidin (1:300; Vector SA-5594) in PBS for 30 min at RT before mounting with ProLong Gold mounting medium with DAPI (ThermoFisher Scientific #P36931). The sections were washed in PBS after each step, beginning with the fixation. The data were expressed as the proportion of F4/80+ macrophages that were also CCL2+ out of the total F4/80+ macrophage population ([F4/80+CCL2+ cells]/[total F4/80+ cells]). Cell counts were performed on a Leica DMRXA fluorescence microscope. Confocal images were acquired on a Leica TCS-SP5 confocal microscope.

The distribution of CD68+ macrophages relative to sites in muscle that were enriched in dMHC+ fiber was assayed in muscle sections following fixation in acetone cooled to −80°C. The sections were blocked in M.O.M. blocking buffer (Vector #PK-2200) for 1 h at RT. The sections were then incubated in rat anti-CD68 (1:100; Serotec #MCA 1957) and mouse anti-dMHC (1:100; Novocastra #NHC-MHCd) overnight at 4°C in M.O.M. protein dilute (Vector #PK-2200). The sections were incubated with anti-rat (1:200; DyLight 594; Abcam #ab102260) and anti-mouse (1:200; DyLight 488; Vector #DI-594) fluorescent antibodies for 30 min at RT before mounting with ProLong Gold Mounting medium with DAPI. The sections were washed in PBS following each step of their processing. Data were collected by identifying sites containing dMHC+ fibers and then counting the numbers of CD68+ macrophages in a standardized volume of 289 000 μm^3 surrounding the dMHC+ fibers. The volume utilized was calculated using a point-counting technique to calculate the area of the field of view surrounding dMHC+ sites (28 900 μm^2) and multiplying the area by the section thickness (10 µm). All sites containing dMHC+ fibers in each sample were used for data collection. An equivalent number of healthy sites of equal volume were used to quantify the numbers of CD68+ macrophages at sites without dMHC+ fibers in each sample. The data were expressed as the density of CD68+ cells per mm^3 (CD68+ cells/mm^3). Cell counts were performed on an Olympus BH2 fluorescence microscope.

Table 1.

Gene	Forward	Reverse
tpt1	GGAGGGCAAGATGGTCAGTAG	CGGTGACTACTGTGCTTTCG
rnps1	AGGCTCACCAGGAATGTGAC	CTTGGCCATCAATTTGTCCT
hprt1	GCTGACCTGCTGGATTACATTAAAG	CCACCAATAACTTTTATGTCCCC
lif	GTCTTGGCCGCAGGGATTG	GCACAGGTGGCATTTACAGG
ccl2	GCTCAGCCAGATGCAGTTAAC	CTCTCTCTTGAGCTTGGTGAC

Confocal images were acquired on a Leica TCS-SP5 confocal microscope.

The relative quantity of LIF in LIF/*mdx* and WT/*mdx* muscle fibers was assayed by determining the mean fluorescence intensity (MFI) of muscle fibers following labeling with anti-LIF and a fluorescent secondary antibody. Sections were fixed in 2% PFA cooled to 4°C. PFA-induced autofluorescence was quenched by submerging the sections in 0.1 M glycine in PBS for 5 min. The sections were incubated with goat anti-LIF (1:66; R&D Systems #AB-449) overnight at 4°C. The sections were then incubated with a biotinylated anti-goat secondary antibody (1:200; Vector #BA-9500) for 30 min at RT. The sections were incubated with a fluorophore-conjugated streptavidin (1:300; DyLight 594; Vector #SA-5594) for 30 min at RT before mounting with ProLong Gold Mounting medium with DAPI. The sections were washed in PBS after each step. The MFI of 20 randomly selected muscle fibers in each sample was quantified using ImageJ (National Institutes of Health). Images used for MFI measurements were acquired on an Olympus BH2 fluorescence microscope. Confocal images were acquired on a Leica TCS-SP5 confocal microscope.

Myofiber number quantification and CSA measurements

Cross-sections from the TA muscle mid-belly were stained with hematoxylin (Vector #H-3401) for 10 min. Muscle fiber CSA was quantified using ImageJ (National Institutes of Health). The average CSA of each sample was calculated from 500 randomly sampled fibers. The classification for large or small fibers was determined by setting three standard deviations from the mean CSA for the control group at each time-point as previously described (76). Fibers were considered to be small or large in 1-month TAs if the CSA was less than 796 μm^2 or greater than 1785 μm^2, respectively. Fibers were considered to be small or large in 3-month TAs if the CSA was less than 2000 μm^2 or greater than 4414 μm^2, respectively. Fibers were considered to be small or large in 12-month TAs if the CSA was less than 832 μm^2 or greater than 3453 μm^2, respectively. Fibers were considered normal if their CSA was between the threshold measurements for small and large fibers. Images used for CSA measurements were acquired on an Olympus BH2 microscope equipped with Nomarski optics.

RNA isolation and quantitative PCR

Cell cultures were washed with Dulbecco's phosphate-buffered saline (DPBS, Sigma-Aldrich #5652) cooled to 4°C and the RNA was isolated in TRIzol Reagent (Ambion #15596018) according to the manufacturer's protocol. The isolated RNA was further cleaned and concentrated using an RNA Clean and Concentrator-5 kit (Zymo Research #R1014). The RNA was quantified, reversed transcribed to cDNA, and used for qPCR as previously described (18,77). We followed established guidelines for experimental design, data normalization and data analysis (78–80). Primer sequences used for qPCR are listed in Table 1.

Muscle macrophage isolation

Skeletal muscles from male and female, 1-month-old *mdx* mice were minced in 1.25 mg/ml collagenase types IA and IV (Sigma-Aldrich #C9891, #C5138) in Dulbecco's Modified Eagle medium (Sigma #D1152) and digested at 37°C for 1 h with gentle trituration each 15 min. The digestate was diluted with DPBS, filtered through 70 µm mesh filters and the liberated cells collected by centrifugation. The cells were resuspended in DPBS, overlaid on Histopaque-1077 (Sigma-Aldrich #1077-1) and centrifuged at 400 x g for 30 min at RT. Macrophages were collected from the DPBS-Histopaque interface and RNA isolated from the cells as described above. QPCR was performed using *tpt1* and *hprt1* as house-keeping genes. Muscle macrophages were collected from five WT/*mdx* and three LIF/*mdx* mice.

Preparation of BMDMs for RNA analysis

BMCs were aseptically flushed from femurs and tibiae with DPBS and treated with ACK lysis buffer (Lonza #10-548E) to lyse red blood cells. BMCs from three male mice of the same genotype were pooled together to generate CD11b/LIF- and CD11b/LIF+ BMDMs. Following a wash with DPBS and filtration through a 70 µm mesh filter, the BMCs were plated in 6-cm tissue culture dishes (1×10^7 cells/dish) in macrophage growth medium (RPMI-1640 (Sigma #R6504), 20% heat-inactivated fetal bovine serum (HI-FBS, Omega Scientific #FB-11), 100 U/ml penicillin +100 µg/ml streptomycin (1% Pen/Strep, Gibco #15140-122), 10 ng/ml macrophage colony-stimulating factor (M-CSF, Cell Applications Inc. #RP2008)) at 37°C in 5% CO_2 for 6 days. The macrophage growth medium was replenished on days 3 and 5 post-plating. On day 6, adherent cells were activated to an M1-biased or M2-biased phenotype in macrophage activation medium (DMEM (Sigma-Aldrich #D1152), 0.25% HI-FBS, 1% Pen/Strep, 10 ng/ml M-CSF and either Th1 cytokines (10 ng/ml IFNγ and 10 ng/ml TNFα; BD Pharmingen #554587 and 554 589) or Th2 cytokines (25 ng/ml IL-4 and 10 ng/ml IL-10; BD Pharmingen #550067 and 550 070)) for 48 h. The activation medium was replenished after the first 24 h of activation. Th0 BMDMs were generated by culturing the adherent cells in macrophage activation medium without Th1 or Th2 cytokines. RNA from the cells was isolated as described above. QPCR was performed using *tpt1* and *rnps1* as house-keeping genes.

ELISA analysis of CCL2 in BMDM conditioned media

CCL2 secretion by BMDMs was measured as previously described (1). Briefly, BMDMs from wild-type, WT/*mdx* and LIF/*mdx* mice were generated as described above. BMCs from two male mice of each genotype were pooled to generate the BMDMs. On the sixth day of culture, the BMDMs were switched to DMEM containing

0.25% HI-FBS, 1% Pen/Strep and 10 ng/ml M-CSF, with or without 10 ng/ml recombinant mouse LIF (eBioscience #14-8521). After 24 h of stimulation, the conditioned media were collected, briefly centrifuged to remove particulates, and analyzed for BMDM-secreted CCL2 (Duoset ELISA, R&D Systems, #DY479) according to the manufacturer's instructions.

Cytotoxicity assay

Macrophage-mediated cytotoxicity was assessed using co-cultures of BMDMs and C2C12 muscle cells. BMDMs from one female mouse of each genotype (WT/*mdx* and LIF/*mdx*) were generated as described above with the following modifications. Freshly isolated BMCs were plated at 5×10^6 cells per 10-cm, low-adherence dish (Eisco #CH0372C) in macrophage growth medium for 6 days. Adherent cells were activated to a cytotoxic, M1-biased phenotype using activation medium containing Th1 cytokines for 24 h. Unstimulated BMDMs were cultured in activation medium without Th1 cytokines. Following activation, the BMDMs were washed with DPBS and detached from the dishes using Cellstripper (Corning #25-056-Cl) for 10 min. The detached BMDMs were centrifuged at 526 x g for 5 min, resuspended in DPBS, and total cell numbers were calculated using a hemocytometer. BMDMs were resuspended in cytotoxicity assay medium (Hank's balanced salt solution (HBSS; Sigma-Aldrich #H1387), 0.25% HI-FBS, 400 µM L-arginine).

One day prior to co-culture, 12-well plates were prepared by adding 8-mm glass coverslips coated with 2% gelatin to each well. C2C12 muscle cells were plated in the 12-well plates at 5.94×10^4 cells per well in growth medium (DMEM (Sigma-Aldrich #D1152), 10% FBS, 1% Pen/Strep) for 24 h to allow the cells to reach 70% confluency and attach to the glass coverslips. The muscle cells were then washed with DPBS and fluorescently labeled with CFDA-SE (Accurate Chemical #14456) to allow visual differentiation from unlabeled BMDMs. The muscle cells were incubated in labeling medium (HBSS, 0.1% BSA, 5 µM CFDA-SE) for 10 min at 37°C in 5% CO_2. CFDA-SE is a cell membrane-permeable dye that does not cause cytotoxicity at the concentration used. Intracellular CFDA-SE is cleaved by endogenous esterases to form cell membrane-impermeable CFSE. CFSE is a fluorescent molecule (488 nm emission) that binds intracellular proteins, permanently labeling cells. The cells were washed with growth medium to remove residual CFDA-SE from each well. The cells were then incubated in growth medium for 5 min at 37°C in 5% CO_2 to allow unreacted CFDA-SE to flow out of the cells and avoid labeling BMDMs. The labeled cells received a final wash using HBSS to remove residual growth medium.

The BMDMs were added to the muscle cultures at 1.3×10^6 BMDMs/well in cytotoxicity assay medium. Following 6 h of co-culture at 37°C in 5% CO_2, each co-culture well was washed with DPBS. GelRed (Biotium #41003-1) diluted in cytotoxicity assay medium (1:2500 dilution) was added to each well for 10 min at 37°C in 5% CO_2 to label permeabilized muscle cells. GelRed is a cell membrane-impermeable, fluorescent dye (593 nm emission) that binds to nucleic acids. Following a final DPBS wash, the glass coverslips were removed from each well and mounted onto glass microscope slides using Fluoro-Gel (Electron Microscopy Sciences #17985-10).

Fluorescence microscopy with an Olympus BH2 microscope was used to collect cytotoxicity data based on the following criteria: BMDMs were CFSE-GelRed-, non-permeabilized muscle cells were CFSE+GelRed- and permeabilized muscle cells were CFSE+GelRed+. Data were expressed as the proportion of permeabilized muscle cells out of total C2C12 cells ([CFSE+GelRed+ cells]/[total CFSE+ cells]) on each coverslip. Three coverslips were included per group. The proportion of permeabilized muscle cells was quantified from 15 randomly chosen fields per coverslip. The average proportion of permeabilized muscle cells per coverslip was calculated and used as a single datum to calculate the mean and SEM for each group. The data were normalized to a muscle cell-only control group. Data were verified by repeating the experiment in triplicate.

In a separate experiment, we verified the sensitivity of this assay by testing the influence of increasing numbers of Th1-stimulated BMDMs on muscle cell lysis. The experiment was repeated as described above. The muscle cell cultures were co-cultured with no BMDMs, low numbers of BMDMs (6.55×10^5 cells), medium numbers of BMDMs (1.30×10^6 cells) or high numbers of BMDMs (2.60×10^6 cells). Because the wells containing high numbers of BMDMs prevented accurate counts of total muscle cells, data were expressed as GelRed+ cells/mm^2.

Chemotaxis assay

BMDMs were isolated from two male mice of each genotype (WT/*mdx* and LIF/*mdx*) using the following strategy. BMCs were aseptically flushed from the femurs and tibiae as described earlier. The BMCs were plated at 1.0×10^7 cells per 6-cm, ultra-low attachment dish (Corning #3261) in macrophage growth medium containing Th1 or Th2 cytokines for 24 h at 37°C in 5% CO_2. Unpolarized BMDMs were cultured in macrophage growth medium without additional cytokines. The cells were washed with DPBS and adherent cells were detached using Cellstripper as described previously. The cells were collected and BMDMs were purified using a Histopaque-1077 gradient (Sigma-Aldrich #10771) according to the manufacturer's instructions. The BMDMs were resuspended in chemotaxis medium (RPMI-1640, 1% Pen/Strept, 1% BSA).

We tested the chemotactic ability of the BMDMs in response to CCL2 using a chemotaxis chamber (Neuro Probe #AP48) following the manufacturer's protocol. We used 10 ng/ml of CCL2 (R&D Systems #479-JE/CF) in chemotaxis medium to measure chemotaxis. Spontaneous migration was measured using chemotaxis medium without CCL2. Cells in the chemotaxis chamber were incubated for 2 h at 37°C in 5% CO_2.

Three wells were included in each group. The numbers of migratory cells were quantified in five randomly chosen fields per well. The average number of migratory cells per field in each well was calculated and used as a single datum to calculate the mean and SEM for each group. Data were verified by repeating the experiment in triplicate. Data were collected using an Olympus BX50 microscope equipped with Nomarski optics.

Statistical analysis

All data are presented as mean ± SEM. Statistical significance was calculated using an unpaired Student's t-test, one-way analysis of variance (ANOVA) with Tukey's multiple comparisons test, or two-way ANOVA with Tukey's multiple comparisons test using Prism 7 (GraphPad). Differences with a P-value < 0.05 were considered statistically significant.

Acknowledgements

Confocal laser scanning microscopy was performed at the California NanoSystems Institute Advanced Light Microscopy-/Spectroscopy Shared Resource Facility at UCLA. DNA microinjections for the production of the CD11b/LIF transgenic mice

were performed at the University of California, Irvine Transgenic Mouse Facility. The Pax7 hybridoma developed by T.M. Jessell, Columbia University, was obtained from the Developmental Studies Hybridoma Bank, created by the NICHD of the NIH and maintained at The University of Iowa, Department of Biology, Iowa City, IA 52242.

Funding

This work was supported by the National Institute of Arthritis and Musculoskeletal and Skin Diseases of the National Institutes of Health under award numbers F31AR071783 (to IF), F32AR065845 (to SSW) and RO1AR066036, RO1AR062579 and R21AR066817 (to JGT).

Conflict of interest

The authors have no competing interests to declare.

Abbreviations

Duchenne muscular dystrophy = DMD
leukemia inhibitory factor = LIF.
bone marrow cells = BMCs.
bone marrow-derived macrophages = BMDMs.
C-C motif chemokine ligand-2 = CCL2.
recombinant LIF = rLIF.
tibialis anterior = TA.
developmental myosin heavy chain = dMHC.
C57BL/10ScSn-Dmd*mdx*/J mice = *mdx* mice.
paraformaldehyde = PFA.
room temperature = RT.
bovine serum albumin = BSA.
phosphate buffered saline = PBS.
mean fluorescence intensity = MFI.
Dulbecco's phosphate-buffered saline = DPBS.
heat-inactivated fetal bovine serum = HI-FBS.
penicillin/streptomycin = Pen/Strep.
macrophage colony-stimulating factor = M-CSF.
Dulbecco's modified eagle medium = DMEM.
Hank's balanced salt solution = HBSS.

References

1. Welc, S.S., Flores, I., Wehling-Henricks, M., Ramos, J., Wang, Y., Bertoni, C. and Tidball, J.G. (2019) Targeting a therapeutic LIF transgene to muscle via the immune system ameliorates muscular dystrophy. *Nat. Commun.*, **10**, 1–17.
2. Dadgar, S., Wang, Z., Johnston, H., Kesari, A., Nagaraju, K., Chen, Y., Hill, D.A., Partridge, T.A., Giri, M., Freishtart, R.J. *et al.* (2014) Asynchronous remodeling is a driver of failed regeneration in Duchenne muscular dystrophy. *J. Cell Biol.*, **207**, 139–158.
3. Austin, L. and Burgess, A.W. (1991) Stimulation of myoblast proliferation in culture by leukaemia inhibitory factor and other cytokines. *J. Neurol. Sci.*, **101**, 193–197.
4. Austin, L., Bower, J., Kurek, J. and Vakakis, N. (1992) Effects of leukaemia inhibitory factor and other cytokines on murine and human myoblast proliferation. *J. Neurol. Sci.*, **112**, 185–191.
5. Broholm, C., Laye, M.J., Brandt, C., Vadalasetty, R., Pilegaard, H., Pedersen, B.K. and Scheele, C. (2011) LIF is a contraction-induced myokine stimulating human myocyte proliferation. *J. Appl. Phys.*, **111**, 251–259.
6. Spangenburg, E.E. and Booth, F.W. (2002) Multiple signaling pathways mediate LIF-induced skeletal muscle satellite cell proliferation. *Am. J. Physiol. Cell Physiol.*, **283**, C204–C211.
7. Hunt, L.C., Upadhyay, A., Jazayeri, J.A., Tudor, E.M. and White, J.D. (2011) Caspase-3, myogenic transcription factors and cell cycle inhibitors are regulated by leukemia inhibitory factor to mediate inhibition of myogenic differentiation. *Skelet. Muscle*, **1**, 17.
8. Gao, S., Durstine, J.L., Koh, H.-J., Carver, W.E., Frizzell, N. and Carson, J.A. (2017) Acute myotube protein synthesis regulation by IL-6-related cytokines. *Am. J. Physiol. Cell Physiol.*, **313**, C487–C500.
9. Barnard, W., Bower, J., Brown, M.A., Murphy, M. and Austin, L. (1994) Leukemia inhibitory factor (LIF) infusion stimulates skeletal muscle regeneration after injury: injured muscle expresses lif mRNA. *J. Neurol. Sci.*, **123**, 108–113.
10. Finkelstein, D.I., Bartlett, P.F., Horne, M.K. and Cheema, S.S. (1996) Leukemia inhibitory factor is a myotrophic and neurotrophic agent that enhances the reinnervation of muscle in the rat. *J. Neurosci. Res.*, **46**, 122–128.
11. Kurek, J.B., Bower, J.J., Romanella, M., Koentgen, F., Murphy, M. and Austin, L. (1997) The role of leukemia inhibitory factor in skeletal muscle regeneration. *Muscle Nerve*, **20**, 815–822.
12. Austin, L., Bower, J.J., Bennett, T.M., Lynch, G.S., Kapsa, R., White, J.D., Barnard, W., Gregorevic, P. and Byrne, E. (2000) Leukemia inhibitory factor ameliorates muscle fiber degeneration in the mdx mouse. *Muscle Nerve*, **23**, 1700–1705.
13. Mori, M., Yamaguchi, K., Honda, S., Nagasaki, K., Ueda, M., Abe, O. and Abe, K. (1991) Cancer cachexia syndrome developed in nude mice bearing melanoma cells producing leukemia-inhibitory factor. *Cancer Res.*, **51**, 6656–6659.
14. Tisdale, M.J. (2002) Cachexia in cancer patients. *Nat. Rev. Cancer*, **2**, 862–871.
15. Seto, D.N., Kandarian, S.C. and Jackman, R.W. (2015) A key role for leukemia inhibitory factor in C26 cancer cachexia. *J. Biol. Chem.*, **290**, 19976–19986.
16. Hunt, L.C., Upadhyay, A., Jazayeri, J.A., Tudor, E.M. and White, J.D. (2013) An anti-inflammatory role for leukemia inhibitory factor receptor signaling in regenerating skeletal muscle. *Histochem. Cell Biol.*, **139**, 13–34.
17. Duluc, D., Delneste, Y., Tan, F., Moles, M., Grimaud, L., Lenoir, J., Preisser, L., Anegon, I., Catala, L., Ifrah, N. *et al.* (2007) Tumor-associated leukemia inhibitory factor and IL-6 skew monocyte differentiation into tumor-associated macrophage-like cells. *Blood*, **110**, 4319–4330.
18. Villalta, S.A., Deng, B., Rinaldi, C., Wehling-Henricks, M. and Tidball, J.G. (2011) IFN-γ promotes muscle damage in the mdx mouse model of Duchenne muscular dystrophy by suppressing M2 macrophage activation and inhibiting muscle cell proliferation. *J. Immunol.*, **187**, 5419–5428.
19. Wehling-Henricks, M., Jordan, M.C., Gotoh, T., Grody, W.W., Roos, K.P. and Tidball, J.G. (2010) Arginine metabolism by macrophages promotes cardiac and muscle fibrosis in mdx muscular dystrophy. *PLoS One*, **5**, e10763.
20. Deng, B., Wehling-Henricks, M., Villalta, S.A., Wang, Y. and Tidball, J.G. (2012) IL-10 triggers changes in macrophage phenotype that promote muscle growth and regeneration. *J. Immunol.*, **189**, 3669–3680.
21. Welc, S.S., Wehling-Henricks, M., Antoun, J., Ha, T.T., Tous, I. and Tidball, J.G. (2020) Differential effects of myeloid cell

PPARδ and IL-10 in regulating macrophage recruitment, phenotype, and regeneration following acute muscle injury. *J. Immunol.*, **205**, 1664–1677.
22. Villalta, S.A., Nguyen, H.X., Deng, B., Gotoh, T. and Tidball, J.G. (2009) Shifts in macrophage phenotypes and macrophage competition for arginine metabolism affect the severity of muscle pathology in muscular dystrophy. *Hum. Mol. Genet.*, **18**, 482–496.
23. Villalta, S.A., Rinaldi, C., Deng, B., Liu, G., Fedor, B. and Tidball, J.G. (2011) Interleukin-10 reduces the pathology of mdx muscular dystrophy by deactivating M1 macrophages and modulating macrophage phenotype. *Hum. Mol. Genet.*, **20**, 790–805.
24. Wehling-Henricks, M., Lee, J.J. and Tidball, J.G. (2004) Prednisolone decreases cellular adhesion molecules required for inflammatory cell infiltration in dystrophin-deficient skeletal muscle. *Neuromuscul. Disord.*, **14**, 483–490.
25. Nguyen, H.X., Lusis, A.J. and Tidball, J.G. (2005) Null mutation of myeloperoxidase in mice prevents mechanical activation of neutrophil lysis of muscle cell membranes in vitro and in vivo. *J. Physiol.*, **565**, 403–413.
26. Wehling-Henricks, M., Sokolow, S., Lee, J.J., Myung, K.H., Villalta, S.A. and Tidball, J.G. (2008) Major basic protein-1 promotes fibrosis of dystrophic muscle and attenuates the cellular immune response in muscular dystrophy. *Hum. Mol. Genet.*, **17**, 2280–2292.
27. Tidball, J.G. and Villalta, S.A. (2010) Regulatory interactions between muscle and the immune system during muscle regeneration. *Am. J. Physiol. Regul. Integr. Comp. Physiol.*, **298**, R1173–R1187.
28. Locati, M., Mantovani, A. and Sica, A. (2013) Chapter Six - Macrophage Activation and Polarization as an Adaptive Component of Innate Immunity. In *Advances in Immunology, Development and Function of Myeloid Subsets*. Academic Press, Vol. **120**, pp. 163–184.
29. Murray, P.J., Allen, J.E., Biswas, S.K., Fisher, E.A., Gilroy, D.W., Goerdt, S., Gordon, S., Hamilton, J.A., Ivashkiv, L.B., Lawrence, T. *et al.* (2014) Macrophage activation and polarization: nomenclature and experimental guidelines. *Immunity*, **41**, 14–20.
30. Mills, C.D., Kincaid, K., Alt, J.M., Heilman, M.J. and Hill, A.M. (2000) M-1/M-2 Macrophages and the Th1/Th2 paradigm. *J. Immunol.*, **164**, 6166–6173.
31. Tidball, J.G. (2017) Regulation of muscle growth and regeneration by the immune system. *Nat. Rev. Immunol.*, **17**, 165–178.
32. Lang, R., Patel, D., Morris, J.J., Rutschman, R.L. and Murray, P.J. (2002) Shaping gene expression in activated and resting primary macrophages by IL-10. *J. Immunol.*, **169**, 2253–2263.
33. Mosser, D.M. (2003) The many faces of macrophage activation. *J. Leukoc. Biol.*, **73**, 209–212.
34. Mosser, D.M. and Zhang, X. (2008) Interleukin-10: new perspectives on an old cytokine. *Immunol. Rev.*, **226**, 205–218.
35. Martinez-Pomares, L., Reid, D.M., Brown, G.D., Taylor, P.R., Stillion, R.J., Linehan, S.A., Zamze, S., Gordon, S. and Wong, S.Y.C. (2003) Analysis of mannose receptor regulation by IL-4, IL-10, and proteolytic processing using novel monoclonal antibodies. *J. Leukoc. Biol.*, **73**, 604–613.
36. Hakim, C.H., Grange, R.W. and Duan, D. (2011) The passive mechanical properties of the extensor digitorum longus muscle are compromised in 2- to 20-mo-old mdx mice. *J. Appl. Physiol.*, **110**, 1656–1663.
37. Hourdé, C., Joanne, P., Noirez, P., Agbulut, O., Butler-Browne, G. and Ferry, A. (2013) Protective effect of female gender–related factors on muscle force-generating capacity and fragility in the dystrophic mdx mouse. *Muscle Nerve*, **48**, 68–75.
38. Wehling-Henricks, M., Li, Z., Lindsey, C., Wang, Y., Welc, S.S., Ramos, J.N., Khanlou, N., Kuro-o, M. and Tidball, J.G. (2016) Klotho gene silencing promotes pathology in the mdx mouse model of Duchenne muscular dystrophy. *Hum. Mol. Genet.*, **25**, 2465–2482.
39. Mojumdar, K., Liang, F., Giordano, C., Lemair, C., Danialou, G., Okazaki, T., Bourdon, J., Rafei, M., Galipeau, J., Divangahi, M. and Petrof, B.J. (2014) Inflammatory monocytes promote progression of Duchenne muscular dystrophy and can be therapeutically targeted via CCR2. *EMBO Mol. Med.*, **6**, 1476–1492.
40. Lu, H., Huang, D., Ransohoff, R.M. and Zhou, L. (2011) Acute skeletal muscle injury: CCL2 expression by both monocytes and injured muscle is required for repair. *FASEB J.*, **25**, 3344–3355.
41. Lu, H., Huang, D., Saederup, N., Charo, I.F., Ransohoff, R.M. and Zhou, L. (2010) Macrophages recruited via CCR2 produce insulin-like growth factor-1 to repair acute skeletal muscle injury. *FASEB J.*, **25**, 358–369.
42. Zhao, W., Wang, X., Ransohoff, R.M. and Zhou, L. (2016) CCR2 deficiency does not provide sustained improvement of muscular dystrophy in mdx5cv mice. *FASEB J.*, **31**, 35–46.
43. Warren, G.L., Hulderman, T., Mishra, D., Gao, X., Millecchia, L., O'Farrell, L., Kuziel, W.A. and Simeonova, P.P. (2004) Chemokine receptor CCR2 involvement in skeletal muscle regeneration. *FASEB J.*, **19**, 413–415.
44. Warren, G.L., O'Farrell, L., Summan, M., Hulderman, T., Mishra, D., Luster, M.I., Kuziel, W.A. and Simeonova, P.P. (2004) Role of CC chemokines in skeletal muscle functional restoration after injury. *Am. J. Physiol. Cell Physiol.*, **286**, C1031–C1036.
45. Porter, J.D., Guo, W., Merriam, A.P., Khanna, S., Cheng, G., Zhou, X., Andrade, F.H., Richmonds, C. and Kaminski, H.J. (2003) Persistent over-expression of specific CC class chemokines correlates with macrophage and T-cell recruitment in mdx skeletal muscle. *Neuromuscul. Disord.*, **13**, 223–235.
46. Summan, M., McKinstry, M., Warren, G.L., Hulderman, T., Mishra, D., Brumbaugh, K., Luster, M.I. and Simeonova, P.P. (2003) Inflammatory mediators and skeletal muscle injury: a DNA microarray analysis. *J. Interf. Cytokine Res.*, **23**, 237–245.
47. Kurihara, T., Warr, G., Loy, J. and Bravo, R. (1997) Defects in macrophage recruitment and host defense in mice lacking the CCR2 chemokine receptor. *J. Exp. Med.*, **186**, 1757–1762.
48. Amano, H., Morimoto, K., Senba, M., Wang, H., Ishida, Y., Kumatori, A., Yoshimine, H., Oishi, K., Mukaida, N. and Nagatake, T. (2004) Essential contribution of monocyte chemoattractant protein-1/C-C chemokine ligand-2 to resolution and repair processes in acute bacterial pneumonia. *J. Immunol.*, **172**, 398–409.
49. Rollins, B.J. (1996) Monocyte chemoattractant protein 1: a potential regulator of monocyte recruitment in inflammatory disease. *Mol. Med. Today*, **2**, 198–204.
50. Tidball, J.G. and Wehling-Henricks, M. (2007) Macrophages promote muscle membrane repair and muscle fibre growth and regeneration during modified muscle loading in mice in vivo. *J. Physiol.*, **578**, 327–336.
51. Nguyen, H.X. and Tidball, J.G. (2003) Interactions between neutrophils and macrophages promote macrophage killing of rat muscle cells in vitro. *J. Physiol.*, **547**, 125–132.
52. Cornelio, F. and Dones, I. (1984) Muscle fiber degeneration and necrosis in muscular dystrophy and other muscle

diseases: Cytochemical and immunocytochemical data. *Ann. Neurol.*, **16**, 694–701.
53. Briguet, A., Courdier-Fruh, I., Foster, M., Meier, T. and Magyar, J.P. (2004) Histological parameters for the quantitative assessment of muscular dystrophy in the mdx-mouse. *Neuromuscul. Disord.*, **14**, 675–682.
54. Coulton, G.R., Morgan, J.E., Partridge, T.A. and Sloper, J.C. (1988) The mdx mouse skeletal muscle myopathy: I. A histological, morphometric and biochemical investigation. *Neuropathol. Appl. Neurobiol.*, **14**, 53–70.
55. Cai, B., Spencer, M.J., Nakamura, G., Tseng-Ong, L. and Tidball, J.G. (2000) Eosinophilia of dystrophin-deficient muscle is promoted by perforin-mediated cytotoxicity by T cell effectors. *Am. J. Pathol.*, **156**, 1789–1796.
56. Wehling, M., Spencer, M.J. and Tidball, J.G. (2001) A nitric oxide synthase transgene ameliorates muscular dystrophy in mdx mice. *J. Cell Biol.*, **155**, 123–132.
57. Hodgetts, S., Radley, H., Davies, M. and Grounds, M.D. (2006) Reduced necrosis of dystrophic muscle by depletion of host neutrophils, or blocking TNFα function with Etanercept in mdx mice. *Neuromuscul. Disord.*, **16**, 591–602.
58. Capote, J., Kramerova, I., Martinez, L., Vetrone, S., Barton, E.R., Sweeney, H.L., Miceli, M.C. and Spencer, M.J. (2016) Osteopontin ablation ameliorates muscular dystrophy by shifting macrophages to a pro-regenerative phenotype. *J. Cell Biol.*, **213**, 275–288.
59. Sugiura, S., Lahav, R., Han, J., Kou, S.-Y., Banner, L.R., Pablo, F.D. and Patterson, P.H. (2000) Leukaemia inhibitory factor is required for normal inflammatory responses to injury in the peripheral and central nervous systems in vivo and is chemotactic for macrophages in vitro. *Eur. J. Neurosci.*, **12**, 457–466.
60. Tofaris, G.K., Patterson, P.H., Jessen, K.R. and Mirsky, R. (2002) Denervated Schwann cells attract macrophages by secretion of leukemia inhibitory factor (LIF) and monocyte chemoattractant protein-1 in a process regulated by interleukin-6 and LIF. *J. Neurosci.*, **22**, 6696–6703.
61. Shireman, P.K., Contreras-Shannon, V., Ochoa, O., Karia, B.P., Michalek, J.E. and McManus, L.M. (2007) MCP-1 deficiency causes altered inflammation with impaired skeletal muscle regeneration. *J. Leukoc. Biol.*, **81**, 775–785.
62. Martinez, C.O., McHale, M.J., Wells, J.T., Ochoa, O., Michalek, J.E., McManus, L.M. and Shireman, P.K. (2010) Regulation of skeletal muscle regeneration by CCR2-activating chemokines is directly related to macrophage recruitment. *Am. J. Physiol. Regul. Integr. Comp. Physiol.*, **299**, R832–R842.
63. Brigitte, M., Schilte, C., Plonquet, A., Baba-Amer, Y., Henri, A., Charlier, C., Tajbakhsh, S., Albert, M., Gherardi, R.K. and Chrétien, F. (2010) Muscle resident macrophages control the immune cell reaction in a mouse model of notexin-induced myoinjury. *Arthritis Rheum.*, **62**, 268–279.
64. Henriques-Pons, A., Yu, Q., Rayavarapu, S., Cohen, T.V., Ampong, B., Cha, H.J., Jahnke, V., Van der Meulen, J., Wang, D., Jiang, W. *et al.* (2014) Role of toll-like receptors in the pathogenesis of dystrophin-deficient skeletal and heart muscle. *Hum. Mol. Genet.*, **23**, 2604–2617.
65. Wang, Y., Wehling-Henricks, M., Samengo, G. and Tidball, J.G. (2015) Increases of M2a macrophages and fibrosis in aging muscle are influenced by bone marrow aging and negatively regulated by muscle-derived nitric oxide. *Aging Cell*, **14**, 678–688.
66. Pascual-García, M., Bonfill-Teixidor, E., Planas-Rigol, E., Rubio-Perez, C., Lurlaro, R., Arias, A., Cuartas, I., Sala-Hojman, A., Escudero, L., Martinez-Ricarte, F. *et al.* (2019) LIF regulates CXCL9 in tumor-associated macrophages and prevents CD8+ T cell tumor-infiltration impairing anti-PD1 therapy. *Nat. Commun.*, **10**, 2416.
67. Hunt, L.C., Tudor, E.M. and White, J.D. (2010) Leukemia inhibitory factor-dependent increase in myoblast cell number is associated with phosphotidylinositol 3-kinase-mediated inhibition of apoptosis and not mitosis. *Exp. Cell Res.*, **316**, 1002–1009.
68. Blau, H.M., Webster, C. and Pavlath, G.K. (1983) Defective myoblasts identified in Duchenne muscular dystrophy. *Proc. Natl. Acad. Sci. U. S. A.*, **80**, 4856–4860.
69. Webster, C. and Blau, H.M. (1990) Accelerated age-related decline in replicative life-span of Duchenne muscular dystrophy myoblasts: implications for cell and gene therapy. Somat. *Cell Mol. Genet.*, **16**, 557–565.
70. Sacco, A., Mourkioti, F., Tran, R., Choi, J., Llewellyn, M., Kraft, P., Shkreli, M., Delp, S., Pomerantz, J.H., Artandi, S.E. and Blau, H.M. (2010) Short telomeres and stem cell exhaustion model Duchenne muscular dystrophy in mdx/mTR mice. *Cell*, **143**, 1059–1071.
71. Lu, A., Poddar, M., Tang, Y., Proto, J.D., Sohn, J., Mu, X., Oyster, N., Wang, B. and Huard, J. (2014) Rapid depletion of muscle progenitor cells in dystrophic mdx/utrophin−/− mice. *Hum. Mol. Genet.*, **23**, 4786–4800.
72. Gregorevic, P., Hayes, A., Lynch, G.S. and Williams, D.A. (2000) Functional properties of regenerating skeletal muscle following LIF administration. *Muscle Nerve*, **23**, 1586–1588.
73. Sandow, A. and Brust, M. (1958) Contractility of dystrophic mouse muscle. *Am. J. Phys.*, **194**, 557–563.
74. Hete, B. and Shung, K.K. (1995) A study of the relationship between mechanical and ultrasonic properties of dystrophic and normal skeletal muscle. *Ultrasound Med. Biol.*, **21**, 343–352.
75. Virgilio, K.M., Martin, K.S., Peirce, S.M. and Blemker, S.S. (2015) Multiscale models of skeletal muscle reveal the complex effects of muscular dystrophy on tissue mechanics and damage susceptibility. *Interface Focus*, **5**, 20140080.
76. White, J.P., Baltgalvis, K.A., Sato, S., Wilson, L.B. and Carson, J.A. (2009) Effect of nandrolone decanoate administration on recovery from bupivacaine-induced muscle injury. *J. Appl. Physiol.*, **107**, 1420–1430.
77. Wehling-Henricks, M., Welc, S.S., Samengo, G., Rinaldi, C., Lindsey, C., Wang, Y., Lee, J., Kuro-O, M. and Tidball, J.G. (2018) Macrophages escape Klotho gene silencing in the mdx mouse model of Duchenne muscular dystrophy and promote muscle growth and increase satellite cell numbers through a Klotho-mediated pathway. *Hum. Mol. Genet.*, **27**, 14–29.
78. Bustin, S.A., Benes, V., Garson, J.A., Hellemans, J., Huggett, J., Kubista, M., Mueller, R., Nolan, T., Pfaffl, M.W., Shipley, G.L., Vandesompele, J. and Wittwer, C.T. (2009) The MIQE guidelines: minimum information for publication of quantitative real-time PCR experiments. *Clin. Chem.*, **55**, 611–622.
79. Nolan, T., Hands, R.E. and Bustin, S.A. (2006) Quantification of mRNA using real-time RT-PCR. *Nat. Protoc.*, **1**, 1559–1582.
80. Vandesompele, J., De Preter, K., Pattyn, F., Poppe, B., Van Roy, N., De Paepe, A. and Speleman, F. (2002) Accurate normalization of real-time quantitative RT-PCR data by geometric averaging of multiple internal control genes. *Genome Biol.*, **3**, research0034.1.

Supplementary Figure 1

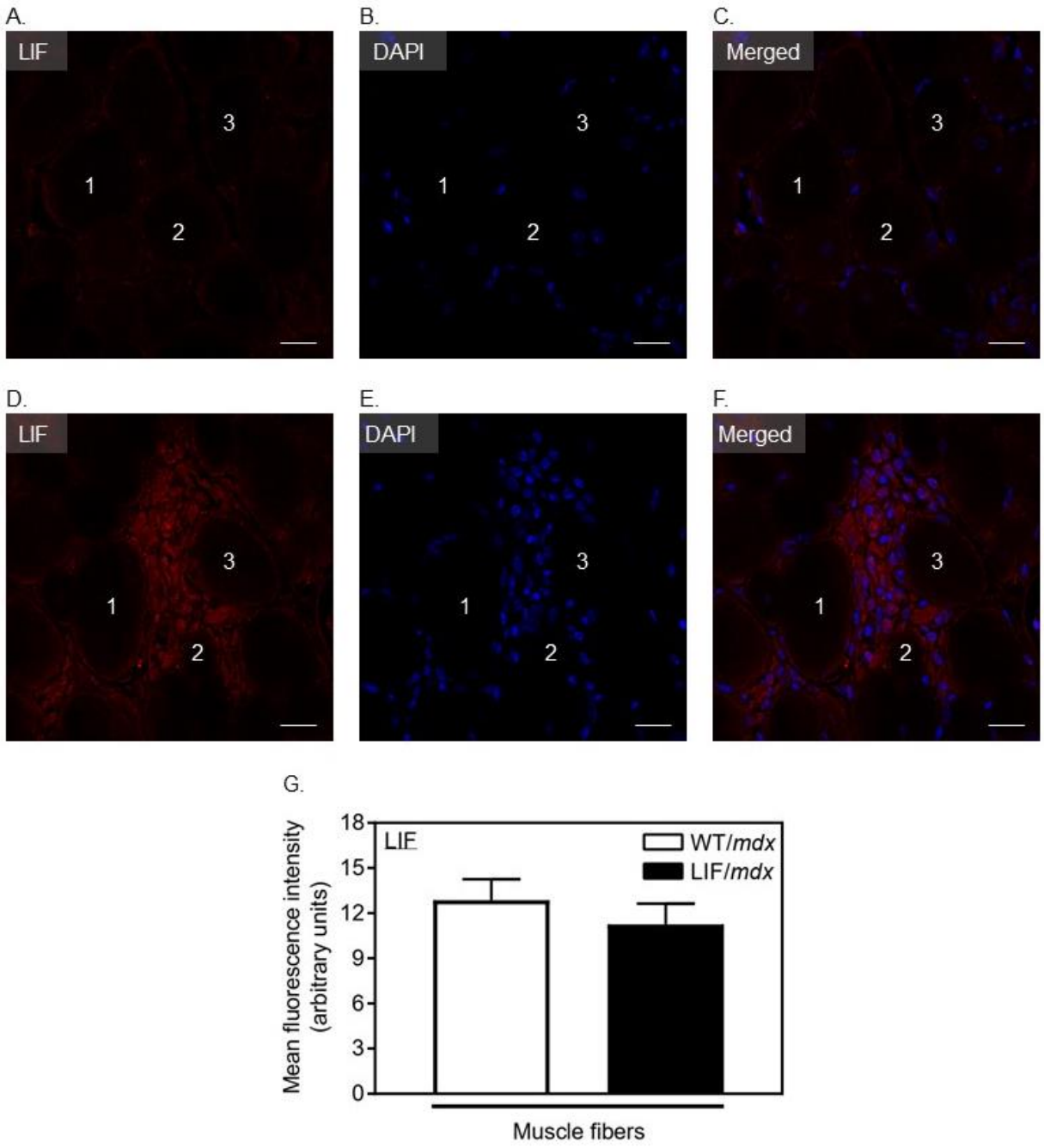

Supplemental figure 1. Muscle fibers of LIF/*mdx* mice do not exhibit ectopic expression of the CD11b/LIF transgene. Cross-sections immunolabeled with anti-LIF **(A, D)** show no LIF protein expression at sites devoid of inflammatory lesions **(A-C)** in muscles of LIF/*mdx* mice. LIF protein expression is present in inflammatory lesions containing mononuclear cells but not in the surrounding

fibers **(D-F)** of LIF/*mdx* mice. Fibers that are numbered "1," "2" or "3" represent the same fiber in each fluorescence channel. Scale bars = 20 μm. Histogram showing no difference in LIF MFI in the fibers of 1-month-old LIF/*mdx* muscles compared to WT/*mdx* fibers **(G)**. *P*-values are based on a two-tailed t-test. *N* = 5 for both groups. Bars = SEM.

Chapter 4:

Conclusions

In this investigation, we showed that genetically-modified macrophages can be utilized as vectors for the targeted delivery of transgenic LIF to dystrophic muscles in a manner that is responsive to the magnitude of pathology. Muscles from LIF/*mdx* mice contained elevated levels of LIF protein at sites occupied by M1-biased macrophages. QPCR analysis of CD11b/LIF+ BMDMs validated the observation that transgenic LIF is primarily delivered to dystrophic muscles by macrophages activated to an M1-biased phenotype. Additionally, we observed no difference in the levels of LIF protein in muscle fibers or sera of LIF/*mdx* and WT/*mdx* mice. These observations show that the CD11b promoter provides targeted delivery of transgenic LIF without off-target transgene expression. Transplantation of CD11b/LIF+ BMCs to non-transgenic, *mdx* mice (LIF BMT/*mdx*) showed that BMT is a viable treatment strategy for the long-term delivery of therapeutic molecules to dystrophic muscles after a single intervention.

The primary benefit of CD11b/LIF transgene expression in dystrophic muscles was a reduction in fibrosis and stiffness of *mdx* muscles. Our present findings indicate that LIF can reduce fibrosis through multiple mechanisms. Transgenic LIF reduced the proportion of macrophages that express TGF-β in LIF BMT/*mdx* muscles, while LIF stimulation reduced the expression and secretion of TGF-β by BMDMs *in vitro*. The reduced expression of TGF-β by macrophages *in vivo* was associated with a reduction in the number of FAPs in LIF BMT/*mdx* muscles. The reduction in FAP numbers may be caused by increased FAP apoptosis due reduced availability of TGF-β to protect FAPs against TNF-α-mediated apoptosis [1]. The anti-fibrotic effects of LIF were also observed in muscle cells. Myogenic progenitor cells isolated from LIF/*mdx* muscles showed reduced expression of fibronectin and collagen type 3. *In vitro*, LIF inhibited the TGF-β-mediated increase in the expression of CTGF in myoblasts and myotubes. These findings indicate that LIF can reduce fibrosis of dystrophic muscles by reducing the amount of TGF-β produced by macrophages and by reducing TGF-β-mediated fibrogenesis of myogenic cells.

Muscle fibrosis can also be affected by changes in the activity and numbers of macrophages, which were affected in both of our mouse models.

Elevated expression of LIF reduced the intramuscular numbers of F4/80+ macrophages in LIF/*mdx* and LIF BMT/*mdx* muscles. Because CCL2 is a potent macrophage chemoattractant, we assessed whether LIF could reduce CCL2-CCR2 signaling in macrophages [2,3]. We found that the CD11b/LIF transgene reduced the proportion of F4/80+ macrophages that expressed CCL2 in the muscles of LIF/*mdx* and LIF BMT/*mdx* muscles. Additionally, *in vitro* experimentation showed that elevated LIF can reduce the expression and secretion of CCL2 by BMDMs and reduce the chemotactic response of BMDMs to CCL2. These data indicate a novel role for LIF in reducing macrophage recruitment to dystrophic muscles by inhibiting CCL2's chemotactic effect on macrophages. However, the finding that CD163+ and CD206+ macrophage numbers were reduced in the muscles of both mouse models without affecting the numbers of CD68+ macrophages indicates that LIF may also inhibit the transition of macrophages from an M1-biased to an M2-biased phenotype.

The shift in macrophages away from an M2-biased phenotype may be explained by changes in the expression of SOCS3 in *mdx* muscles caused by the CD11b/LIF transgene, as discussed in Chapter 2. However, recent investigations have shown that CCL2-CCR2 signaling is also involved in promoting the M2-biased phenotype. For example, gene expression was compared between human macrophages that were stimulated to an M1-biased or M2-biased phenotype. M1-biased macrophages expressed greater levels of CCR2, while M2-biased macrophages expressed and secreted greater levels of CCL2 [4]. Culturing the human macrophages in the presence of a CCL2-neutralizing antibody showed that the amount of endogenous CCL2 secreted by macrophages is enough to promote the expression of genes related to the M2-

biased phenotype. A similar study showed that human macrophage cultures stimulated with CCL2 have a greater proportion of CD206+ macrophages in comparison to unstimulated or IL-6-stimulated macrophages [5]. Additionally, muscles from CCR2-null, *mdx* mice expressed reduced levels of the M2-biased macrophage markers CD206, Arg-1, and Ym1 [6]. In the context of these studies, our data suggest that CD11b/LIF-mediated reductions in expression and responsiveness to CCL2 by macrophages may reduce the transition to an M2 phenotype, in addition to reducing macrophage recruitment.

Our findings indicate that macrophages recruited to lesions in LIF/*mdx* muscles encounter elevated levels of LIF that may act as a chemoattractant to prevent macrophage dispersion to other portions of the muscles. This effect may be amplified by increased HMGB1-TLR4 signaling that occurs in *mdx* muscle [7]. Activation of TLR4 signaling can drive CD11b expression, which could increase expression of the CD11b/LIF transgene and amplify the chemotactic effect of LIF in transgenic muscles [8,9]. Thus, the overall chemotactic effect of the transgene may be a reduction in the CCL2-mediated recruitment of macrophages from the bone marrow and circulation to injured muscles, but decreased macrophage dispersal from the original site of infiltration due to localized elevations of LIF and HMGB1 associated with increased muscle damage.

Our cytotoxicity assay data indicate that the CD11b/LIF transgene does not increase the cytolytic effect of macrophages on muscle cells. Rather, the increase in muscle fiber damage in LIF/*mdx* muscles (1-month time-point) was associated with the increased accumulation of cytolytic, M1 macrophages at inflammatory lesions. Increases in fiber damage were absent in LIF/*mdx* muscles at later stages of the pathology (3-month and 12-month time-points) or in LIF BMT/*mdx* muscles (6-month time-point) that received BMT at 2-months of age. These

observations suggest that transplantation of CD11b/LIF+ BMCs to non-transgenic *mdx* mice should be done at a time-point past the onset of acute onset of inflammation. This strategy would provide the anti-fibrotic effects of the transgene and reduce the possibility of increasing muscle fiber damage.

Applications of other therapies for DMD in conjunction with CD11b/LIF+ BMT may further improve the treatment outcomes achieved by BMT. For example, using safe dietary supplements that act as ROS scavengers in conjunction with CD11b/LIF+ BMT may be a viable strategy to reduce the fiber damage seen in LIF/*mdx* mice at early stages of the pathology. Vitamin E and N-acetylcysteine (NAC) are oral supplements that can reduce the effect of ROS in acutely injured and *mdx* muscles [10,11]. Oral administration of vitamin E to 2-week-old *mdx* mice for 2 weeks reduced oxidative stress and the number of IgG+, necrotic fibers in the diaphragm muscles at the 1-month time-point [12]. Vitamin E supplementation also reduced the levels of creatine kinase in the serum of these mice. Elevated levels of creatine kinase are released through damaged sarcolemma of *mdx* and DMD muscles [13–15]. Similarly, oral administration of NAC to *mdx* mice can reduce ROS concentrations and the number of necrotic fibers in limb muscle while reducing creatine kinase levels in the serum [16,17].

While the use of ROS scavengers can reduce the early, detrimental effects of the transgene, the use of anti-fibrotic agents may increase the benefits of the CD11b/LIF transgene. Halofuginone is an anti-fibrotic molecule that has been used to reduce the accumulation of collagens in various organs, including the skin, liver, pancreas, and esophagus [18–20]. It mediates its effect by decreasing fibroblast proliferation and expression of collagens by inhibiting the phosphorylation of Smad3 downstream of TGF-β binding to the TGF-β receptor [21]. Administration of halofuginone to young *mdx* mice prevented age-related increases in fibrosis of the diaphragm

and heart muscles [22]. Treatment of older *mdx* mice demonstrated that halofuginone is also effective in reversing established fibrosis in limb, respiratory, and cardiac muscles [23]. Administration of halofuginone in tandem with CD11b/LIF+ BMT may provide synergistic effects in the reduction of fibrosis of dystrophic muscles.

Analysis of muscles from LIF/*mdx* mice provided evidence for the therapeutic benefit of using the CD11b/LIF transgene in ameliorating the dystrophic pathology. Additionally, the LIF BMT/*mdx* model validated the use of BMT in the long-term delivery of transgenic LIF to dystrophic muscles after a single intervention. However, we believe that the most significant aspect of this investigation is that this approach could be used to drive the expression of other therapeutic molecules to ameliorate chronic pathologies with a significant inflammatory component following a single BMT intervention. For example, elevated expression of follistatin has been shown to reduce the *mdx* pathology and its delivery could be improved by driving its expression by the CD11b promoter in transplanted BMCs [24–26]. Applying this strategy to humans would require *ex vivo* manipulation of macrophages to introduce a therapeutic transgene.

Researchers have shown the feasibility of manipulating primary cells derived from bone marrow prior to transplantation into recipients to influence muscle repair following acute injury. For example, BMCs derived from donor mice were expanded and activated toward an M1-bisaed phenotype prior to their direct transplantation into acutely-injured limb muscles [27]. The transplanted M1 BMDMs reduced fiber permeability and fibrosis when compared to mice receiving unpolarized BMDMs. Additionally, investigators have transfected primary human bone marrow stromal cells with Notch1 intracellular domain (NICD) and transplanted the cells directly to cardiotoxin injured muscles [28]. The transfected cells showed increased expression of genes associated with the myogenic lineage and increased the number of donor-derived nascent fibers

when compared to bone marrow stromal cells without transfection. These observations suggest that BMCs isolated from humans may be transfected with transgenes in which the CD11b promoter drives the expression of pro-regenerative molecules, such as IGF-1 or Klotho, to improve the regenerative capacity of injured muscles and other tissues [29–33].

Although myeloablative pre-conditioning and immunosuppression in BMT may be necessary for the treatment of chronic conditions, they may not be necessary in the context of acute injuries. In a proof-of-concept study, investigators used tail vein injection to transplant microglia derived from donor bone marrow into host mice that did not receive myeloablative pre-conditioning or immunosuppression [34]. One month after transplantation, the investigators found donor-derived microglia in the brain of host mice. The same group used this approach to show that BMDMs transplanted into a mouse model for Alzheimer's disease could reduce amyloid plaque accumulation and cognitive function 5 weeks post-transplantation [35]. While that investigation used a chronic pathology model, other groups have shown success using the same transplantation approach in acute injuries. Researchers showed that human mesenchymal stem cells that are transplanted into hosts experiencing ischemic injuries to the brain or heart, can improve tissue health [36,37]. These observations suggest the possibility of using primary BMCs expressing a transgene driven by the CD11b promoter to improve the health of acutely injured tissues following the same systemic transplantation approach into hosts without myeloablative pre-conditioning or immunosuppression. Using the CD11b promoter would prevent elevated expression of the transgene by the transplanted cells in transit to the site of injury, as suggested by the lack of increased LIF protein content in the sera of LIF/*mdx* mice.

In conclusion, we have shown that cells of the immune system can be used for the targeted expression of therapeutic transgenes to inflamed muscles. Transgenic LIF delivered to

dystrophic muscles using this delivery system was efficient in reducing muscle fibrosis, decreasing the chemotactic effect of CCL2 on macrophage recruitment, and shifting immunity away from a Th2, pro-fibrotic response. Transplantation of genetically-modified BMCs to *mdx* mice allowed us to transfer the beneficial effects of the CD11b/LIF transgene after a single intervention.

References

1. Lemos, D. R., Babaeijandaghi, F., Low, M., Chang, C.-K., Lee, S. T., Fiore, D., Zhang, R.-H., Natarajan, A., Nedospasov, S. A. and Rossi, F. M. V. (2015) Nilotinib reduces muscle fibrosis in chronic muscle injury by promoting TNF-mediated apoptosis of fibro/adipogenic progenitors. *Nat. Med.*, **21**, 786–794.

2. Lu, H., Huang, D., Ransohoff, R. M. and Zhou, L. (2011) Acute skeletal muscle injury: CCL2 expression by both monocytes and injured muscle is required for repair. *FASEB J.*, **25**, 3344–3355.

3. Amano, H., Morimoto, K., Senba, M., Wang, H., Ishida, Y., Kumatori, A., Yoshimine, H., Oishi, K., Mukaida, N. and Nagatake, T. (2004) Essential Contribution of Monocyte Chemoattractant Protein-1/C-C Chemokine Ligand-2 to Resolution and Repair Processes in Acute Bacterial Pneumonia. *J. Immunol.*, **172**, 398–409.

4. Sierra-Filardi, E., Nieto, C., Domínguez-Soto, Á., Barroso, R., Sanchez-Mateos, P., Puig-Kroger, A., Lopez-Bravo, M., Joven, J., Ardavin, C., Rogdriguez-Fernandez, J. L., Sanchez-Torres, C., Mellado, M. and Corbí, A., (2014) CCL2 Shapes macrophage polarization by GM-CSF and M-CSF: identification of CCL2/CCR2-dependent gene expression profile. *J. Immunol.*, **192**, 3858–3867.

5. Roca, H., Varsos, Z. S., Sud, S., Craig, M. J., Ying, C. and Pienta, K. J. (2009) CCL2 and interleukin-6 promote survival of human CD11b+ peripheral blood mononuclear cells and induce M2-type macrophage polarization. *J. Biol. Chem.*, **284**, 34342–34354.

6. Zhao, W., Wang, X., Ransohoff, R. M. and Zhou, L. (2016) CCR2 deficiency does not provide sustained improvement of muscular dystrophy in mdx5cv mice. *FASEB J.*, **31**, 35–46.

7. Giordano, C., Mojumdar, K., Liang, F., Lemaire, C., Li, T., Richardson, J., Divangahi, M., Qureshi, S. and Petrof, B. J. (2015) Toll-like receptor 4 ablation in mdx mice reveals innate

immunity as a therapeutic target in Duchenne muscular dystrophy. *Hum. Mol. Genet.*, **24**, 2147–2162.

8. Lee, S. J., Choi, E. K., Seo, K. W., Bae, J. U., Park, S. Y. and Kim, C. D. (2014) TLR4-mediated expression of mac-1 in monocytes plays a pivotal role in monocyte adhesion to vascular endothelium. *PLoS ONE*, **9**, e104588.

9. Zhou, X., Gao, X.-P., Fan, J., Liu, Q., Anwar, K. N., Frey, R. S. and Malik, A. B. (2005) LPS activation of Toll-like receptor 4 signals CD11b/CD18 expression in neutrophils. *Am. J. Physiol. Lung Cell Mol. Physiol.*, **288**, L655-662.

10. Galli, F., Azzi, A., Birringer, M., Cook-Mills, J. M., Eggersdorfer, M., Frank, J., Cruciani, G., Lorkowski, S. and Özer, N. K. (2017) Vitamin E: Emerging aspects and new directions. *Free Radic. Biol. Med.*, **102**, 16–36.

11. Howard, A. C., McNeil, A. K. and McNeil, P. L. (2011) Promotion of plasma membrane repair by vitamin E. *Nat. Commun.*, **2**, 597.

12. Mâncio, R. D., Hermes, T. de A., Macedo, A. B., Mizobuti, D. S., Valduga, A. H., Rupcic, I. F. and Minatel, E. (2017) Vitamin E treatment decreases muscle injury in mdx mice. *Nutrition*, **43–44**, 39–46.

13. Ozawa, E., Hagiwara, Y. and Yoshida, M. (1999) Creatine kinase, cell membrane and Duchenne muscular dystrophy. *Mol. Cell. Biochem.*, **190**, 143–151.

14. Kobayashi, Y. M., Rader, E. P., Crawford, R. W. and Campbell, K. P. (2012) Endpoint measures in the mdx mouse relevant for muscular dystrophy pre-clinical studies. *Neuromuscul. Disord.*, **22**, 34–42.

15. Zatz, M., Rapaport, D., Vainzof, M., Passos-Bueno, M. R., Bortolini, E. R., Pavanello, R. de C. M. and Peres, C. A. (1991) Serum creatine-kinase (CK) and pyruvate-kinase (PK) activities in Duchenne (DMD) as compared with Becker (BMD) muscular dystrophy. *J. Neurol. Sci.*, **102**, 190–196.

16. Terrill, J. R., Radley-Crabb, H. G., Grounds, M. D. and Arthur, P. G. (2012) N-Acetylcysteine treatment of dystrophic mdx mice results in protein thiol modifications and inhibition of exercise induced myofibre necrosis. *Neuromuscul. Disord.*, **22**, 427–434.

17. Whitehead, N. P., Pham, C., Gervasio, O. L. and Allen, D. G. (2008) N-Acetylcysteine ameliorates skeletal muscle pathophysiology in mdx mice. *J. Physiol.*, **586**, 2003–2014.

18. Pines, M. (2014) Halofuginone for fibrosis, regeneration and cancer in the gastrointestinal tract. *World J. Gastroenterol.*, **20**, 14778–14786.

19. Pines, M., Domb, A., Ohana, M., Inbar, J., Genina, O., Alexiev, R. and Nagler, A. (2001) Reduction in dermal fibrosis in the tight-skin (Tsk) mouse after local application of halofuginone. *Biochem. Pharmacol.*, **62**, 1221–1227.

20. Pines, M. (2008) Targeting TGFβ signaling to inhibit fibroblast activation as a therapy for fibrosis and cancer: effect of halofuginone. *Expert Opin. Drug Discov.*, **3**, 11–20.

21. McGaha, T. L., Phelps, R. G., Spiera, H. and Bona, C. (2002) Halofuginone, an inhibitor of type-I collagen synthesis and skin sclerosis, blocks transforming-growth-factor-beta-mediated Smad3 activation in fibroblasts. *J. Invest. Dermatol.*, **118**, 461–470.

22. Turgeman, T., Hagai, Y., Huebner, K., Jassal, D. S., Anderson, J. E., Genin, O., Nagler, A., Halevy, O. and Pines, M. (2008) Prevention of muscle fibrosis and improvement in muscle performance in the mdx mouse by halofuginone. *Neuromuscul. Disord.*, **18**, 857–868.

23. Huebner, K. D., Jassal, D. S., Halevy, O., Pines, M. and Anderson, J. E. (2008) Functional resolution of fibrosis in mdx mouse dystrophic heart and skeletal muscle by halofuginone. *Am. J. Physiol. Heart Circ. Physiol.*, **294**, H1550–H1561.

24. Nakatani, M., Takehara, Y., Sugino, H., et al. (2008) Transgenic expression of a myostatin inhibitor derived from follistatin increases skeletal muscle mass and ameliorates dystrophic pathology in mdx mice. *FASEB J.*, **22**, 477–487.

25. Zhu, J., Li, Y., Lu, A., Gharaibeh, B., Ma, J., Kobayashi, T., Quintero, A. J. and Huard, J. (2011) Follistatin improves skeletal muscle healing after injury and disease through an interaction with muscle regeneration, angiogenesis, and fibrosis. *Am. J. Pathol.*, **179**, 915–930.

26. Benabdallah, B. F., Bouchentouf, M., Rousseau, J., Bigey, P., Michaud, A., Chapdelaine, P., Scherman, D. and Tremblay, J. P. (2008) Inhibiting myostatin with follistatin improves the success of myoblast transplantation in dystrophic mice. *Cell Transplant.*, **17**, 337–350.

27. Rybalko, V., Hsieh, P.-L., Merscham-Banda, M., Suggs, L. J. and Farrar, R. P. (2015) The Development of Macrophage-Mediated Cell Therapy to Improve Skeletal Muscle Function after Injury. *PLoS ONE*, **10**, e0145550.

28. Dezawa, M., Ishikawa, H., Itokazu, Y., Yoshihara, T., Hoshino, M., Takeda, S., Ide, C. and Nabeshima, Y. (2005) Bone marrow stromal cells generate muscle cells and repair muscle degeneration. *Science*, **309**, 314–317.

29. Tonkin, J., Temmerman, L., Sampson, R. D., Gallego-Colon, E., Barberi, L., Bilbao, D., Schneider, M. D., Musarò, A. and Rosenthal, N. (2015) Monocyte/macrophage-derived IGF-1 orchestrates murine skeletal muscle regeneration and modulates autocrine polarization. *Mol. Ther.*, **23**, 1189–1200.

30. Barton-Davis, E. R., Shoturma, D. I., Musaro, A., Rosenthal, N. and Sweeney, H. L. (1998) Viral mediated expression of insulin-like growth factor I blocks the aging-related loss of skeletal muscle function. *Proc. Natl. Acad. Sci.*, **95**, 15603–15607.

31. Wehling-Henricks, M., Li, Z., Lindsey, C., Wang, Y., Welc, S. S., Ramos, J. N., Khanlou, N., Kuro-o, M. and Tidball, J. G. (2016) Klotho gene silencing promotes pathology in the mdx mouse model of Duchenne muscular dystrophy. *Hum. Mol. Genet.*, **25**, 2465–2482.

32. Ahrens, H. E., Huettemeister, J., Schmidt, M., Kaether, C. and von Maltzahn, J. (2018) Klotho expression is a prerequisite for proper muscle stem cell function and regeneration of skeletal muscle. *Skelet. Muscle*, **8**, 20.

33. Shavlakadze, T., White, J., Hoh, J. F. Y., Rosenthal, N. and Grounds, M. D. (2004) Targeted expression of insulin-like growth factor-i reduces early myofiber necrosis in dystrophic mdx mice. *Mol. Ther.*, **10**, 829–843.

34. Leovsky, C., Fabian, C., Naaldijk, Y., Jäger, C., Jang, H. J., Böhme, J., Rudolph, L. and Stolzing, A. (2015) Biodistribution of in vitro-derived microglia applied intranasally and intravenously to mice: effects of aging. *Cytotherapy*, **17**, 1617–1626.

35. Costa-Marques, L., Arnold, K., Pardon, M.-C., Leovsky, C., Swarbrick, S., Fabian, C. and Stolzing, A. (2019) Transplantation of bone marrow derived macrophages reduces markers of neuropathology in an APP/PS1 mouse model. *Transl. Neurodegener.*, **8**, 33.

36. Sammali, E., Alia, C., Vegliante, G., Columbo, V., Giordano, N., Pischiutta, F., Boncoraglio, G. B., Barilani, M., Lazzari, L., Caleo, M., De Simoni, M.-G., Gaipa, G., Citerio, G. and Zanier, E. R. (2017) Intravenous infusion of human bone marrow mesenchymal stromal cells promotes functional recovery and neuroplasticity after ischemic stroke in mice. *Sci. Rep.*, **7**, 6962.

37. Peng, Y., Chen, B., Zhao, J., Peng, Z., Xu, W. and Yu, G. (2019) Effect of intravenous transplantation of hUCB-MSCs on M1/M2 subtype conversion in monocyte/macrophages of AMI mice. *Biomed. Pharmacother.*, **111**, 624–630.